

**The Toxicological Effects of Engineered Nanoparticles,
Quantum Dots, in Estuarine Fish**

by

Twyla Michelle Blickley

Department of Environment
Duke University

Date: _____

Approved:

Daniel Rittschof, Co-chair

Patricia D. McClellan-Green, Co-chair

Richard T. Di Giulio

David E. Hinton

Eva Oberdörster

Dissertation submitted in partial fulfillment of
the requirements for the degree of Doctor
of Philosophy in the Department of
Environment in the Graduate School
of Duke University

2010

ABSTRACT

**The Toxicological Effects of Engineered Nanoparticles,
Quantum Dots, in Estuarine Fish**

by

Twyla Michelle Blickley

Department of Environment
Duke University

Date: _____

Approved:

Daniel Rittschof, Co-chair

Patricia D. McClellan-Green, Co-chair

Richard T. Di Giulio

David E. Hinton

Eva Oberdörster

An abstract of a dissertation submitted in partial
fulfillment of the requirements for the degree
of Doctor of Philosophy in the Department of
Environment in the Graduate School
of Duke University

2010

Copyright by
Twyla Michelle Blickley
2010

Abstract

Engineered nanoparticles (ENPs) are a part of everyday life. They are incorporated into a wide array of products including sunscreens, clothing, electronics, paints, and automobiles. One particular type of ENP, quantum dots (QDs), are fluorescent semi-conducting nanocrystals, and are touted as the next generation of medical tracers and energy-efficient light bulbs. The continued development and expansion of commercial applications for QDs ensure that they will enter the aquatic environment following manufacture, use, and disposal. Unfortunately, very little information exists on the bioavailability and sub-lethal toxicological effects of QDs in aquatic organisms. The studies described in this dissertation focused on determining the toxicological effects of Lecithin-encapsulated CdSe/ZnS quantum dots in larval and adult *Fundulus heteroclitus* (the mummichog).

Quantum dot dispersion is greatly influenced by environmental parameters such as pH, natural organic matter concentration, and ionic strength. Lecithin-encapsulated core-shell QDs aggregated and precipitated from suspension in 20 ppt seawater. QD aggregates adhered to the exterior chorion of *Fundulus* embryos in aqueous embryo exposures, but did not traverse the chorion and deposit into the body of the fry.

Incidences of developmental abnormalities increased and hatching rates declined in embryos exposed to the highest concentration tested (100 µg/ml).

Dietary assessments showed that QDs were bioavailable to adult *Fundulus*.

While QDs or their degradation products traversed the intestinal epithelial and were deposited to the liver, less than 0.01% of the cadmium from the QDs was retained in the liver and intestinal tissues. QD uptake did not cause significant changes in hepatic total glutathione or lipid peroxidation levels, nor did it statistically alter the expression of genes involved in metal metabolism and oxidative stress— metallothionein, glutathione-s-transferase, glutathione peroxidase, and superoxide dismutases. There was, however, a clear gender-specific trend in the level of Cu/Zn-superoxide dismutase transcription.

In addition, QDs did impact fecundity presumably by feminizing male fish.

Vitellogenin transcription was elevated and relative gonad size reduced in male *Fundulus* consuming 10 µg QD per day. Lastly, QDs or their degradation products were maternally transferred to the eggs following six to eight weeks of parental exposure, thus posing a risk to *Fundulus* progeny. Based on the results of these studies, it is apparent that chronic exposure to QDs could result in adverse effects in teleosts and other organisms inhabiting estuarine environments.

Dedication

For Brandon, Bill, Twyla, Crystal, and Karen for all your love and support.

Contents

Abstract	iv
List of Tables	x
List of Figures	xi
List of Abbreviations	xiv
Acknowledgements	xv
Chapter 1. Quantum Dots: From Synthesis to Degradation (and Everything in Between)	1
1.1 Synthesis	5
1.2 Chemistry & Structure	6
1.3 Optical Properties	9
1.4 Stability	10
1.5 Toxicity & Potential Mechanisms of Action	13
1.5.1 Toxicity of Quantum Dots.....	13
1.5.2 Toxicity of Quantum Dot Components.....	21
1.5.2.1 Cadmium.....	21
1.5.2.2 Selenium	28
1.5.2.3 Lecithin	33
1.5.3 Oxidative Stress	37
Conclusions	51
Chapter 2. Developmental Toxicity of Aqueous CdSe/ZnS QD Exposure in Teleosts	52
Materials and Methods	55

Results	58
Discussion.....	60
Conclusions	62
Chapter 3. Lecithin as an Encapsulating Agent for QDs: A Pilot Study	64
Materials and Methods.....	66
Results	73
Discussion.....	78
Conclusions	81
Chapter 4. Bioavailability and Oxidative Stress from Dietary Quantum Dot Exposure in <i>Fundulus</i>	83
Materials and Methods.....	86
Results	100
Discussion.....	121
Conclusions	129
Chapter 5. Reproductive Toxicity and Maternal Transfer of CdSe/ZnS QDs in Mummichogs.....	131
Materials and Methods.....	133
Results	141
Discussion.....	149
Conclusions	154
Chapter 6. Conclusions: The Potential Consequences of QDs in Estuarine Systems.....	155
Bioavailability	156
Reproductive Effects	157

Developmental Toxicity.....	157
Oxidative Stress	158
Study Implications	158
Future Studies	159
Appendix.....	160
References	166
Biography.....	194

List of Tables

Table 1-1. ROS-related expression cascades.....	47
Table 2-1. Developmental toxicity of aqueous QD exposure.....	60
Table 3-1. QD and Cd content of the diets (5 week exposure).....	68
Table 4-1. QD and Cd content of the diets (12 week exposure).....	89
Table 4-2. Real-Time PCR primer sequences for <i>F. heteroclitus</i>	97
Table 4-3. Tissue cadmium uptake.....	108
Table 5-1. Real-Time PCR primer sequences for <i>F. heteroclitus</i>	138
Table 5-2. Development and hatching of parentally-exposed embryos.....	148

List of Figures

Figure 1-1. Organic ligands.....	7
Figure 1-2. Core-shell QD structure.....	8
Figure 1-3. QD structure with coatings and ligands.....	9
Figure 1-4. QD coating materials.....	12
Figure 1-5. Structure of Lecithin.....	35
Figure 1-6. Reactive oxygen species pathway.....	37
Figure 2-1. Photoluminescent spectrum of the Mixed QD suspension.....	58
Figure 2-2. <i>Fundulus</i> embryos exposed to QDs.....	59
Figure 3-1. Growth and relative liver size.....	74
Figure 3-2. Hepatic total glutathione and lipid peroxidation levels.....	75
Figure 3-3. H&E stained liver sections.....	76
Figure 3-4. Fecundity.....	77
Figure 3-5. Embryo deformities due to Lecithin.....	78
Figure 4-1. Photoluminescent spectrum of the Lecithin-encapsulated QD suspension.....	100
Figure 4-2. Particle sizes of QD and Lecithin suspensions.....	101
Figure 4-3. Transmission electron micrographs of liver slices from SD + Lecithin fed <i>Fundulus</i>	103
Figure 4-4. Transmission electron micrographs of liver slices from <i>Fundulus</i> fed the High QD	104
Figure 4-5. Transmission electron micrographs of liver slices from <i>Fundulus</i> fed the Cd diet	105
Figure 4-6. Cd uptake.....	107

Figure 4-7. Hepatic total glutathione and lipid peroxidation levels.....	111
Figure 4-8. Changes in gene expression.....	112
Figure 4-9. Pathology of a testicular tumor from a Cd-treated <i>Fundulus</i>	114
Figure 4-10. Micrographs of testes from the Standard Diet fed <i>Fundulus</i>	115
Figure 4-11. Micrographs of liver sections from Standard Diet fed <i>Fundulus</i>	117
Figure 4-12. Liver pathology SD + Lecithin treated <i>Fundulus</i>	118
Figure 4-13. Pathology of the liver of <i>Fundulus</i> fed the High QD diet.....	119
Figure 4-14. Liver pathology of <i>Fundulus</i> fed the Cd diet.....	120
Figure 5-1. Growth.....	142
Figure 5-2. Hepatosomatic indices.....	143
Figure 5-3. Fecundity.....	144
Figure 5-4. Acute and chronic fecundity.....	145
Figure 5-5. Male vitellogenin transcription	146
Figure 5-6. Male gonadosomatic indices.....	147
Figure 5-7. Embryo deformities due to parental diet.....	148
Figure A-1. Sex-specific total glutathione levels.....	160
Figure A-2. Sex-specific lipid peroxidation levels.....	161
Figure A-3. Sex-specific metallothionein mRNA levels.....	162
Figure A-4. Sex-specific glutathione-s-transferase mRNA levels.....	162
Figure A-5. Sex-specific glutathione peroxidase mRNA levels.....	163
Figure A-6. Sex-specific Mn-superoxide dismutase mRNA levels.....	163
Figure A-7. Sex-specific Cu/Zn-superoxide dismutase mRNA levels.....	164

Figure A-8. Female vitellogenin transcription.....165
Figure A-9. Female gonadosomatic indices.....165

List of Abbreviations

CAT	Catalase
ENPs	Engineered nanoparticles
ERK	Extracellular signal-regulated kinase
gpx	Glutathione peroxidase mRNA
GSH	Glutathione
gstmu	Glutathione-s-transferase mRNA
ICP-MS	Inductively-coupled plasma mass spectrometry
JNK	c-jun NH ₂ -terminal kinase
LPo	Lipid peroxidation
MAPK	Mitogen-activated protein kinase
Mt	Metallothionein mRNA
MT	Metallothionein protein
PKC	Protein kinase C
QDs	Quantum dots
ROS	Reactive oxygen species
SOD	Superoxide dismutase
sod1	Cu/Zn superoxide dismutase mRNA
sod2	Mn superoxide dismutase mRNA
TEM	Transmission electron microscopy
vtg	Vitellogenin mRNA transcript
VTG	Vitellogenin protein

Acknowledgements

I thank Drs. David Holbrook and Wyatt Vreeland of the National Institute of Standards and Technology (NIST) in Gaithersburg, MD as well as Dr. Cole Matson of the Center for the Environmental Implications of NanoTechnology (CEINT) for performing the confocal microscopy, transmission electron microscopy, flow field-flow fractionation, and quantitative real-time PCR. T.M. Blickley was supported by the Society of Environmental Toxicology and Chemistry (SETAC) Doctoral Fellowship, sponsored by the Procter & Gamble Company. This research was partially supported by the Oak Foundation, Duke University Marine Laboratory, NC State University Center for Marine Sciences and Technology, and the National Science Foundation and the Environmental Protection Agency under NSF Cooperative Agreement EF-0830093, CEINT. Any opinions, findings, conclusions or recommendations expressed in this material are those of the author(s) and do not necessarily reflect the views of the National Science Foundation or the Environmental Protection Agency. This work has not been subjected to EPA review and no official endorsement should be inferred.

Chapter 1. Quantum Dots: From Synthesis to Degradation (and Everything in Between)

In 1985 the field of nanoscience arose as a result of the discovery of the fullerene (C_{60}) by Kroto and Smalley [1]. While early investigators focused on documenting the physical and chemical properties of these novel materials, it is their commercial applications and potential that are driving the nanotechnology revolution.

Nanomaterials are defined as naturally-occurring or engineered particles that are less than 100 nm in any one dimension. The large surface-to-mass ratios of engineered nanoparticles (ENPs) confer unique physical, chemical, electrical, and optical properties that are desirable to many fields including manufacturing, defense, environmental remediation, and medicine. ENPs are being used to develop innovative solutions to timeless dilemmas. For example, clinical scientists are investigating nanotubes as drug delivery devices, fullerenes as potential therapies for neuro-degenerative diseases, and nano-gold as a treatment for cancer. The National Science Foundation has estimated that with increasing production and commercialization, the nanotechnology industry will be worth ~\$1 trillion by 2015 [2].

A wide variety of ENPs exist due to diverse synthesis methods, differing core materials, and an abundance of capping/coating agents. Currently there are 6 classifications of ENPs: fullerenes, carbon nanotubes, quantum dots, zero-valent metals, metal oxides, and dendrimers. Fullerenes (C_{60} , C_{70} , C_{76} , and C_{80}) are carbon molecules

configured in a hollow, spherical structure [1], whereas nanotubes are carbon molecules arranged in a cylindrical structure [3]. Quantum dots (CdTe, CdSe, PbS, and InAs) are semi-conducting nanocrystals composed of alternating layers of metals [4]. Zero-valent metals, such as nano-Au, Ag, and Fe, are transition metals in the nano size range, while metal oxides are composed a metal cation and oxide anion(s) in the nano size range (nano-TiO₂, ZnO, CoO₂, and MnO₃). Dendrimers are branched molecules and are used predominately in the medicinal fields. Scientists have not determined which factors (composition, morphology, size, surface chemistry, aggregation state, or environmental parameters) most influence nanoparticle fate and toxicity. As such, ENPs must be investigated individually for deleterious sequelae.

Accompanying progress in nanoparticle development is a lack of human and environmental health information regarding exposure and effects of ENPs and their degradation products. Given the rapid and substantial increase in commercial applications, ENPs will be released from products into terrestrial and aquatic ecosystems during use and disposal. For example, nanotubes deposited on roadways from tire treads enter ditches and streams via stormwater run-off, while nano-iron is directly injected into aquatic systems as a component of environmental remediation agents. Similarly, degrading electronics in landfills release quantum dots and fullerenes

into terrestrial environments, which then make their way into aquatic environments during storm events. The goal of these studies is to determine if one type of ENP, Lecithin-encapsulated CdSe/ZnS quantum dots, affects biological processes in the estuarine teleost *Fundulus heteroclitus* (the mummichog) including oxidative balance, gene expression changes, reproduction, and embryological development. The generation of this data will help design future ENPs to be safer for both humans and our environment.

Quantum dots (QDs), also known as semi-conducting nanocrystals, are essentially atom clusters of III-V or II-VI metals. QDs in the III-V category are typically made of GaAs, InAs, or InP, while dots that fall into the II-VI group are composed of CdSe, CdS, or CdTe. They are 1-10 nm in diameter and emit tunable, discrete fluorescence when illuminated with visible or near UV wavelengths. QDs are commercially-available as components of light emitting diodes (LEDs), electronic displays, telecommunications components, wiring, lasers, inks, and solar cells [4]. QDs are also being evaluated as potential bio-imaging and bio-labeling agents as they are superior to conventional fluorophores. Given the immense potential of QDs, they need to be evaluated from synthesis to degradation for toxicological effects in organisms. This begins with an extensive review of the QD, cadmium, and selenium literature in

order to highlight potential mechanisms of toxicity. Additionally, because oxidative stress is thought to be the predominate mechanism by which ENPs exert toxicity, a thorough investigation of the toxicological effects of reactive oxygen species will identify potential biomarkers of oxidative stress.

1.1 Synthesis

The initial techniques for synthesizing QDs emerged in the 1980s stemming from research at the AT&T Bell Laboratories [5-7]. Briefly, two organometallic solutions—one containing Cd^{2+} , the other bis(trimethylsilyl) selenium ($\text{Se}(\text{TMS})_2$)—are added to a microemulsion at high temperatures (approximately 350°C). Nucleation and growth of the core occur in a layered one-to-one fashion. After the formation of the appropriate size CdSe core, injection of Zn^{2+} and S^{2-} into the micelle media initiates epitaxial growth of the ions around the cores [6]. Several techniques to synthesize QDs have evolved since then, including pyrolysis [8], molecular beam epitaxy [9, 10] and electron beam lithography [11]. These newer methods of creation enhance both size-selectivity and quality, while reducing cost and the amount of hazardous materials needed to produce the QDs.

1.2 Chemistry & Structure

The properties of QDs are a function of the particles' diameter and coatings. A CdSe/ZnS crystal ranges from 1.9-5.2 nm in diameter and has a molecular weight between 2.7 and 180 $\mu\text{g/nmol}$ [4]. The CdSe core is composed of monodispersed layers of Cd and Se atoms arranged in a nearly wurtzite crystal, thus having an ABABAB... pattern [5, 8]. Like other materials in this size range, Van der Waals forces are responsible for the molecular bonding of the colloid [8]. The molecules are tetrahedrally bonded (109° , sp^3 bond), but the bonds ease (120° , sp^2 bond) as you move outward from the center of the cluster [12]. In this relaxed crystal, the cadmium is drawn inward, while selenium is pushed outward [12]. The surface atoms tend to be unsaturated [13] providing sites for linkages of additional layers. The shapes of these multi-faceted CdSe core dots are generally regular (tetrahedron or hexagonal prism), spherical, or ellipsoidal [8, 13]. However, QDs formed by E-beam lithography can take the form of many shapes including pillars, mushrooms, walls, or crosses [11].

As with most ENPs, particle aggregation is a significant problem that can be avoided with the introduction of a lyophilic coating. Passivating QDs with organic ligands (Fig. 1-1) such as tri-*n*-octylphosphine oxide or hexadecylamine deter aggregation, flocculation, and interactions with surface molecules. Passivating the

surface also allows the molecule to be solubilized in non-polar solvents. It is the cadmium that bonds to the organic material [13].

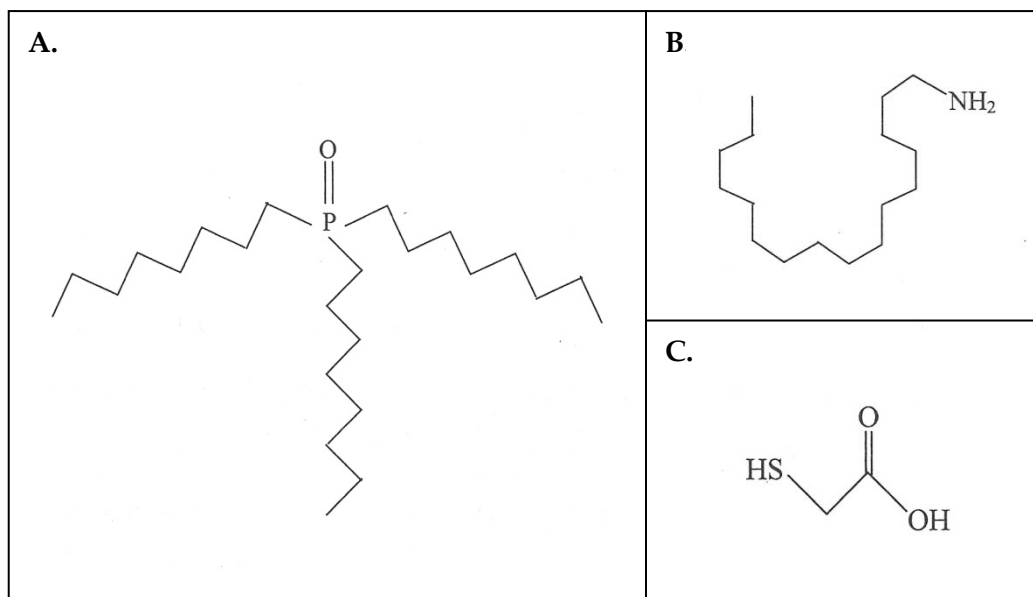


Figure 1-1. Organic ligands (A) tri-*n*-octylphosphine oxide, (B) hexadecylamine, and (C) mercapto-acetic acid are used to hinder aggregation or render QDs water-miscible.

Second generation QDs (Fig. 1-2) are capped with an inorganic shell, usually ZnS, to hinder aggregation, while increasing stability and brightness. Capping the core also reduces photoluminescent degradation and oxidation by sterically hindering bonding with other molecules [14, 15]. ZnS is configured in a tetrahedral pattern like the CdSe core; however, CdSe and ZnS do not have the same bond length. A Cd-Se bond is 13% longer than a Zn-S bond, so the two lattices do not anneal/alloy due to the 2.5%

mismatch [6, 15]. Typically only 1-3 layers of ZnS are grown on to the core because additional coverage leads to unevenness and surface defects [16], which alter optical properties.

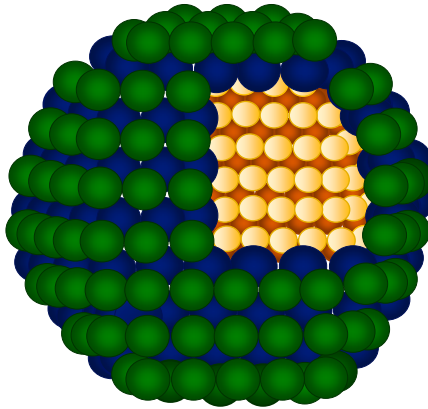


Figure 1-2. Core-shell QD structure. The cadmium selenide core (yellow and orange) is surrounded by a thin zinc sulfide shell (green and blue) [4].

After the addition of proprietary coatings by the manufacturers to deter degradation, ligands (Fig. 1-3) can be attached to the QDs through a variety of conjugation techniques. Coatings (Figures 1-1 and 1-4) such as mercapto-acetic acid [17-19], mercapto-undecanoic acid [20, 21], bovine serum albumin [19], and sheep serum albumin [21] have been coupled to QDs to render the dots water-miscible and decrease interactions with cellular components. Polyethylene glycol has also been used to make QDs biologically inert *in vivo*. Attachment of thiol, carboxyl, or amine groups alter the

QDs surface charge, while allowing additional biomolecules to be coupled to the QD.

DNA, proteins, antibodies, peptides, and neurotransmitters have been attached to QDs for assays and cell-specific targeting [22-27].

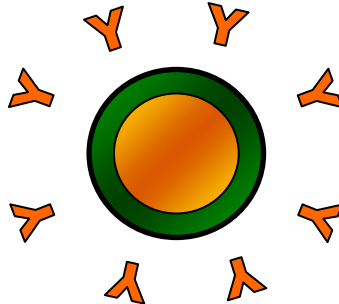


Figure 1-3. This diagram represents a core (orange and yellow) –shell (green) QD with a proprietary coating (black) and a biological macromolecule (Y).

1.3 Optical Properties

Quantum dots are essentially fluorophores emitting in the 465-2300 nm range. Fluorescence occurs when light is absorbed and the electrons jump the band gap to a higher energy state [14], essentially causing the electrons to move from a bonding to anti-bonding orbital [28]. As the energy decays, the excited electrons fall back to the ground state, and emit light at a wavelength that is longer than the excitation wavelength—known as Stokes-shift [4]. When excited at a wavelength less than 400 nm, CdSe cores emit at 465-640 nm and CdSe/ZnS QDs at 490-620 nm [4].

QD fluorescence is discrete and can be tuned to a specific wavelength based on the QDs diameter. As the diameter of the particle decreases, the emission wavelength is shortened [14]. A 5% variation in diameter is all that is needed to vary the color of the emission [4]. Unintentional shifts in the peak wavelength can signal aggregation or degradation. A right shift in the peak signals that aggregation is occurring, while a left shift—termed bluing—is a sign that the QD is degrading.

1.4 Stability

QD stability varies depending on the coating/shell (type and thickness) and environmental conditions (air, light, pH). While coatings and shells have been shown to increase the stability of QDs, the longevity of the coatings is uncertain under environmentally-relevant exposure scenarios. Studies have indicated that QDs can break down and leach toxic metal ions [19, 29]. This risk to environmental and human health signals a need for comprehensive life-cycle and toxicological assessment of QDs.

Oxidation of CdSe QDs in air is thought to be a function of the coating type and shell thickness. Exposure of CdSe QDs and insufficiently shelled CdSe/ZnS QDs to air resulted in the release of SeO₂ and altered Cd:Se ratios within the remaining core [16, 30]. However, QDs that were shelled with 1.3 monolayers of ZnS were sufficiently

protected from oxidation [16]. The CdSe QDs degraded in as little as 16 hours, while those shelled with sufficient layers of ZnS were stable up to 80 hours [16]. Researchers theorize that increased ZnS thickness conveys stability because it takes longer for oxygen to diffuse to the core [31].

CdSe QDs with thiol groups attached to the surface are also unstable in air [29]. In studies conducted by Aldana and colleagues [29], the aliphatic thiol ligands underwent oxidation and disulfide formation after approximately 170 minutes. Core disassociation followed ligand degradation and nanocrystal shrinkage was confirmed by a decreased optical density (absorbance) at the original peak.

QDs are also photo-oxidized by visible light. After the Se is oxidized to selenate and evaporates, free cadmium and an exposed layer of CdSe are left behind [13]. Derfus *et al.* [19] showed that mercapto-acetic acid-solubilized CdSe QDs disassociated in air and light. Non-oxidized QD solutions measured only 6 $\mu\text{g Cd}^{2+}/\text{ml}$, while QDs exposed to air (12 hours) or ultraviolet light (8 hours) resulted in free cadmium levels of 126 and 82 $\mu\text{g}/\text{ml}$, respectively. Shelling CdSe QDs with ZnS eliminated oxidation via air, but not UV illumination. Coating CdSe/ZnS QDs with BSA conveyed additional stability as

it provided another barrier through which oxygen had to diffuse to liberate the core molecules.

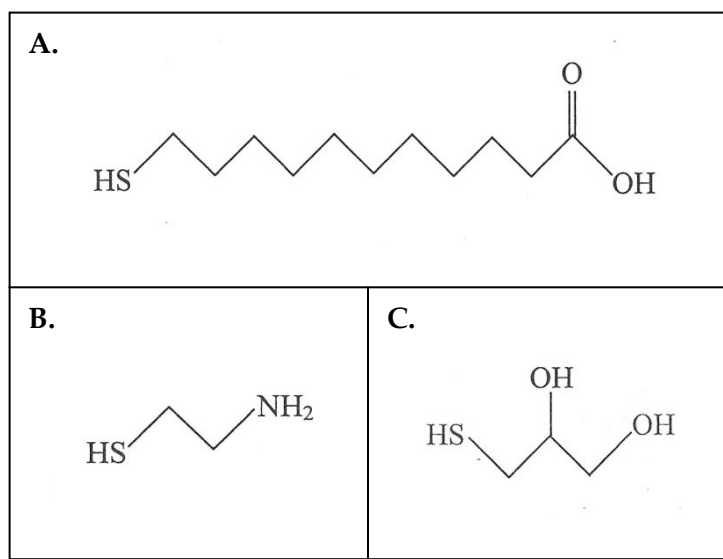


Figure 1-4. The structures of the dispersion coatings (A) mercapto-undecanoic acid, (B) cysteamine, and (C) thioglycerol investigated by Hoshino. *et al.* [20] for toxicological effect.

Hoshino *et al.* [20] investigated the stability of CdSe/ZnS quantum dots coated with mercapto-undecanoic acid, cysteamine, thioglycerol, mercapto-undecanoic acid/thioglycerol, and cysteamine/thioglycerol (Fig. 1-4) at different pHs. All of the modified QDs, both positively and negatively charged, were stable in weakly basic environments (pH 9.0) for approximately 30 minutes. However, only QDs with amine groups, which were positively charged, were stable under acidic conditions (pH 3.0).

Low pH and oxidative sites present in intracellular environments provide a plausible mechanism for QD degradation *in vivo*.

While most environmental conditions seem to favor QD degradation, natural organic matter stabilizes QDs in aqueous environments [32]. When CdSe QDs in hexane were added to samples of natural waters with varying types and degrees of natural organic matter, the QDs quickly flocculated to the water/solvent interface and eventually moved from the hexane into the aqueous phase [32]. This suggests that the inherently lipophilic QDs will become hydrophilic when dispersed in bodies of water. It also implies that there will be a potential increase in risk to aquatic organisms as both water-miscible and lipophilic QDs will enter aqueous systems.

1.5 Toxicity & Potential Mechanisms of Action

1.5.1 Toxicity of Quantum Dots

In Vitro Studies

Cytotoxicity [19, 21, 33, 34], DNA damage [35, 36], and generation of reactive oxygen species (ROS) [37, 38] have all been documented in response to *in vitro* QD exposure. While research is still emerging on the subject, it appears that toxicity can be caused by whole QDs, their degradation products (metallic components), and their

coatings. Hoshino *et al.* [20] determined that the toxicity of CdSe/ZnS QDs was dependent on the coating agents (mercapto-undecanoic acid, cysteamine, thioglycerol, mercapto-undecanoic acid/thioglycerol, and cysteamine/thioglycerol). While mercapto-undecanoic acid-QDs were found to cause significant DNA damage in WTK1 human lymphoma cells at concentrations greater than 1.5 μM , additional testing revealed that mercapto-undecanoic acid alone was severely cytotoxic. Cysteamine was weakly genotoxic, and tri-*n*-octylphosphine oxide was cytotoxic and genotoxic.

Although Hoshino *et al.* [20] indicated that the coatings were responsible for the toxicity, work by Green and Howman [35] proposed an alternate mechanism of action. Investigators discovered that UV-exposed biotinylated CdSe/ZnS QDs caused elevated levels of DNA damage. 56% of the DNA was damaged after exposure to light, whereas only 29% was damaged in darkness. The authors hypothesized that the ZnS shell of the QD was oxidized to SO_2^{\bullet} , which then converted to the superoxide and hydroxyl radicals. Ipe *et al.* [38] later confirmed the generation of ROS, but the phenomenon couldn't be generalized to all QDs. Irradiated CdS QDs generated superoxide and hydroxyl free radicals, while CdSe QDs only generated hydroxyl free radicals. CdSe/ZnS QDs did not generate ROS. This implies that oxidative stress could be the mechanism by which some types of QDs exert toxicity.

Chan *et al.* [39] noted that while CdSe/ZnS QDs had little effect on human neuroblastoma IMR-32 cells (300 μ M, 24 hrs), mercapto-acetic acid-CdSe QDs¹ (150 and 300 μ M) caused significant apoptosis (controlled cell death), but not necrosis (premature cell death due to abnormal stresses). This correlated with increased intracellular ROS generation and pro-apoptotic signaling (activation of caspase-9, stimulation of caspase-3, and the release of cytochrome *c*). CdSe QDs also activated c-jun NH₂-terminal kinase (JNK, pro-apoptotic), downregulated Ras (survival) expression, and increased Bax (pro-apoptotic) protein levels. Conversely, no apoptotic signaling occurred in cells exposed to shelled QDs. Pre-treatment with the ROS scavengers *N*-acetyl cysteine and vitamin E reduced ROS generation and apoptosis suggesting that toxicity is initiated by ROS levels. Taken together, this suggests that unshelled CdSe QDs generated ROS and stressed the cells, which initiated pathways associated with apoptosis to prevent further damage to tissue.

Toxicological studies with CdTe QDs have also shown ROS generation and release of free cadmium [40-42]. Acute exposure to CdTe QDs (≤ 10 μ g/ml, prepared

¹Tetrahydrofuran (THF) was used in the solubilization of these QDs. The toxicity of THF-solubilized fullerene (C₆₀) has been attributed to the THF degradation product, γ -butyrolactone [43]. Up-regulation of antioxidant pathways by THF-C₆₀ and THF-water are consistent with the oxidative injury (lipid peroxidation) reported in other studies [44, 45].

without THF) generated ROS and induced apoptotic signaling pathways in rat pheochromocytoma and human breast cancer cells [40-42]. Cho and colleagues [42] suggest that the combination of free cadmium and ROS induced cell death. Exposure to photo-oxidized mercapto-propionic acid-, cysteamine-, or *N*-acetyl cysteine-capped CdTe QDs resulted in elevated levels of free cadmium (3.77 - 5.62 μM) and significantly decreased metabolic activity. Although irradiated mercapto-propionic acid-CdTe QDs generated singlet oxygen, QDs coated with the antioxidant *N*-acetyl cysteine did not, suggesting that cadmium acted by an alternate pathway to alter metabolic activity. Cd has been known to cause non-ROS related metabolic dysfunction by altering osmotic/ionic imbalance and energy production processes/strategies [46-48].

Gagné *et al.* [49] explored the effects of free Cd^{2+} from QDs by exposing rainbow trout hepatocytes to aged cysteamine-CdTe QDs. Both QDs (aged 2 months and 2 years) were cytotoxic in acute aqueous exposures (48-hr, $\leq 250 \mu\text{g/ml}$). Metallothionein and heat shock protein 72 were also significantly increased at concentrations of 2-250 $\mu\text{g/ml}$. While lipid peroxidation was minimally decreased with 2-month old QDs, there was a significant dose-dependent decrease in lipid peroxidation with 2-year old QDs. Researchers concluded that while labile cadmium was responsible for some of the

toxicity, QD properties such as surface charge and size may have also contributed to toxicity.

Pharmacokinetic Studies

Rodent pharmacokinetic studies have concluded that the kidney, liver, and spleen are the primary sites of QD deposition [22, 50-53]. Though the route of exposure was not environmentally-relevant (injection), the deposition pattern is similar to that of bulk cadmium in fish [54-58]. In Sprague-Dawley rats, mercapto-undecanoic acid-coated, lysine-crosslinked (LM) and bovine serum albumin-coated (BSA) CdSe/ZnS QDs were cleared from the plasma quickly, 0.84 ± 0.3 ml/min/kg for LM-QDs and 1.22 ± 0.2 ml/min/kg for BSA-QDs. There was minimal binding to blood components such as erythrocytes. The QDs were sequestered primarily in the liver, but were also found in the spleen, lung, bone marrow, and lymph nodes. Further examination revealed the QDs were localized to the liver sinusoid or trapped in Kupffer cell vesicles [51].

In Balb/c *nu/nu* nude mice (immunodeficient, T-cells absent) injected with CdSe/ZnS QDs coupled to target-specific peptides, mononuclear phagocytes of the reticuloendothelial system removed the QDs from circulation and deposited them in the liver and spleen. Additional studies revealed that accumulation was reduced by 95%

when the QDs were coated in polyethylene glycol (PEG), thus minimizing the phagocytes ability to detect the invading particles [22]. In Balb/c mice, CdSe/ZnS-PEG QDs were deposited in liver, bone marrow, and lymph nodes, and the fluorescent signal was visible for at least 1 month post-injection [50]. CdSe/CdS-PEG QDs were also deposited in the lymphatic system [52]. Light and fluorescence microscopy of hematoxylin stained frozen spleen sections revealed that the QDs were concentrated in the vacuoles of phagocytic cells [50].

In studies conducted by Yang *et al.* [53], ICR mice administered CdTe/ZnS-mPEG QDs had the same distribution patterns with spleen, liver, and kidney being the predominant sites of deposition. The plasma half-life suggested that the QDs did not bind with red blood cells. Light and fluorescence microscopy of paraffin embedded sections revealed that the QDs (fluorescent red granules) were deposited in vascular-rich areas in the organs including the linings of the hepatic sinusoids, red pulps of the spleen, renal vessels, and glomerular vasculature of the kidneys. Pathological examination showed no microscopic abnormalities in the liver and kidneys; however, sinusoidal congestion and multinucleated giant cells were observed in the spleen.

In each of these rodent model studies, elimination was virtually non-existent. In one study, QDs were only minimally detected in urine (0.01-0.04%) up to 28 days post-exposure with no detection in the feces [53]. In another, fluorescence in the intestine suggested metabolism by the liver and excretion; however, fluorescence was detected *in vivo* for at least 4 months [50] signifying that elimination of these potentially harmful metallic clusters was very slow and/or that QDs were subject to re-uptake and enterohepatic circulation. Conversely, QD excretion (as whole QDs or Cd²⁺) did not occur in either urine or feces during a 10 day study suggesting that sequestration, not metabolism or excretion, occurred [51].

Keeping in mind that the pharmacokinetic studies previously mentioned utilized injection as the means of exposure, toxicity should differ when exploring environmentally-relevant pathways of exposure. Dermal *in vitro* studies suggest skin penetration depends on the surface charge [59]. Recent studies have confirmed that consumed CdSe/ZnS QDs are degraded by enzymes in the digestive tract [60], suggesting that QD toxicity will manifest as Cd toxicity. Additional *in vivo* studies employing environmentally-relevant exposure routes are needed to clarify uptake, depuration, and toxicological effects of QDs.

Ecotoxicity

While screening via cell culture provides rapid assessment for toxicity, these studies show only a snap-shot of what is occurring. *In vitro* studies do not encompass the multitude of pathways, defensive cascades, and feedback loops affected by a chemical insult. Currently, there are a limited number of *in vivo* studies regarding QD (CdSe, CdTe, and CdS) toxicity. In freshwater mussels (*Elliptio complanata*) CdTe QDs deposited to the gill > digestive gland > gonad and caused oxidative stress, immune system dysfunction, and genotoxicity (24 hrs, $\leq 8 \mu\text{g/ml}$) [61, 62]. Lipid peroxidation was significantly elevated, while metallothionein was significantly reduced in the gills at a concentration of $8 \mu\text{g/ml}$. Conversely, the digestive gland had a dose-dependent decrease in lipid peroxidation and significantly elevated metallothionein at 1.6 and $4 \mu\text{g/ml}$ QD. Phagocytic ability and hemocyte viability were significantly reduced at all concentrations tested (1.6, 4, and $8 \mu\text{g/ml}$). Investigators attributed the effects to the release of free cadmium and colloidal interactions (aggregates). While individual QDs are thought to go undetected by the body's defense system, at higher QD concentrations where aggregation is increased, gill filaments trap and pass the particles to the digestive system. Gill damage (i.e. elevated lipid peroxidation) likely occurred due to the decrease in immune response; however, damage in the digestive gland was probably circumvented by the increased metallothionein levels.

1.5.2 Toxicity of Quantum Dot Components

1.5.2.1 Cadmium

As previously mentioned, coated and uncoated QDs leach cadmium ions under various environmental conditions. Cadmium (bulk) has been associated with oxidative stress, behavioral abnormalities, neurotoxicity, nephrotoxicity, genotoxicity, teratogenesis, and carcinogenesis. Because cadmium has multiple targets, determining the mechanism of toxicity has proven difficult. The prevailing mechanism of action is substitution. Transition metals—those in groups 3 through 12 on the periodic table—have similar physico-chemical properties (size, 2s electrons, ionization potential), which allows them to be substituted in place of one another in proteins and enzymes.

Cadmium has the ability to mimic and/or displace other divalent cations such as Cu, Fe, Ca, and Zn. One example is the exchange of Cd for Zn in metallothionein. In Cd exposed organisms, the metal is bound to albumin, an abundant plasma transport protein, and transported to the liver where it is conjugated to glutathione for excretion via the bile or bound to metallothionein [63]. Metallothionein (MT)—a low-molecular weight protein containing thiol groups—binds, transports, stores, and regulates metal ion concentrations in organisms. Consequently, exposure to cadmium induces metallothionein synthesis [64-68]. Zinc is displaced from metallothionein by cadmium,

and the increase in free zinc ion levels signals for the up-regulation of metallothionein [67].

Uptake and Deposition

Uptake and deposition of bulk Cd is dependent on the route of exposure. When injected (i.v. injection in the tail or jugular vein of rodents versus i.p. injected in fish), the deposition pattern of free cadmium in fish is similar to that of CdSe/ZnS QD-injected rodents. Rodents accumulated Cd in the liver, kidney, and spleen [51, 53], whereas rainbow trout (*Oncorhynchus mykiss*, formally *Salmo gairdneri*) accumulated Cd²⁺ in the liver, kidney, and gills [57]. Though the trout only retained about 37% of the intended dose, elimination of the remaining cadmium was extremely slow. There was no loss of Cd from the organs 98 days post-injection [57]. Similar conclusions regarding elimination were drawn in the QD rodent studies.

Currently there are very few publications regarding oral/dietary exposure of organisms to QDs. Karabanovas *et al.* [60] reported that CdSe/ZnS QD suspensions in fat or sonicated in water crossed the esophagus in Wistar rats. Photoluminescence was detected in the internal and external walls of the esophagus 30 minutes post-exposure. While the photoluminescent spectra were not detectable in the esophagus, stomach,

duodenum, or small intestine at 1 hour post-exposure, the left-shift (bluing) in the peak wavelength after 30 minutes suggests degradation occurred in the stomach, most likely due to the acidic environment. No data was collected regarding cadmium concentrations, so uptake and deposition patterns could not be discerned.

Despite the lack of distribution information from dietary QD studies, exposure of fish to dietary Cd suggests that uptake from ingestion is limited and will result in little toxicological risk. Rainbow trout that were fed 500 mg/kg Cd for 28 days retained less than 1% of the dose from the diet (40% in the kidney and liver and 20-35% in the stomach and intestine) [55]. Similarly, an infusion of Cd²⁺ (0.1617 mg/kg) into the stomachs of rainbow trout resulted in only 2.4% of the dose diffusing across the gut wall, while 17% remained in the gut tissue and 27% in the lumen [69]. Given that our study involves dietary QD uptake, Cd is expected to accumulate in the gastrointestinal tract and traces may be detected in the liver.

Fish embryos can also be exposed to free cadmium *in ovo* through a process referred to as maternal transfer [70, 71]. In 1980, Shackley *et. al.* [71] reported that natural populations of blennies (*B. pholis*) collected from intertidal pools in Mumbles Head, U.K. showed an increase in gut cadmium levels from March to July, which

coincides with the spawning period. The liver and ovaries accumulated Cd from March to April, but the metal concentration decreased from April to May. The investigators theorized that the lost cadmium was transported from the liver to the oocytes via the yolk as a way of eliminating the metal from the body.

Sellin and Kolok [70] later reported that larval fathead minnows (*Pimephales promelas*) exposed *in ovo* to aqueous Cd (0-100 µl/l) displayed a positive trend in cadmium body content with increasing maternal exposure concentration. Though reproduction (spawning rate, clutch size, fertilization rate, and hatch rate) was not negatively impacted, larval mortality was significantly increased at concentrations of 25 and 100 Cd µg/l. The mechanism for maternal transfer was confirmed when *in vitro* studies reported that vitellogenin (VTG), the egg yolk protein precursor, bound cadmium by displacing calcium and zinc [72]. When the VTG-Cd complex was injected into female Atlantic croaker (*Micropogonias undulatus*), 69% was incorporated into the ovaries within 48 hours versus free cadmium (26%). This suggests that vitellogenesis mobilizes Cd accumulated in the liver by binding to vitellogenin and moving it to the ovaries for sequestration to the eggs.

Toxicological Effects of Cd

It is well known that cadmium can generate ROS [73, 74]. Although it is not a Fenton metal and cannot directly generate ROS, Cd displaces Fenton metals such as iron and copper from intracellular proteins such as ferritin or apoferritin, thus indirectly causing the generation of superoxide anion, hydroxyl radicals, and hydrogen peroxide (for reviews, see [75, 76]). Generation of ROS can lead to oxidative imbalance, otherwise known as oxidative stress. Section 1.5.3 discusses the effects of oxidative stress in more detail.

Antioxidant levels, though tissue- and species-dependent, are affected by cadmium exposure. Basha and Rani [77] evaluated superoxide dismutase, xanthine oxidase, glutathione peroxidase, and catalase in tilapia exposed to 5 µg/ml CdCl₂—one tenth of the 48-hour LC₅₀ value. The liver and kidney tissues of the sub-chronically exposed tilapia (*Oreochromis mossambicus*) were collected at sacrifice on days 1, 7, 15, or 30. For both organs, there were significant increases in all antioxidant enzyme levels from day 7 through day 15, followed by a decrease at day 30 that still remained above control levels. Studies employing juvenile tilapia (*Oreochromis niloticus*) chronically exposed to 0.35-3.0 µg/ml CdCl₂ reported that liver superoxide dismutase was significantly increased at all concentrations. Liver glutathione peroxidase was increased

at 1.5 and 3.0 $\mu\text{g/ml}$ CdCl_2 , and lipid peroxidation levels were significantly reduced when the glutathione peroxidase levels were at their highest. Although white muscle showed increased superoxide dismutase and glutathione peroxidase levels at all concentrations tested, superoxide dismutase was depleted in red muscle at 1.5 and 3.0 $\mu\text{g/ml}$ cadmium. Therefore, white muscle was effectively quenching ROS as evidenced by the lack of lipid peroxidation at all concentrations despite 60 days of continuous exposure [78].

DNA damage and impairment of repair mechanisms have been noted in response to Cd exposure [66, 79-81]. Dally and Hartwig [79] found that HeLa cells incubated with 1, 5, 10, or 50 μM CdCl_2 for 5 hours caused a significant increase in the number of DNA strand breaks at 10 and 50 μM Cd. No DNA lesions (adducts) were reported. Further investigation revealed that Cd affected the ability of the nucleotide excision repair machinery to recognize and/or excise light-induced DNA damage at low, non-cytotoxic concentrations ($< 25 \mu\text{M}$ CdCl_2) by causing a dose-dependent reduction of protein binding to DNA [79, 80]. ZnCl_2 was able to restore binding (DNA-protein interactions) and repair the DNA. This suggests that cadmium's ability to displace Zn at critical binding motifs is responsible for altering the functioning of nucleotide excision repair machinery [80]. In the case of base excision repair dysfunction, cadmium

essentially hinders the expression, protein translation, and catalytic ability of an essential DNA repair enzyme, 8-oxoguanine-DNA glycosylase [81].

Cadmium can affect regulatory gene expression during embryonic development resulting in teratogenesis. Zebrafish embryos (*Danio rerio*) exposed to 1-1000 μM CdCl_2 for 18 hours showed a wide range of morphological deformities, specifically cranial hypoplasia, hypopigmentation, heart edema, yolk sac abnormalities, spinal curvature, and tail alterations. Additional studies found that embryos exposed to 100 μM CdCl_2 had altered expression of select genes including sonic hedgehog (*shh*), even-skipped (*eve1*), and no tail (*nt1*) in the malformed areas [82]. Examination of embryos displaying spinal curvature revealed misshapen myotomes [82, 83], while immunostaining showed a 45.3 - 74% decrease in the motor protein myosin [82]. Markers for fast and slow muscles showed a significant loss of fast muscle fibers in areas of axial curvature. *In situ* hybridization with *myoD* showed myogenic cells developing in place of somitic cells and expressing *myoD* in areas of the tail region where a notochord failed to develop [83]. Studies also found that cadmium-treated embryos experienced stunted growth in primary and secondary motor neurons. Motor neuron axon extension into myotome regions was limited in embryos with and without trunk malformations [83]. Chan *et al.* [84] noted that embryos treated with 100 μM CdCl_2 possessed a significantly increased

number of apoptotic cells (2440 ± 1764 cells/embryo vs. 94 ± 54 cells/embryo in Controls), and the location of these apoptotic cells corresponded to areas with morphological abnormalities.

Larval behavior of fry exposed to Cd during embryonic development is also altered. In touch tests, Cd-treated zebrafish embryos displaying abnormal skeletal curvature did not display typical coiling or avoidance behaviors. Treated embryos without abnormal axial curvature still experienced reduced coiling activity and were slow to swim away from the stimulus [83]. These diminished or absent tactile responses could be attributed to muscle loss and the lack of motor neuron extension previously described.

1.5.2.2 Selenium

Selenium, in contrast to cadmium, is an essential micronutrient. Selenium is biotransformed to selenophosphate and then used to synthesize selenoproteins. Selenomethionine can be substituted into proteins for methionine, and selenocysteine is a co-factor for glutathione peroxidase [63]. However, at elevated levels selenium causes teratogenesis and neurotoxicity [85]. Effects of selenosis—high selenium levels—in adult fish include gill swelling, increased immune response, anemia, cataracts, popeye,

edema, and reproductive failure [86, 87]. While mechanisms of selenium toxicity are still being evaluated, two prominent hypotheses have emerged: (1) thiol substitution of Se for S, and (2) generation of ROS.

Uptake and Deposition

Selenium uptake in fish is a function of chemical speciation, species, and gender. Inorganic forms of selenium include elemental selenium (Se^0), selenides (Se^{2-}), selenite (Se^{4+}), and selenate (Se^{6+}), while organic forms include selenomethionine, selenocysteine, and selenophosphate. Kleinow and Brooks [88] reported that dietary selenomethionine accumulated to a greater extent in fathead minnow than selenite (SeO_3) or selenate (SeO_4). Regardless of the form, Se deposited preferentially to the liver. The heart was the secondary site of selenomethionine deposition, while inorganic forms of Se deposited in high concentrations to the kidney and digestive system. Although the distribution pattern of inorganic Se is consistent with the work of Hilton *et al.* [89] and Sato *et al.* [90], others have reported that Se deposits primarily to the gonads [91-93]. Baumann and Gillespie [91] found that in natural fish populations, females had large amounts of Se in the ovaries, while testis did not. This may be because in reproductively-active females, Se (mainly in the form of selenomethionine) is

redistributed after the initial uptake and sequestered to the ovaries for ovo-deposition [88, 91-93].

Toxicological Effects of Se

Selenium has the ability to generate ROS including superoxide and hydrogen peroxide (for reviews see [94, 95]). The generation of these species is thought to occur via thiol oxidation. Ironically, Se-generated ROS are enhanced by the addition of excess glutathione [96, 97]. Shen *et al.* [98] noted that HepG₂ cells (human hepatoma) experienced a dose- and time-dependent depletion of intracellular glutathione when exposed to 10 μ M Na₂SeO₃. Shen *et al.* [96] later reported that while HepG₂ cells exposed to selenite showed increased generation of ROS, co-treatment with selenite and glutathione more than doubled the amount of ROS generated. This is because various forms of selenium can oxidize glutathione to form selenodiglutathione (GS-Se-SG) instead of GSSG. Selenodiglutathione has the ability to oxidize a cysteine residue of thioredoxin [99]—a ubiquitous oxidoreductase enzyme responsible for reducing proteins [100]. While thioredoxin reductase or glutathione reductase can directly reduce selenodiglutathione, the oxidation of thioredoxin inhibits it from functioning properly [99, 100].

As mentioned previously, antioxidant levels are affected by exposure to selenium; however, the toxicological effects are species-dependent. In juvenile rainbow trout, acute aqueous exposure to selenite (0- 3.60 mg/l for 96 hr) caused a significant depletion of glutathione stores at concentrations of 2.52 and 3.60 mg/l. Although lipid peroxidation levels fluctuated, they remained at or below normal levels despite increasing Se concentrations [101]. Similarly, in studies involving male Kunming mice, glutathione peroxidase and glutathione-s-transferase levels were significantly increased, while reduced glutathione levels were significantly depleted by dietary selenite or Nano-Se (elemental) (0-6 mg/kg, 12 days). Superoxide dismutase and catalase activities were significantly decreased by dietary selenite, but not Nano-Se. At a dietary dose of 6 mg/kg Se, hepatic lipid peroxidation levels were significantly reduced by Nano-Se and significantly increased by selenite [102]. This illustrates that selenite has a greater propensity to cause oxidative imbalance than Nano-Se.

As with cadmium, selenium has been linked to DNA damage and repair inhibition. Acute exposure of mouse L1210 cells (leukemia) to 0-10 μ M selenite resulted in increased single and double DNA strand breaks [103]. Zhou *et al.* [104] confirmed that selenite was able to cause chromosomal strand breaks in HL-60 cells, while selenocysteine and selenomethionine did not. Studies examining the ability of inorganic

selenium to alter DNA repair in U₂OS cells (human osteosarcoma) revealed that low concentrations of SeO₃ (0.01- 10 μM) significantly decreased DNA repair via the transcription coupled repair pathway. It was suggested that selenium substituted for the sulfur in the sulfhydryl group of DNA repair proteins, thus altering their structures and subsequent catalytic activities [105]. Alternately, Blessing *et al.* [106] hypothesized that selenium-containing compounds were able to oxidize thiol groups of proteins causing a release of zinc from binding motifs and altering the enzymatic activity of the DNA repair enzymes formamidopyrimidine-DNA glycosylase (FPG) and xeroderma pigmentosum group A (XPA). While FPG activity was not affected by up to 1 mM selenomethionine, it was significantly reduced (~90%) by 150 μM selenocysteine during *in vitro* assays involving DNA from the marine bacterium *Alteromonas espejiana*. XPA binding to DNA was also affected by selenocysteine, possibly through thiol oxidation and disulfide bond formation. Selenocysteine caused a dose-dependent increase in free zinc with treatment with as low as 6 μM selenocysteine causing a release of zinc from the XPA-zinc finger.

Despite the varied reports that fish accumulate large amounts of Se in the ovaries, reproduction (spawning frequency, clutch size, and hatchability) does not seem to be significantly altered by high Se burdens [92, 93, 107-109]. However, larval

mortality and incidences of morphological abnormalities are increased by selenium whether parentally- or environmentally-exposed [107, 108, 110]. Adult fathead minnows aqueously exposed to SeO_3 or SeO_4 transferred selenium to their offspring resulting in lordosis and edema [107, 110]. Parental dietary exposure of bluegills (*Lepomis macrochirus*) to selenite and selenomethionine resulted in fry with skeletal and jaw abnormalities. Fry also experienced a decrease ability to swim up, or surface for food once the yolk sac was absorbed [111]. Sacramento splittail embryos (*Pogonichthys macrolepidotus*) acutely exposed to 0, 5, and 15 $\mu\text{g/ml}$ selenite displayed scoliosis, kyphosis, lordosis, and tail loss [108]. Other teratogenic deformities observed in natural populations of fish from selenium-contaminated waters include missing or deformed fins, gills, gill covers, and eyes [86]. The hypothesized mechanism of embryonic malformation is the substitution of selenium for sulfur during amino acid and protein synthesis and disruption of disulfide bonds resulting in impaired musculo-skeletal development [108].

1.5.2.3 Lecithin

Lecithin, also referred to as phosphatidylcholine, is a phospholipid found in biological membranes and acts as natural surfactant (for review, see [112]). It is derived from egg yolk and soy, and is found in all organisms. It is used in foods as an

emulsifying agent, in pharmaceuticals as a drug delivery device, and in cosmetics as a skin-conditioning and emulsifying agent. Lecithin has also been used as a medicinal supplement to lower cholesterol and triglyceride levels [113, 114].

Encapsulation technique

Lecithin is composed of a large polar head and two non-polar hydrocarbon chains (Fig. 1-5). The hydrocarbon chains vary in length, but are usually between 12 and 18 carbons in length with varying degrees of saturation [115]. While Lecithin is insoluble in water, it organizes to form monolayers when dispersed in organic solvents such as toluene and chloroform. Micelles spontaneously form in solution when the threshold surfactant concentration is reached or surpassed—known as the critical micelle concentration.

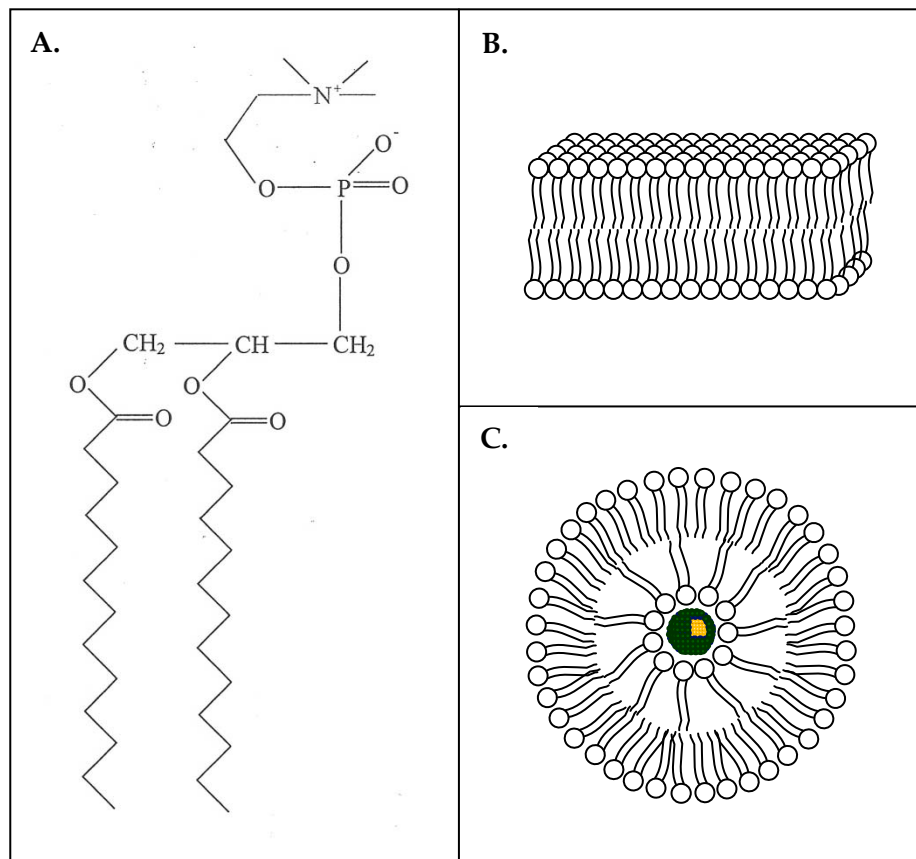


Figure 1-5. The structure of (A) Lecithin, (B) a lipid bilayer, and (C) a cross section of a liposome.

Various methods have been devised to create phospholipid vesicles—liposomes—in aqueous solution [116-120]. Briefly, the lipids are mixed in organic solvent for a period of time after which the solvent is removed under a stream of nitrogen gas. The remaining film is dispersed in water via shaking and sonication to yield multilamellar vesicles and small unilamellar vesicles [112]. Nanoparticles or other

materials such as pharmaceuticals can be incorporated into the internal space of the vesicles if added to the solution prior to sonication or stirring. Gold nanoparticles have already been successfully rendered water-miscible using Lecithin [121].

Toxicological Effects of Lecithin

Only a limited number of human, animal, and ecological toxicological studies have been conducted with Lecithin. Reports confirm that it is neither a reproductive, nor developmental toxicant; evidence also suggests it is not mutagenic [122]. Mice (Webster-derived CD-1) receiving a single injection of 150 μ L of soybean Lecithin (20% w/w phosphatidylcholine) showed no behavioral or toxicological effects 15 days post-injection [123]. Pikeperch (*Sander lucioperca*) exposed via diet to increasing amounts of soybean Lecithin (1.4, 4.7, and 9.5% of dry matter) showed significantly improved growth and no change in the percentage of larva with deformities [124]. White-leg shrimp (*Penaeus vannamei*) fed diets supplemented with 1.5% soybean Lecithin also had significantly improved growth as well as a reduced sensitivity to osmotic stress [125]. Thus, in the absence of sufficient toxicological data, the Food & Drug Administration regards Lecithin as safe for human consumption as long as good manufacturing processes are upheld [126].

1.5.3 Oxidative Stress

Oxidative stress is a condition that occurs when an organism is experiencing an imbalance in pro-oxidant and antioxidant processes. The ROS that is generated by contaminants can bind to enzymes and proteins causing abnormal activity or complete dysfunction. ROS can also disrupt membranes through lipid peroxidation. Basal levels of antioxidants such as superoxide dismutase, catalase, and glutathione are available to neutralize endogenous sources of ROS (Fig. 1-6), but these levels are tissue- and species-dependent. Exogenous sources of ROS induce upregulation of these protective enzymes. If the oxidation and subsequent damage overwhelms the organism's defenses, oxidative stress occurs.

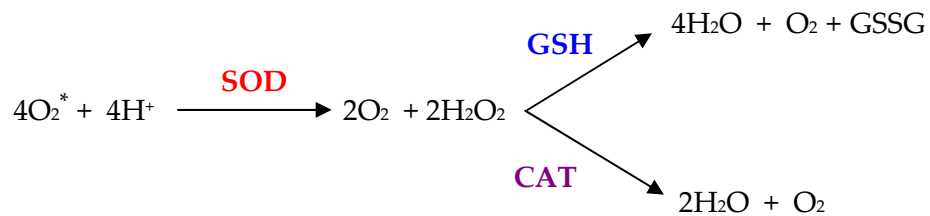


Figure 1-6. Conversion of reactive oxygen species via SOD, CAT, and GSH.

Glutathione levels can be an indicator of oxidative stress. The sulfhydryl groups in GSH are responsible for reducing radicals. The accumulation of oxidized glutathione

(GSSG) and a subsequent increase in the GSSG/GSH ratio is indicative of an organism suffering from oxidative stress. If glutathione reductase doesn't efficiently return the enzyme to its reduced form, the increased GSSG levels leads to increases in the number of protein-mixed disulfides (protein-SSG) [127]. Female C57BL/6J mice injected with 5 µg/kg/day 2,3,7,8-tetrachlorodibenzo-p-dioxin exhibited elevated GSSG levels after 1 week of treatment and elevated protein-glutathione mixed disulphide levels after 8 weeks of exposure [127]. When a critical thiol of an enzyme, protein, receptor, or signaling molecule is compromised, it will not function properly and will be targeted for degradation [128]; alterations in proteins responsible for proliferation regulation (Fos, Jun, PKC, etc.) could lead to carcinogenic lesions [127].

Lipid peroxidation (LPO) also serves as a biomarker for oxidative stress. It occurs when ROS attack lipids, such as those found in biologic membranes, and antioxidants are unable to quench the reaction. LPO propagates the oxyradical cycle through its by-products malonaldehyde and 4-hydroxynonenal, which in turn causes enzyme inhibition, DNA damage, protein modification, and more [129-132].

Reactive Oxygen Species

ROS (superoxide anion radical, hydroxyl radical, peroxy radical, alkoxy radical, hydroperoxyl radical, hydrogen peroxide, singlet oxygen, and peroxynitrite) are frequently generated in organisms by endogenous sources—xanthine oxidase, nitric oxide synthase, fatty acid oxidase, metals, and the electron transport chain. A basal amount of ROS is biologically necessary; it is utilized by phagocytic cells as a weapon against invading microbes, as second messengers in signaling cascades, and in cellular respiration (oxidative phosphorylation). Exogenous substances known to generate ROS include quinones, polycyclic aromatic hydrocarbons, polychlorinated biphenyls, brominated flame retardants, dioxins, estrogenic compounds, and metals such as Fe, Cu, Cr, and Se. For reviews, see [128, 133-136]. While the body has the means to manage exogenous sources of ROS, the insult can overwhelm antioxidant resources (superoxide dismutase, catalase, glutathione, glutathione peroxidase, and vitamin E) leading to inhibition of enzymes, alteration of appropriate cellular signaling, and damage to biological macromolecules.

The response to ROS is a function of cell, tissue, or species type as well as being time- and concentration-dependent [137]. Low levels of oxidants (3-15 μM H_2O_2) actually stimulate growth in cells (HA-1 cell line, Chinese hamster ovary fibroblasts)

because the oxidant acts as a cellular proliferation signal. Moderate levels can cause senescence (120-150 $\mu\text{M H}_2\text{O}_2$) or permanent growth arrest (250-400 $\mu\text{M H}_2\text{O}_2$). This keeps DNA from being uncoiled and replicated in its damaged state [137]. Apoptosis and necrosis are exhibited at the highest concentrations of ROS (0.5 mM to 10mM H_2O_2) [129, 138, 139]. Apoptotic signaling does not cause inflammation or result in additional oxidative damage, whereas, necrosis leads to the demise of surrounding cells and further perpetuates the ROS cycle.

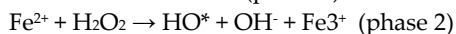
Studies have reported that QDs and/or their degradation components generate reactive oxygen species [38, 40-42]. Free cadmium ion indirectly generates superoxide anion, hydrogen peroxide, and hydroxyl radicals by displacing metals (from proteins) that can generate ROS when labile [73-76]. Selenium generates superoxide anion and hydrogen peroxide via thiol oxidation [94, 95]. Thus, QDs through the generation of ROS have the potential to: cause DNA damage, incorrectly activate or inactivate enzymes, alter antioxidant levels, modify cellular signaling, and affect embryonic development. The remainder of this chapter is dedicated to reviewing the toxicological effects of other contaminants that generate ROS to identify targets of ROS that should be studied with *in vivo* QD exposures.

DNA Damage

Exposure to ROS has been linked to DNA damage such as adducts, strand breaks, base modifications, and cross-links. ROS reacts with proteins, nucleic acids, sugar moieties, and the phosphate backbone resulting in structural and functional modifications that can affect transcription and translation. For reviews, see [136, 140-142].

When ROS are accompanied by Fenton metals², the damage is increased. Metals can modify the strand structure by bringing the components closer together, thus facilitating the formation of ionic and covalent bonds (cross-linking). It may also enhance base oxidation [143]. Exposure of salmon sperm DNA to hydrogen peroxide and the metals Cu, Fe, or Ni caused intrastrand cross-links, adducts, and strand breaks (both single and double). The reduction of H₂O₂ by the metals led to the formation of hydroxyl radicals [144]. Similarly, the hydroxyl radicals generated in the livers of male Fischer rats after exposure to the arsenical metabolite trimethylarsine oxide (1.47 mM, 20 days) caused DNA adducts and substantially elevated expression of the repair enzyme

²Fenton metals are reduced (gain an electron) during the first phase of the Fenton reaction, when superoxide anion is converted to oxygen. The metal loses the electron when it is oxidized by H₂O₂ for form a hydroxyl radical [145]. The Fenton reaction: $^*O_2 + Fe^{3+} \rightarrow O_2 + Fe^{2+}$ (phase 1)



8-oxoguanine-DNA glycosylase [146]. In some instances, exposure to chelating agents, such as EDTA, prior to the insult decreased DNA damage [144, 147].

Industrial chemicals can also cause DNA damage through the generation of ROS. Wang and colleagues [147] showed that the carcinogen 4-aminobiphenyl and its isomer 2-aminobiphenyl caused single strand breaks and alkali-labile sites in HepG₂ cells by generating H₂O₂. Pre-exposure to iron and copper chelating agents (desferrioxamine and neocupronine, respectively) decreased DNA damage. This suggests that ions are involved in the formation of the strand breaks.

Enzymes

Pharmaceuticals given for their therapeutic effects can alter enzymes as a result of oxidative stress. Acetaminophen has been shown to generate superoxide anion in Swiss mice that were given a single injection (375 mg/kg). Consequently, the mice suffered from elevated liver enzymes (lactate dehydrogenase, alanine aminotransferase, and aspartate aminotransferase) signifying that damage had occurred. Antioxidant levels and activities were also compromised [148].

As briefly mentioned, the by-products of lipid peroxidation can cause inhibition of enzymes. Thioredoxin is an antioxidant enzyme that inhibits ASK-1 (apoptosis), activates NF- κ B (cell survival), has the ability to refold proteins, and can reduce ROS by providing a disulphide complex [149, 150]. Thioredoxin reductase is responsible for returning it back to thioredoxin for further reactions. However, the LPO by-product 4-hydroxynonenal has been linked to the inactivation of thioredoxin reductase (in conjunction with the inactivation of the tumor suppressor p53), thus the ability of the cells to combat the oxidant imbalance is compromised [132].

The activity of Protein Kinase C (PKC), an enzyme that mediates growth, proliferation, differentiation, and expression by phosphorylating various proteins in signaling cascades [151, 152], can be altered by ROS. Modification of PKC's regulatory or catalytic domains as a result of increased ROS levels can cause abnormal activation or inactivation of the enzyme. The enzyme's binding domain contains a zinc-finger that is susceptible to oxidation. When it is compromised, DNA cannot bind properly to the domain [153, 154], thus altering the necessary signaling for growth, proliferation, differentiation, or apoptosis.

Antioxidants

Antioxidant levels fluctuate in response to oxidative insults and enzymatic damage. Studies using Caco-2 cells (human colon carcinoma) noted that administration of hydrogen peroxide (50-250 μM) induced an antioxidant response. The cells responded to the oxidative imbalance with an increase in catalase activity at all concentrations and in increase in glutathione peroxidase activity at concentrations ≥ 150 μM H_2O_2 . Superoxide dismutase activity was elevated at lower H_2O_2 concentrations (50 μM), but was significantly inhibited at higher concentrations (≥ 150 μM). Investigators hypothesized that the inhibition of SOD at higher concentrations could be occurring as a result of oxidative damage at a key histidine site or structural alterations that might restrict binding [155].

Cellular Signaling

Oxidative stress can trigger the activation of a variety of signaling cascades responsible for growth, proliferation, differentiation, apoptosis, necrosis, or survival. The exact pathway is determined by factors such as the type of toxin, concentration, duration of exposure, and tissues type. AP-1, NF- κB , myb, p53, HIF-1, and NFAT are a few of the transcription factors that are activated by elevated levels of ROS levels. Other

responses to oxidative stress include kinase phosphorylation, altered gene expression, and caspase cleavage. For reviews, see [132, 138, 149, 150, 156-158].

Kinase phosphorylation is one response to oxidative stress. Two genes that are phosphorylated in response to oxidants, mitogen-activated protein kinases (MAPKs) and PKC, show dual redox-activities and can signal for death or survival [157, 159]. MAPKs are a family of serine/threonine protein kinases that are responsible for transmitting various signals into the nucleus of the cell. Types of MAPKs that have redox-sensitive sites include: (1) extracellular signal-regulated kinases (ERK), which is involved in cellular proliferation, differentiation, and development; (2) JNK, which can cause apoptosis; and (3) p38 mitogen-activated protein kinases (p38 MAPK), which is associated with cell differentiation and apoptosis [160]. Phosphorylation of ERK has been linked with both pro- and anti-apoptotic signaling [161]. Researchers suggest that the actions of ERK are mediated by the duration of the oxidant exposure; transient ERK activation leads to survival, whereas, prolonged activation causes growth arrest and apoptosis [137].

The pathways activated by ROS are a network of competing interests, survival and growth versus arrest and cell death. Moreover, cross-talk and redox-sensitive steps

in each pathway can cause contrasting results. In the study conducted by Turner *et al.* [162], investigators suggested that oxidative stress had activated three distinct pathways based on their findings: (i) MEK-1/2 and ERK-1/2; (ii) MKK-4, JNK, c-Jun, and ATF-2; and (iii) MKK-3 and p38 MAPK. In this scenario, ERK activation seemed to be associated with necrosis, while JNK phosphorylation led to apoptotic death and p38 activation caused senescence. In reviewing the oxidative stress literature, Martindale and Holbrook [157] felt that there was a balance between ERK and JNK activity, and alteration of this balance would determine cell survival. They also noted that pathways had check points in redox-signaling that measure changing levels of ROS and respond accordingly.

Table 1-1 shows the progression from anti-apoptotic to apoptotic cell signaling as hydrogen peroxide concentrations are increased *in vitro*. Exposure to oxidants at low concentrations or for short durations increased antioxidant levels. H₂O₂ and 4-hydroxynonenal (LPO by-product) activate transcription factors that phosphorylate various kinases, such as PKC and PKD, resulting in cell stabilization because they signal for increased production of glutathione or other antioxidants to prevent further oxidative injury [163-165]. Anti-apoptotic signaling also occurs to assist in saving the

cells. Phospholipase C- γ 1(PLC- γ 1, cell motility) is a pro-survival pathway that inhibits or suppresses apoptosis [157, 166].

Table 1-1. Signaling cascades affected by H₂O₂ exposure.

Cell line	Conc. (μ M)	Effect	Ref.
HeLa	10	Transient \uparrow PKD	[164]
HeLa, Rat1, NIH 3T3, PC12	50 200	Transient \uparrow ERK2, c-jun, and c-fos; \uparrow JNK	[167]
AR42J	80	\uparrow SOD, glutathione reductase, XPG, NF- κ B, GADD, p53	[168]
Jurkat	100-200	\uparrow PKC and MAPK activity	[169]
H9c2 cardiac muscle	400	Cytochrome c release; casp-3 cleavage; transient \uparrow in JNK	[170]
Swiss 3T3 fibroblasts, COS-7, HeLa, NIH 3T3 fibroblasts	10-500	\uparrow PKD	[171]
Mouse embryonic fibroblasts	0-600	Phosphorylation of PLC- γ 1	[166]
H9c2 cardiac muscle	0-1000	caspase activation; phosphorylation of ERK2, JNK, p38 MAPK, MEK-1/2, MKK-4, ATF-2, c-jun	[162]
COS-7	5000	Activation of all PKC isoforms tested	[154]

Activation of p53 and p38 MAPK are associated with arrest, but also with apoptosis [156, 157, 172]. When an organism experiences oxidative stress at high levels

or for a prolonged period of time and cannot compensate by upregulating the production of antioxidants, then apoptotic signaling usually occurs. This is a protective mechanism which halts the replication of damaged DNA and keeps inflammation from affecting surrounding tissues. Apoptosis consists of cell shrinkage, nuclear condensation, and membrane blebbing [173]. Pro-apoptotic signaling, such as the release of cytochrome c and cleavage of caspases, leads to DNA fragmentation [132, 170].

When the cellular damage from ROS is too extensive, necrotic signaling occurs. Necrosis—uncontrolled cell death—is marked by caspase (pro-apoptotic) suppression [149]. Cellular debris leaking from necrotic cells alters signaling cascades and causes inflammation in the surrounding tissues. This can lead to additional ROS generation and subsequent damage.

Again, signaling pathways are not always linear. A variety of genes and transcription factors have multiple responses, some contradictory. The literature shows that activation of the transcription factor nuclear factor kappa-light-chain-enhancer of activated B cells (NF- κ B) initiates genes associated with immune response, cell growth, survival, and apoptosis [137, 160]. Therefore, exposures to contaminants such as QDs

will need to evaluate multiple points along various signaling pathways to determine how the organism is responding to the oxidative insult.

Developmental Toxicity

Various metals (including Se), pharmaceuticals, and industrial chemicals that generate ROS and cause oxidative stress have been linked with developmental toxicity. Wistar rats that were maternally exposed to aluminum (345 mg/kg/day orally) displayed reduced bone ossification that was reversible with the administration of therapeutic agents glutathione and/or Tiron. A decrease in fetal glutathione and glutathione-s-transferase coupled with an increase in catalase and lipid peroxidation suggests oxidative stress was occurring and may be responsible for the lack of bone ossification [174]. Increased selenium has been shown to affect bone development in birds; altered GSH and GSSG levels as well as increased lipid peroxidation suggests that oxidative stress was the cause of the avian deformities [175].

Tamoxifen, which is used in the treatment of breast cancer, caused an increase in superoxide production and lipid peroxidation in sea urchin embryos (10^{-8} – 10^{-6} M). Embryolethality and developmental defects occurred in a dose-dependent fashion. Examination of oxidative DNA damage (8-OHdG) revealed that genetic damage

occurred at low tamoxifen concentrations, and therefore could be responsible for lethality and mitotic arrest [176].

Nicotine is another substance known to cause developmental abnormalities via oxidative stress. C57BL/6J mouse embryos grown in culture with nicotine (0.6, 1, 3, 6 μM ; 48 hours) showed deformities at the highest two concentrations. Deformities included an open neural tube, smaller forebrain, and underdevelopment of the lower portion of the spine. TUNEL-assays confirmed that apoptosis was occurring at malformation sites. Additional studies with mouse embryos exposed to 3 μM nicotine for 24 hours discovered increased ROS and Ca^{2+} levels in tissues where the malformations occurred. Co-exposure to nicotine and an antioxidant or Ca chelator showed ROS levels and incidences of malformation consistent with Controls [177].

Other compounds including dichloroacetate (a by-product of water treatment processes) [178], diepoxybutane (a metabolite of 1,3-butadiene) [179], and PAH derivatives [180] have also induced morphological deformities attributable to oxidative stress. These studies noted altered levels or activities of antioxidant enzymes, or directly measured ROS production to conclude redox imbalance as the cause of the developmental toxicity.

Conclusions

Quantum dots have the potential to alter biological processes in a variety of ways. Studies have shown that QDs and their degradation components affect ionic homeostasis, genetic stability, oxidative balance, cellular proliferation, and embryonic development. As the study of QDs continues, it is important to scrutinize the composition and stability of QDs in aqueous environments as well as monitor the biological pathways mentioned in this chapter to determine how QDs affect organisms.

Chapter 2. Developmental Toxicity of Aqueous CdSe/ZnS QD Exposure in Teleosts

Reproduced in part with permission from Marine Environmental Research, submitted.

Given the increased production and commercialization of engineered nanomaterials, contamination of aquatic ecosystems is inevitable [181, 182]. Yet virtually nothing is known about the effects of engineered nanoparticles on developing fish. Studies have confirmed that certain types and forms of nanoparticles are bioavailable and can affect embryonic development in fish. Lee *et al.* [183] published that nano-silver was able to diffuse through the chorionic pore canals of developing zebrafish (*Danio rerio*) and subsequently deposit in the retina, brain, heart, gill, and tails. Morphological abnormalities included tail fin truncation, heart malformation, yolk sac edema, head edema, and eye anomalies. This concurs with a study in which zebrafish were exposed to BSA or starch-capped Ag nanoparticles at concentrations up to 100 µg/ml; researchers found that nano-sized Ag depressed heart rates and caused abnormal twisting of the notochord [184]. In contrast, water-stirred C₆₀ (aqua-nC₆₀) did not affect the embryonic development of zebrafish and mummichogs (*Fundulus heteroclitus*) [43, 185]. The lack of morphological abnormalities associated with aqua-nC₆₀ exposure was attributed to aggregation and the adherence of fullerene aggregates to the chorion of the teleost [185]. Similarly, single-walled carbon nanotubes did not alter zebrafish development (conc. < 360 mg/l) because the nanotubes were not bioavailable due to their length. Hatching delays did occur, but were most likely caused by nanotube aggregates that were attached to the chorionic surface, which may have altered embryonic oxygen

levels [186]. Thus, the developmental effects caused by ENPs in fish appear to be a factor of composition and aggregation state.

Fundulus embryos are at risk of encountering QDs in nature. The ionic strength of estuarine water results in the agglomeration and precipitation of engineered nanomaterials from the water column [185, 187]. While the eggs spawned on or buried in the sediment have a protective chorion, fish chorions are pervious to exogenous contaminants including nano-silver [183], polystyrene beads [188], 2,3,7,8-tetrachlorodibenzo-*p*-dioxin [189, 190], and benzo[*a*]pyrene [190]. Morphological deformities arising from Cd exposure include cranial hypoplasia, hypopigmentation, heart edema, yolk sac abnormalities, spinal curvature, and tail alterations [191]. Therefore, the goal of this study was to determine whether aqueous exposure to Lecithin-encapsulated CdSe/ZnS QDs adversely affected the development of *Fundulus* embryos.

Materials and Methods

Chemicals

CdSe/ZnS Evidots (ED-C11-TOL) were purchased from Evident Technologies (Troy, NY, USA). Lecithin (102147) was purchased from MP Biomedicals, Inc. (Solon, OH, USA). Gelatin (G-9382) was purchased from Sigma (St. Louis, MO, USA).

Quantum Dot Preparation

A Mixed QD suspension containing orange (4.0 nm, $\lambda=600$ nm), green (2.4 nm, $\lambda=540$ nm), and blue (1.9 nm, $\lambda=490$ nm) QDs [4] was prepared according to Dubertret *et al.* [192] with slight modifications. QDs were precipitated from toluene using 5 volumes of methanol and dried under vacuum. The precipitate was dissolved in chloroform and sonicated in a Branson 1200 bath sonicator (Danbury, CT, USA) for 5-10 minutes (50/60 Hz, 117 V, 0.7 Amps) to disperse the QDs. Lecithin (from soy) was added to the chloroform mixture in a 1:2 QD:Lecithin ratio (by weight). The solution was stirred in darkness at a speed of 400-500 rpms overnight to encourage monolayer and micelle formation. The solvent was then evaporated under a steady stream of N₂. The residue was heated in a water-bath at 80°C for 5 minutes. Sterile deionized (DI) water was added and the suspension was sonicated briefly (15-20 seconds) to re-suspend the film. The suspension was centrifuged at ~ 125,000 g for 8 hrs in a Beckman L8-80M

ultracentrifuge (Palo Alto, CA, USA) with a type 55.2 Ti fixed-angle rotor to break apart empty micelles containing residual solvent. After the supernatant was discarded, sterile DI water was added. The material was vortexed briefly, transferred to a glass vial, and sonicated 3-5 minutes to acquire the final QD suspension. The Mixed QD suspension had a nominal concentration of 400 µg/ml. A Lecithin suspension containing no QDs was prepared via an identical process and had a nominal concentration of 730 µg/ml. All suspensions were stored in darkness at 4°C prior to exposure.

QD Characterization

The emissions profile of the Mixed QD suspension was acquired on a SpectraMax M2 fluorometer (Sunnyvale, CA, USA). The excitation wavelength was 320 nm and the emissions were recorded from 460 to 680 nm in 5 nm increments. The QD's photoluminescent spectrum was compared to that of sterile DI water.

Aqueous Embryo Exposures

Eggs and sperm were obtained from our breeding colony of *Fundulus heteroclitus* and *in vitro* fertilization was carried out in the laboratory. When eggs reached the 2- to 4-cell stage they were randomly divided among the treatment regimes and housed in 6-well plates. Each well contained 10-15 developing eggs and the treatment solution

volume was adjusted appropriately so that each well contained 0.2 ml of treatment solution per embryo. The Mixed QD stock suspension was diluted with 0.22 μm filtered seawater to obtain the appropriate QD concentrations at a salinity of 17 ppt. Final nominal concentrations were 0, 1, 5, 10, 50, and 100 μg QD/ml. Lecithin was tested for developmental effects by exposing embryos to 0, 100, and 200 μg Lecithin/ml. Embryos were monitored on days 2, 3, 5, 8, and hatching (~14 to 15 days post-fertilization) for morphological variations in the notochord, eyes, brain, heart, bladder, trunk, and fins [193]. At the conclusion of the exposures, embryos were imaged using a Leitz Laborlux 12 fluorescent microscope (Wetzlar, Germany) with a DAPI filter cube (type A, Leitz #513596, excitation $\lambda = 340\text{-}380$ nm). Images were taken with a Canon Powershot A650 IS with microscope adapter. A subset of QD-exposed eggs was also examined with confocal microscopy to determine if QDs could be visualized within the embryo. The study was replicated 3 times; in total, 40 eggs were exposed to each concentration.

Statistics

Embryonic development was assessed using a χ^2 test ($\alpha=0.05$) in Excel (Microsoft Corporation, Redmond, WA).

Results

Prior to embryonic exposures, the Lecithin-encapsulated QD suspension was examined for degradation via the fluorescence emission spectrum. The photoluminescent spectrum of the Mixed QD suspension (Fig. 2-1) showed a right shift of 15 nm in the intensity peak of the blue (490 nm) QDs and a 5 nm shift of the orange (600 nm) QDs suggesting the particles were larger than when manufactured. The green (540 nm) QDs peak emission was not affected.

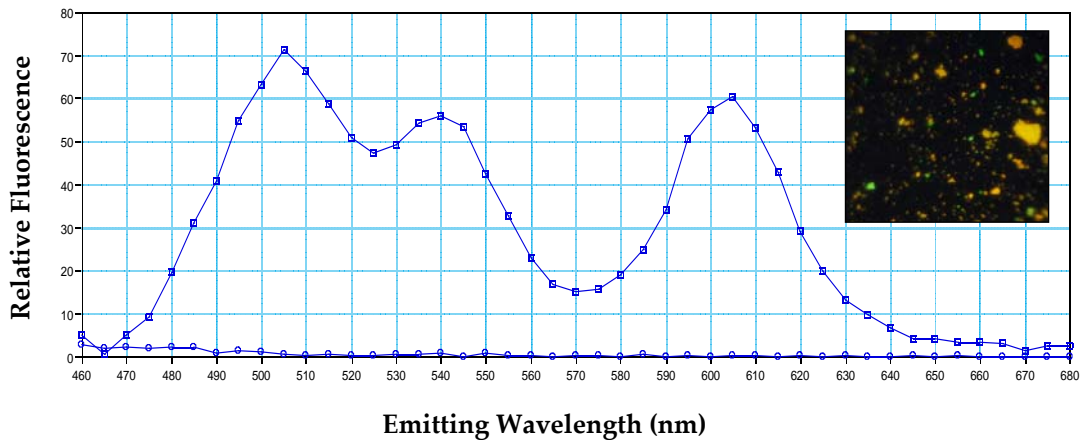


Figure 2-1. The emission profiles of the Mixed QD suspension (\square) versus sterile de-ionized water (\circ). Fluorescence intensity peaks are at 505 (blue), 540 (green), and 605 nm (orange). The insert in the upper right corner is a fluorescent micrograph of the QD aggregates in suspension.

CdSe/ZnS QDs aggregated in seawater and adhered to the exterior chorion of the mummichog embryos in an apparent dose-dependent fashion (Fig. 2-2); however, no QDs were visualized within the embryos [194].

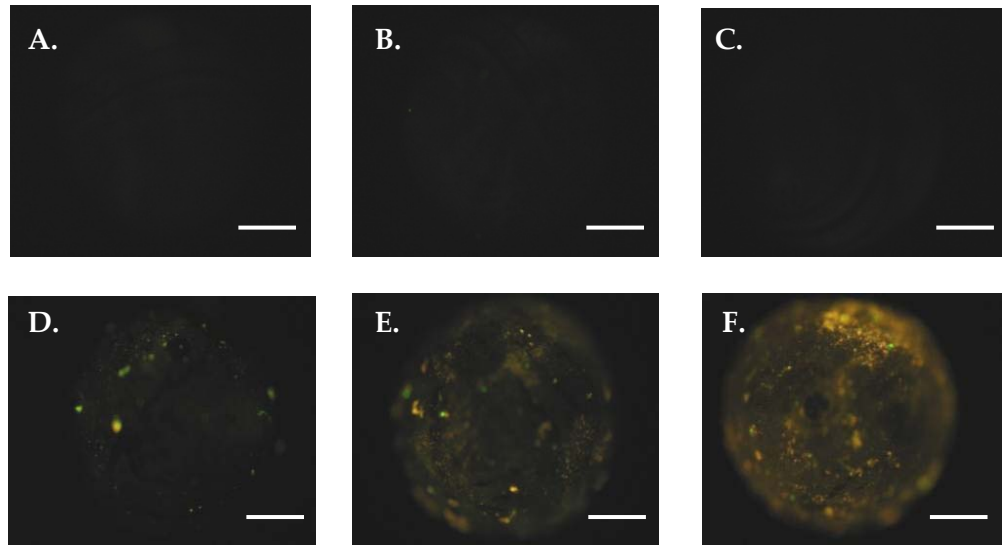


Figure 2-2. Fluorescent micrographs of embryos that have undergone static exposure to (A) 0, (B) 1, (C) 5, (D) 10, (E) 50, and (F) 100 µg/ml CdSe/ZnS QDs for 16 days. While no QD signal is visible in A-C, micrographs D-F show an apparent dose-dependent increase in the chorionic surface area that is covered by QDs. Scale bars = 0.5 mm.

Levels of abnormal development—early mortality and sub-lethal morphological deformities—were significantly elevated in the 100 µg/ml Mixed QD treatment and marginally elevated in the 200 µg/ml Lecithin treatment, 10% in each treatment versus 2.5-5% in their respective Controls (Table 2-1). The types of physical deformities

observed included hemorrhages and pectoral fin deformities. The hatching rate at 100 $\mu\text{g/ml}$ QD (72.5%) was significantly lower than Controls (85.0%). Lecithin did not affect hatching success.

Table 2-1. Developmental toxicity of aqueous QD exposure

Treatment	% abnormal ^a	% hatched ^b
0	2.5	85.0
1	2.5	85.0
5	2.5	85.0
10	2.5	90.0
50	2.5	77.5
100 $\mu\text{g/ml}$ QD	10.0*	72.5*
0	5.0	95.0
100	2.5	92.5
200 $\mu\text{g/ml}$ Lecithin	10.0	90.0

^a includes lethal and sub-lethal deformities, ^b includes both normally- and abnormally-developed fry; * $\alpha = 0.05$.

Discussion

Embryos exposed to the Lecithin-encapsulated CdSe/ZnS QD suspension in seawater developed normally with very few incidences of morphological abnormalities. QDs were prepared with a 1:2 QD: Lecithin ratio, so increasing the QD concentration proportionally increased the Lecithin concentration. The elevated percentage of abnormally developed embryos in the highest QD dose (100 $\mu\text{g/ml}$ QD, 200 $\mu\text{g/ml}$

Lecithin) was the same as the corresponding Lecithin control treatment, 200 µg/ml Lecithin (no QDs). Thus, it appears that exposure to Lecithin accounts for the increase in developmental toxicity.

The lack of developmental abnormalities in the aqueous QD exposures contradicts a recent study by King-Heiden and colleagues [195] in which polyethylene glycol (PEG)-coated CdSe/ZnS QDs caused morphological defects in chorionated zebrafish embryos/larvae. The investigators reported that QDs coated with PEG₅₀₀₀ were an order of magnitude more toxic than CdCl₂ and displayed deformities such as edema, bent spine, tail malformation, and yolk sac malformation, which are all deformities typical of aqueous cadmium exposure [191]. Alternately, QDs coated with PEG₃₅₀ were virtually non-toxic. The investigators observed that PEG₃₅₀-QDs aggregated heavily in embryo rearing medium, whereas PEG₅₀₀₀-QDs did not. Thus, the disparity in the developmental toxicity of differently sized PEG-coated QDs may be due to the size of the aggregates limiting their bioavailability.

Qualitative assessments of eggs exposed to QDs support the hypothesis that QDs do not penetrate the chorion. Detection of the signature fluorescent signal of the QDs was limited to the chorion. The large aggregate size and surface chemistry of the

chorion likely impedes movement through the chorionic pores. Similar observations have been noted with other engineered nanomaterials in solution including fullerenes [185] and carbon nanotubes [186]. It is also likely that the chorion functions as a barrier to degradation products of QDs such as free cadmium. In Japanese medaka eggs (*Oryzias latipes*) exposed to 10 µg/ml Cd, 94% of the cadmium was loosely bound to the chorion and 5% was detected in the body of the fry [196].

As was the case with embryos exposed to PEG₃₅₀-QDs [195], our Lecithin-encapsulated QDs aggregated in seawater. The salts in seawater act as counter ions to disrupt repulsive forces, so the QDs form large aggregates that are not bioavailable. These aggregates may be responsible for the decline of hatching in the 100 µg/ml QD treatment. The QD aggregates on the chorion could be affecting hatching enzymes, physically stabilizing the chorion, or altering the reception of hatching cues such as dissolved oxygen and light [197].

Conclusions

This study has shown that Lecithin-encapsulated QDs are developmentally toxic to *Fundulus* embryos only at high concentrations, beyond what would currently be considered as environmentally-relevant. Teleost embryos in estuarine systems are

protected from QDs by their outer chorion. The structure and charge of the chorion combined with the size and charge of the QD aggregates prevents the QDs from entering the embryo and interfering with development. Future advances in QD synthesis and composition (coatings and shelling materials) may prevent aggregation from occurring in saline environments. At such a time, it would be necessary to re-evaluate the potential toxicity of QDs to estuarine fish embryos.

Chapter 3. Lecithin as an Encapsulating Agent for QDs: A Pilot Study

Reproduced in part with permission from Marine Environmental Research, submitted.

The vast majority of studies investigating QD toxicity have been acute *in vitro* exposures. These studies report that QDs are cytotoxic [21, 33, 34, 42], genotoxic [36, 198], and capable of generating reactive oxygen species [38]. While *in vitro* exposures provide information rapidly, they do not examine systemic physiological processes such as growth and reproduction, nor do they take into account the multitude of pathways that organisms have for responding to exogenous contaminants (metallothionein, the immune system, and antioxidants). To date, there are 5 publications on the toxicity of QDs in aquatic organisms. CdTe QDs reportedly altered oxidative stress biomarkers (lipid peroxidation) and metallothionein levels in freshwater mussels (*Elliptio complanata*) [61, 62]. CdS QDs induced liver injury and increased oxidized glutathione levels in sticklebacks (*Gasterosteus aculeatus*) [199], and developmental malformations occurred in zebrafish embryos (*Danio rerio*) that were aqueously exposed to CdSe/ZnS QDs [195]. Cadmium ions and the generation of ROS are thought to be the main culprits in the toxicity of both shelled and unshelled QDs.

Our model organism *Fundulus heteroclitus*, the mummichog, is abundant in estuarine waters from Maine to the Gulf of Mexico. Adult and larval stages are opportunistic feeders that will encounter QDs while swimming in the water column or foraging on the sediments. The ability of QDs to aggregate and be transferred up the

food chain [200] increases the likelihood that these fish will be exposed via their diet. Given that QDs are degraded by enzymes in the digestive tract [60], possible effects of the free cadmium and selenium include oxidative stress, behavioral abnormalities, reproductive toxicity, and teratogenesis. Therefore, the objectives of this study were to determine if Lecithin-encapsulated CdSe/ZnS QDs adversely affected the development of *Fundulus* embryos when parentally-exposed, and whether QDs caused oxidative stress or altered fecundity in adult *Fundulus heteroclitus*.

Materials and Methods

Chemicals

CdSe/ZnS Evidots (ED-C11-TOL) were purchased from Evident Technologies (Troy, NY, USA). Lecithin (102147) was purchased from MP Biomedicals, Inc. (Solon, OH, USA). Gelatin (G-9382) was purchased from Sigma (St. Louis, MO, USA).

Quantum Dot Preparation

Maple red-orange QDs with a diameter of 5.2 nm (emit $\lambda = 620$ nm) were encapsulated in Lecithin as previously mentioned (Chapter 2). The suspension, herein referred to as the Maple QD stock, had a nominal QD concentration of 377 $\mu\text{g/ml}$. The

Lecithin suspension (no QDs) made by an identical processes had a concentration of 793 $\mu\text{g}/\text{ml}$.

Adult Dietary Exposures

Eighteen male-female pairs of sexually mature *Fundulus heteroclitus* obtained from tidal creeks in Morehead City, NC were randomly assigned to one of three treatment groups: Standard Diet (SD), Lecithin (0 μg QD and 20 μg Lec./day), and QD (10 μg QD and 20 μg Lec./day). Pairs were housed in segmented tanks containing ~15 liters of filtered seawater. Water parameters were held at ~23°C and a salinity of 20 ± 2 ppt with a 16:8 photoperiod. Partial water changes (1/3 of the tank volume) occurred daily. The Standard Diet consisted of 112.5 mg/ml ground tropical fish flake food (Aquatic Ecosystems, Apopka, FL), 250 $\mu\text{l}/\text{ml}$ shrimp puree (puree=1 shrimp per 10 ml of DI water), and 2% type B gelatin prepared in sterile DI water. The treatments—water, Lecithin, or Maple QD suspension—were added to the food slurries and stirred to obtain a homogeneous mixture. The mixture was pipetted (250 μl per well) into 96-well plates and frozen at -20°C until administered. The contents of 2 wells (a total of 500 μl) were considered a single dose and fed daily to each fish to equal the treatment concentrations described above. Feeding was observed to ensure the fish consumed the entire dose.

Table 3-1. QD and Cd content in the diets.

Treatment	Target Dose^a		Measured Dose^a
Standard Diet	0 µg Lec.	0 µg QD	0.00 µg Cd
Lecithin	10 µg Lec.	0 µg QD	0.00 µg Cd
QD	10 µg Lec.	5 µg QD	1.04 µg Cd

^a content is listed for 1 food cube. Daily diets consisted of 2 food cubes per fish.

The cadmium content (Table 3-1) of the diets was confirmed with inductively coupled plasma mass spectrometry (ICP-MS). Briefly, individual food cubes were digested in 200 µl of ~7 N nitric acid for 1 hour. Samples were homogenized for 20 seconds with a battery-operated hand-held grinder. Then, 800 µl of 7 N nitric acid was added to each tube and the samples were digested overnight at room temperature. The following day, the samples were sonicated for 5 minutes (Branson 2510, Danbury, CT), and then ~90 µl of H₂O₂ was added to each sample. The samples were vortexed intermittently over the next 5 hours. Next, the samples were combined with 10 ml of internal standard solution and centrifuged at ~1,300 X g for 10 minutes. One milliliter of supernatant was moved to a fresh tube with 10 ml of internal standard solution and run on a VG Plasmaquad 3 ICP-MS (Thermo Scientific, Waltham, MA). The internal standard solution consisted of 10 ppb In, Tm, and Bi in ~2 % HNO₃. The detection limit was 0.0005 µg of total Cd per sample or 0.002 ng/ml [201].

All pairs received the Standard Diet for 12 days and were observed to confirm spawning activity. After 12 days of observation, the fish received the SD, Lecithin, or QD diets daily for 35 days. Eggs were collected daily from spawning traps. Reproductive output was based on the total number of eggs spawned that had a hardened chorion—an indication of fertilization [202, 203]. Spawning activity was divided into three time-periods based on a semi-lunar spawning cycle: observation (days 1-13), transition (days 14-30), and acute (days 31-47). Fecundity was determined for each pair by calculating the average number of eggs spawned per day in each of the 3 spawning periods. The observation rate for each pair was set as the baseline (100%) and the transition and acute spawning rates were calculated as a percent based on the observation rate. For the embryonic development assessment, 4 subsets of eggs per treatment were collected and reared in 24-well plates in 20 ppt seawater. Development was monitored for morphological deformities of the notochord, eyes, brain, heart, bladder, trunk, and fins [193]. Embryos with deformities were imaged using a Meiji Techno R2 dissecting microscope (Japan) and captured with a T45 camera (Diagnostic Images, Inc., Sterling Heights, MI) using Image-Pro Plus software (MediaCybernetics, Inc, Bethesda, MD). Hatching was also recorded. At the conclusion of the study, adult *Fundulus* were humanely euthanized in accordance with North Carolina State University policy and tissues were collected. The livers were quickly removed and a portion was

fixed in 10% neutral buffered formalin for histopathology. The remaining liver tissues were stored at -80°C until analyzed for oxidative stress biomarkers (total glutathione and lipid peroxidation).

Total Glutathione (GSH) Assay

Total glutathione (N=6 individuals per treatment) was determined using the DTNB-GSSG Recycling Assay [204, 205] modified for 96-well plates. Livers were homogenized in 10 volumes of 5% sulfosalicylic acid (SSA) and then centrifuged to obtain the supernatant. The supernatant was diluted 1:10 with SSA. A 10 µl aliquot of the sample was combined with 195 µl of reaction cocktail consisting of 0.238 mg/ml NADPH buffer, 10mM 5, 5'-dithiobis (2-nitrobenzoic acid), and sterile DI water. Glutathione reductase (50 U) was added to each well and read at 405 nm every 10 seconds for 2 - 2½ minutes on a SpectraMax 190 UV/VIS spectrophotometer (Sunnyvale, CA, USA). Samples were compared to a GSH standard curve and analyzed by linear regression. Samples and standards were run in triplicate. Concentrations were expressed as nmol GSH per mg of tissue.

Lipid Peroxidation (LPo) Assay

Liver samples (N=10-12 individuals/treatment) were prepared and analyzed according to the protocols of Ringwood *et al.* [204] adapted from Ohkawa *et al.* [206]. Tissues were homogenized in 4 volumes of 150 mM TRIS, pH 7.5, 1mM EDTA buffer and then centrifuged at 4°C [207]. A 100 µl aliquot of supernatant was combined with 1.4 ml 0.375% thiobarbituric acid and 14 µl 2% butylated hydroxytoluene. The samples were heated in a water-bath at 100°C for 15 minutes and centrifuged at 13,000 g for 5 minutes at room temperature. Then, 200 µl aliquots of the supernatant were measured spectrophotometrically at 532 nm and compared against a malondialdehyde tetraethylacetal (MDA) standard curve. Samples and standards were run in triplicate. Concentrations were expressed as nmol MDA per mg protein.

Protein Assay

Liver protein content was determined using a Pierce Coomassie Protein Kit (Rockford, IL, USA). Briefly, a 5 µl aliquot of supernatant from the LPo assay was reacted with 250 µl of Coomassie blue reagent at room temperature. The solution was measured spectrophotometrically at 595nm. Samples were compared to a bovine serum albumin standard curve.

Histopathology

Liver samples were preserved in 10% neutral buffered formalin for approximately 1 month. Samples were then rinsed with DI water and transferred to a 0.1 M Tris solution, pH 7.4 until processing. The samples were dehydrated in a graded series of ethanol solutions, cleared in Citrisolv™ (Fisher Scientific, Pittsburgh, PA), and embedded in Paraplast® Plus (Oxford Labware, St. Louis, MO) using a Leica EG 1160 Embedding Center. The embedded livers were sectioned (7 µm thickness) using a HM 340E rotary microtome and mounted on glass histology slides. Following removal of paraffin, sections were hydrated and stained with hematoxylin and eosin for survey. Slides were imaged using a Nikon Eclipse E600 microscope and captured with a T45 camera (Diagnostic Images, Inc., Sterling Heights, MI) using Image-Pro Plus software (MediaCybernetics, Inc, Bethesda, MD).

Data Analysis and Statistics

Body weights were taken at the beginning and end of the exposure period to determine growth (g). The hepatosomatic indices were calculated by comparing the liver wet weight to the final body weight, $HSI = \text{liver wt (g)} / \text{body wt (g)} \times 100$. Growth, hepatosomatic indices, and liver total glutathione and lipid peroxidation levels were analyzed with a Kruskal-Wallis non-parametric ANOVA with a Dunn's test post-hoc

($\alpha=0.05$) [208]. Average fecundity, deformity, and hatching (expressed as a percent) were assessed using a Kruskal-Wallis ANOVA with a Dunn's comparison post-hoc ($\alpha=0.05$). Since no statistical difference existed between the averages of the 4 subsets of developing embryos, the data were combined and presented as total embryos that developed normally, expressed as a percent. Statistical analysis was performed using GraphPad Prism, version 5.0 (GraphPad Software, San Diego, CA).

Results

Fundulus were observed closely for mating aggression, which can result in the loss of scales and fins. All pairs in the SD group completed the study. One pair from the Lecithin group was removed from the study during the observation period because of severe mate aggression. All data from this pair was omitted in the analysis. Another mating pair in the Lecithin group was separated on the 25th day of exposure due to the male's aggressive behavior. The pair was not included in the acute fecundity data as it did not complete the entire spawning interval, but dietary QD treatment continued so the individuals could be assessed for oxidative stress biomarkers. All the QD pairs completed the study without incident.

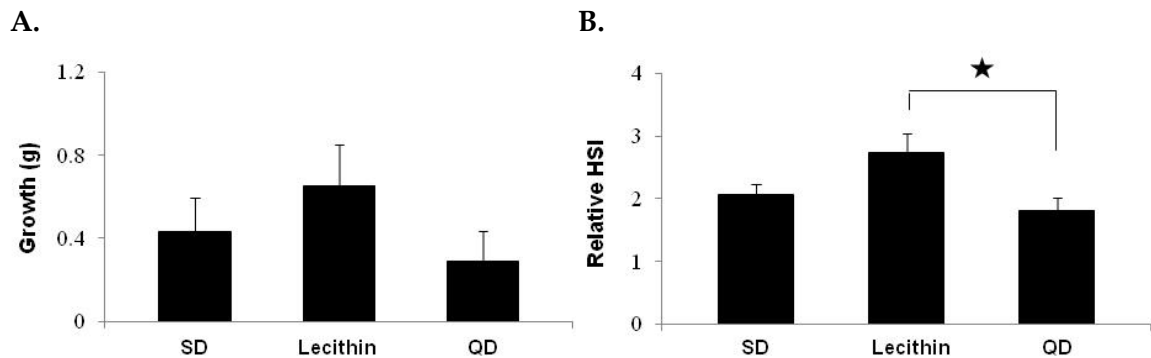


Figure 3-1. Growth and relative liver size. The average (A) growth and (B) hepatosomatic indices of adult *Fundulus* after 5 weeks of dietary treatment. HSI = liver wt (g)/body wt (g) X 100. Bars are mean \pm standard error, $\alpha = 0.05$.

Lecithin-encapsulated CdSe/ZnS QDs were not acutely toxic to adult *Fundulus*, but they did have sub-lethal effects on the fish. Fish consuming QDs had hepatosomatic indices that were significantly lower than fish consuming the Lecithin diet (Fig. 3-1B). Growth was also reduced in the QD diet versus the Lecithin treatment, though it was not statistically different (Fig. 3-1A).

Total liver glutathione and lipid peroxidation levels in the adults were unaltered by treatment (Fig. 3-2). Lecithin had slightly lower GSH (1.47 ± 0.17 nmol/mg tissue) when compared to the SD (1.60 ± 0.05 nmol/mg), while QD treatment slightly increased

GSH levels (1.82 ± 0.18 nmol/mg). Lipid peroxidation levels followed the same trend as GSH. Lecithin had the lowest LPO (0.93 ± 0.13 nmol/mg protein), followed by the SD (0.99 ± 0.12 nmol/mg) and QD (1.25 ± 0.17 nmol/mg).

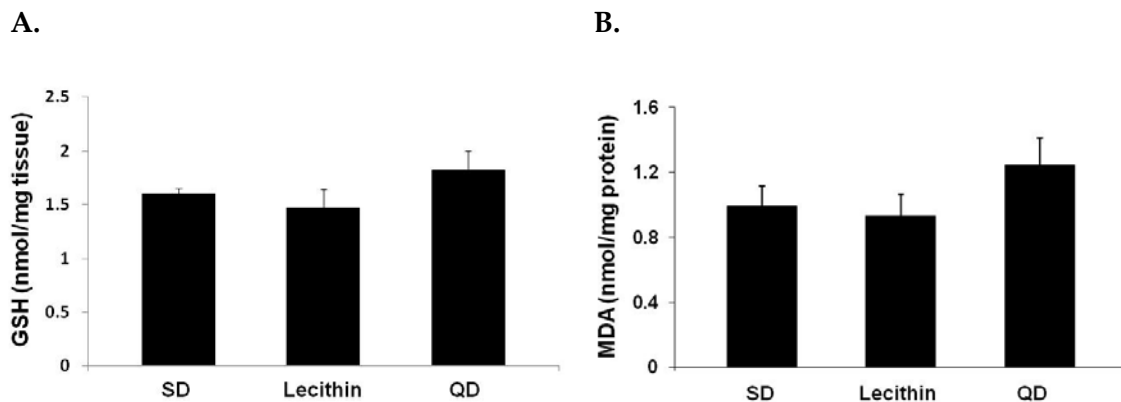


Figure 3-2. The average (A) total glutathione and (B) lipid peroxidation levels of adult livers after 35 days of treatment. Bars are mean \pm standard error.

Livers of *Fundulus* fed the Standard, Lecithin, and QD diets were analyzed using survey histopathology and results are shown in Figure 3-3. *Fundulus* fed the Standard, Lecithin, or the QD diets had rounded, apparently enlarged hepatocytes whose cytoplasm did not stain, but was filled with large vacuoles of smooth margin. The vacuoles were apparently due to lipid inclusion, the presence of which was not detected in hematoxylin and eosin stains due to removal during ethanol dehydration phases of histologic processing.

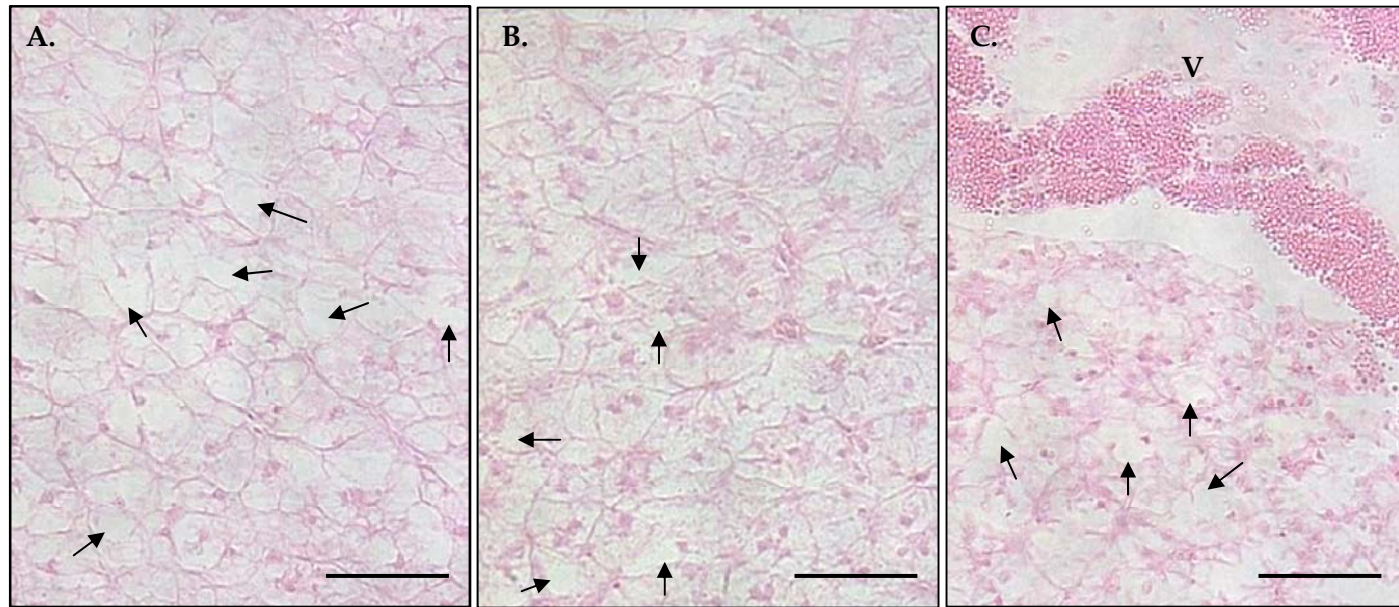


Figure 3-3. Micrographs of H&E stained liver sections (7 μm) from male *Fundulus* fed the (A) Standard, (B) Lecithin, and (C) QD diets for 5 weeks. Hepatocyte margins are indicated by the staining of plasma membranes. Nuclei were apparent. The empty vacuoles characterized hepatocytes of all *Fundulus* (arrows). Figure 3-3C shows numerous erythrocytes in the large hepatic vessel (V) at the top of the field. Magnification: 400X. Scale bars = 50 μm .

Fecundity was positively impacted by the addition of Lecithin or QDs to the Standard Diet (Fig. 3-4). The addition of Lecithin to the diet significantly increased fecundity during the transition spawn (+390.2%), while co-exposure to QDs diminished the nutritional benefit of the Lecithin (+18.3%). No significant effect on fecundity was noted during the acute spawning interval.

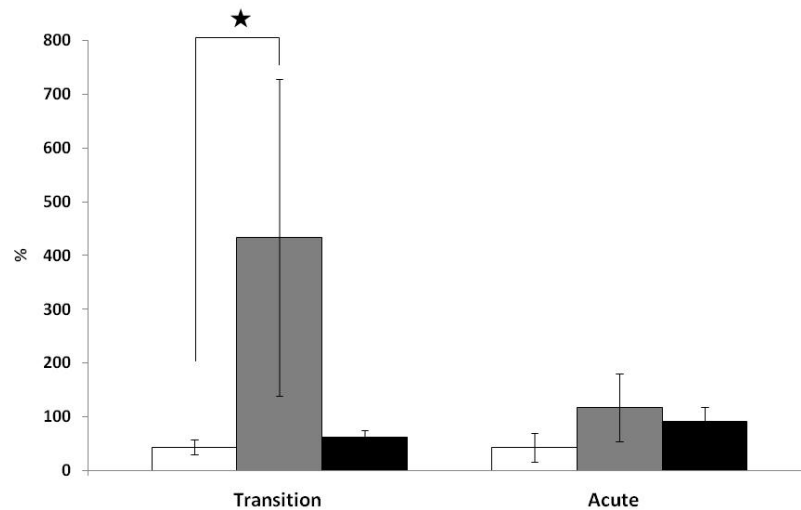


Figure 3-4. Fecundity. Spawning rates (eggs/day) as a percent based on the observational spawning rates for the Standard Diet (white), Lecithin (gray), and QD (black). Bars are mean \pm standard error, $\alpha=0.05$.

Parentally-exposed embryos had few incidences of severe morphological abnormalities, most of which were associated with the Lecithin group (Fig. 3-5). Hemorrhages and fin deformities were the most common malformations recorded. The

proportion of embryos that developed correctly was 96.4% for the SD treatment, 94.1% for Lecithin treatment, and 95.8% in the QD treatment. Neither the percentage of deformed embryos, nor the hatching rates (data not shown) were significantly altered by treatment.

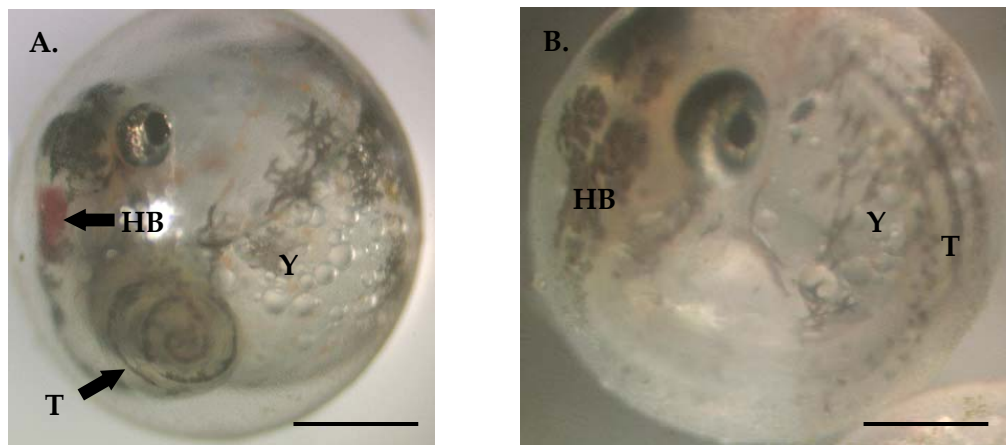


Figure 3-5. Light micrographs of embryos from the Lecithin treatment group. The embryo on the left (A) has a deformed, apparently spiral tail shape (T) and hemorrhage in the hind brain (HB). The embryo on the right (B) has developed normally with the tail extending over the yolk (Y) and caudal portion of the fin resting near the head. Embryo B is also considerably larger in size despite being at a similar stage in development. Scale bar = 0.5 mm.

Discussion

Dietary delivery of Lecithin-encapsulated CdSe/ZnS core-shell QDs had little impact on adults or embryos. After ingestion, digestive processes should have removed the Lecithin coating from the QDs and exposed the ZnS shell. While the core and shell

dissociate in acidic environments [20], *Fundulus* have an alkaline digestive tract [209] and the shell would remain stable under these conditions. Adult hepatic glutathione and lipid peroxidation levels were not significantly altered after 5 weeks of QD exposure. The lack of an oxidative stress response indicates either low uptake across the gut or protection from degradation by the ZnS shell. A study of CdTe and CdSe/ZnS QD toxicity by Cho and colleagues [42] noted that unshelled CdTe QDs leached free Cd²⁺, while the ZnS-shelled QDs showed no detectable levels of free cadmium at 24 hours. In effect, placing a shell on the QD core deters oxidation [16, 31] and conveys additional stability. Thus, the elevated LPO levels of freshwater mussel gills after acute CdTe QD exposure (24 hr, 8 µg/ml) reported by Gagné *et al.* [61] appear to be a function of leached cadmium ions.

As we conceived this study, Hoshino *et al.* [20] published that cytotoxicity in QD exposures was due to the coating agents. To avoid potential negative effects of the coating, we chose Lecithin, otherwise known as phosphatidylcholine, which is a membrane phospholipid found in all organisms. *Fundulus* fecundity is dependent on a variety of factors including the age of the fish, nutritional status, temperature, salinity, and photoperiod [210]. Our results suggest that Lecithin acted as a nutrient because supplementation of the Standard Diet with Lecithin resulted in significantly increased

fecundity. Growth and relative liver size were also increased, though not significantly, with the addition of Lecithin to the diet. This increase in body and liver size could have contributed to the significant increase in fecundity during the transition period. In contrast, *Fundulus* ingesting 10 µg QD per day did not show increased fecundity despite co-ingestion with Lecithin. This suggests that fecundity would be reduced if QDs were coated in a less nutritious material such as PEG or silica.

While Lecithin improved fecundity in the transition period, fecundity of the Lecithin group was not significantly different from the Standard Diet during the acute spawning interval. Daily ingestion of phospholipid could have caused hepatic steatosis (fatty liver), a condition in which normal functioning of the liver is disrupted by the accumulation of lipid droplets [211]. Pathological examination of several livers indicated the condition could be occurring, though an exhaustive examination was not conducted.

Based on the literature reports for QD deposition and our understanding of egg maturation in fish, we predicted that QDs would be maternally transferred to the eggs. Pharmacokinetic studies with rodents have shown QDs primarily deposit to and accumulate in the liver [51, 53]. Thus, QDs accumulate in the organ where

vitellogenin—the egg yolk protein precursor—is synthesized. Vitellogenin is then transported via the blood to the ovaries where it is deposited into the developing ova. Development was monitored in parentally-exposed embryos to evaluate the hypothesis that whole or degraded QDs are maternally transferred to developing progeny. While we did not directly measure the cadmium content of the embryos, we did examine the offspring pre- and post-hatch for QD presence via fluorescent microscopy. No visible red-orange QD signal was detected. Moreover, incidences of gross morphological abnormalities were consistent between all diets. Although this suggests that whole QDs were not maternally transferred to offspring, dissociated cadmium may still be sequestered *in ovo*. Studies have shown that cadmium can bind with vitellogenin and be ovo-deposited to fish embryos [70, 72]. In the future, tests for evidence of maternal transfer of QDs or free Cd will be pursued with longer dietary exposures.

Conclusions

Various mechanisms of action have been theorized for the toxicity of QDs including, but not limited to: generation of reactive oxygen species, oxidative stress, DNA damage, developmental toxicity, and changes in gene expression. This study has shown that in adult *Fundulus*, CdSe/ZnS QD consumption for 35 days did not elicit an oxidative stress response, nor did it alter reproduction when packaged with Lecithin.

Future studies should explore chronic exposures and alternate coating materials to determine if the core-shell QDs are truly benign in fish.

Chapter 4. Bioavailability and Oxidative Stress from Dietary Quantum Dot Exposure in *Fundulus*

Reproduced in part with permission from Environmental Science & Technology, submitted.
Unpublished work copyright 2010 American Chemical Society.

Recent reports of the release of engineered nanoparticles from commercially-available products raise concerns regarding the environmental fate and toxicity of nanotechnology [181, 182]. The available literature shows that in aquatic systems ENPs complex with organic debris and adhere to organisms living in the water column [32, 212]. In waters with high salinities (ionic strength), ENPs form large aggregates that precipitate to the sediments where they interact with benthic dwellers and bottom feeders [185, 187, 213, 214]. Yet, little information is available on the bioavailability and subsequent toxicity of ENPs in environmentally relevant situations.

Quantum dots are ENPs that emit tunable, discrete fluorescence when excited by visible and near UV wavelengths. This tunable fluorescence, which is based upon particle diameter, has spurred their incorporation into commercially-available products such as light emitting diodes (LEDs), security inks, solar cells, and telecommunication components. Applications for QDs continue to flourish; therefore environmental fate and toxicity studies are needed to determine the risk QDs and their degradation products pose to aquatic organisms.

Several studies have shown that QDs are cytotoxic, genotoxic, and able to generate reactive oxygen species [33, 35, 36, 38, 42]. Green and Howman [35] theorized

that the DNA damage that occurred following acute exposure to UV-exposed biotinylated CdSe/ZnS QDs was the result of ROS interaction. They hypothesized that the ZnS shell of a QD was oxidized to $\text{SO}_2\cdot$, which was then converted to the superoxide and hydroxyl radicals. Ipe and colleagues [38] reported that although no sulfur-containing radicals were observed in their studies, irradiated CdSe QDs generated hydroxyl radicals and CdS QDs generated both superoxide and hydroxyl radicals. QD constituents (cadmium and selenium) also generate ROS [73-76, 94, 95]. Given that QDs and their degradation products generate ROS, oxidative stress—the imbalance of pro- and anti-oxidant processes—could be the mechanism by which QDs exert toxicity.

The goal of this study was to determine if an oxidative stress response occurred in the mummichogs (*Fundulus heteroclitus*) exposed via diet to Lecithin-encapsulated CdSe/ZnS QDs. Hepatic total glutathione and lipid peroxidation levels were measured as oxidative stress biomarkers. Furthermore, quantitative real-time PCR (qPCR) was used to evaluate changes in the expression of metallothionein (mt), glutathione-S-transferase (gstmu), glutathione peroxidase (gpx), Cu/Zn-superoxide dismutase (sod1), and Mn-superoxide dismutase (sod2).

Materials and Methods

Chemicals

CdSe/ZnS Evidots (cat. # ED-C11-TOL-0620) were purchased from Evident Technologies (Troy, NY). CdCl₂ (202908) and Gelatin (G-9382) were purchased from Sigma-Aldrich (St. Louis, MO). Lecithin (102147) was purchased from MP Biomedicals, Inc. (Solon, OH, USA). Optima™ trace-metal free HNO₃ and H₂O₂ were purchased from Fisher (Pittsburgh, PA). The cadmium standard (CLCD-2-2Y) was purchased from Spex CertiPrep (Metuchen, NJ).

Quantum Dot Preparation

Suspensions of Lecithin encapsulated CdSe/ZnS quantum dots (diameter = 5.2 nm, emit $\lambda = 620$ nm [4]) were prepared as previously mentioned (see Chapter 2) with modifications to decrease liposome size and increase dispersion [119, 121, 215]. The QDs were precipitated from toluene with 5 volumes of methanol, dried under vacuum, dissolved in chloroform, and sonicated for 10 minutes in a Branson 1200 bath sonicator (Danbury, CT). The solution was then divided equally into two glass vials—each vial undergoing identical treatment. The solutions were mixed on a bench-top stirrer for 1 hour. Refined Lecithin (from soy) was added in a 1:1 Lecithin:QD ratio (by weight) to the chloroform-QD mixture and stirred in darkness at a speed of 400-500 rpms overnight

to encourage mono and bi-layer formation. Then, the solvent was evaporated under a stream of N₂ and the residue was heated in a water-bath at 80°C for 5 minutes. The film was dried *in vacuo* overnight at room temperature to remove any traces of residual solvent. The following day, sterile de-ionized water was added and the vials were sonicated briefly (1 minute) to re-suspend the film. Each suspension was mixed for 2 hours and then sonicated for 30 minutes to form small, uniform unilamellar vesicles. The suspension was centrifuged in a Beckman L8-80M ultracentrifuge (Palo Alto, CA) with a type 55.2 Ti fixed-angle rotor at 125,000 g for 8 hrs to break apart empty micelles [192]. The supernatant was discarded and sterile DI water was added to each vial. The material was then vortexed, transferred to a fresh glass vial, and sonicated for 5 minutes to acquire the final QD suspension. The vials were combined to form a uniform suspension with a nominal concentration of 730 µg/ml QD and 730 µg/ml Lecithin. A Lecithin suspension with a concentration of 730 µg/ml Lecithin (no QDs) was prepared in the same fashion. The stock suspensions were stored at 4°C in darkness for up to 1 week until used as components of the diets.

QD Characterization

Photoluminescence

QDs precipitated from suspension while being stored in darkness at 4°C; thus, prior to use the QD stock suspension was sonicated for 1 minute to re-suspend the nanoparticles and obtain a homogenous mixture. A fluorescence profile for Lecithin encapsulated-CdSe/ZnS QDs was acquired with a SpectraMax M2 fluorometer (Sunnyvale, CA). The excitation wavelength was 355 nm and the emissions were recorded from 450 to 680 nm in 10 nm increments. The QD suspension was compared to the Lecithin suspension and sterile DI water.

Particle Size

QD and Lecithin suspensions were sonicated for 30 seconds in a bath sonicator, and then a 200 µl aliquot from each suspension was used to determine particle size. High-resolution size-based separation of the particle population was carried out using Asymmetric Flow Field-Flow Fractionation AF4 with tandem multiangle laser light scattering (MALLS) detection and characterization (model DAWN EOS, Wyatt Technology, Santa Barbara, CA). Static light scattering intensity was measured at 12 angles simultaneously and used to calculate the excess Rayleigh ratio of the particles in solution as they eluted from the AF4 separation. Light scattering data were analyzed

using Zimm formalism. The radii of the eluted fractions were monitored using the MALLS with data processing using software supplied by the vendor (ASTRA, Wyatt Technology, Santa Barbara, CA).

Diet Preparation

Five diets were prepared: a Standard Diet (SD), SD + Lecithin, Low QD, High QD, and Cd (Table 4-1). Each diet contained 112.5 mg/ml ground tropical fish flakes (Aquatic Ecosystems, Apopka, FL), ~2% gelatin, 250 µl/ml shrimp puree (1 homogenized shrimp/10 ml of DI water) for flavoring, and sterilized DI water. The appropriate amount of the QDs, Lecithin, and/or CdCl₂ were added to each food mixture and stirred for 5-10 minutes to obtain a homogeneous slurry. The liquid diets were pipetted in 250 µl aliquots onto wax paper. The discs were allowed to solidify briefly at room temperature and then stored at -20°C until administered. The daily dose was achieved by feeding each fish 2 discs per day.

Table 4-1. QD and Cd content^a in the diets

Treatment	Target dose		Measured dose
Standard Diet (SD)	0 µg Lec.	0.0 µg QD	0.00 µg Cd
SD + Lecithin	5 µg Lec.	0.0 µg QD	0.00 µg Cd
Low QD	5 µg Lec.	0.5 µg QD	0.07 µg Cd
High QD	5 µg Lec.	5.0 µg QD	0.74 µg Cd
Cd	5 µg Lec.	1.7 µg Cd	1.42 µg Cd

^a amounts are for an individual food disc. Each fish received 2 food discs per day.

The cadmium concentrations of the food discs (Table 4-1) were measured with inductively coupled plasma mass spectrometry. Cubes were homogenized in acid-washed polypropylene tubes for 30 seconds with a battery-operated hand-held grinder in 200 μ l of 7 N nitric acid. Then, 800 μ l of 7 N nitric acid was added to each tube and the samples were allowed to digest overnight. In the morning, the samples were sonicated for 5 minutes (Branson 2510, Danbury, CT) and then approximate 90 μ l of H₂O₂ was dispensed into each mixture. The samples were vortexed intermittently over the next 6 hours and then transferred to trace-metal free 15 ml vials. Each sample was combined with 10 ml of internal standard solution and then centrifuged at ~1,300 g for 10 minutes. One milliliter of supernatant was transferred to a fresh tube with 10 ml of internal standard solution and analyzed on a VG Plasmaquad 3 ICP-MS (Thermo Scientific, Waltham, MA). The internal standard solution consisted of 10 ppb In, Tm, and Bi in ~2 % HNO₃. The detection limit was 0.0005 μ g of total Cd per sample or 0.002 ng/ml [201]. Recovery of cadmium spiked SD + Lecithin food discs was 86.8%.

Research Design

Thirty male-female pairs of sexually mature *Fundulus heteroclitus* were obtained from tidal creeks in Morehead City, NC. After an appropriate laboratory acclimation period, mating pairs were housed in segmented tanks containing ~ 15 liters of natural

filtered seawater at ~23°C and 20 ± 2 ppt salinity with a 16:8 light:dark cycle. Partial water changes were performed daily. Each pair received the Standard Diet for 27 days. Following the observation period, the treatment diets were administered daily for 85 days. Two food discs were administered to each male-female pair and feeding was observed to ensure each fish consumed a disc. The process was then repeated with a second set of discs to reach the proper daily dose. The fish were given additional tropical flake food once or twice daily (after the food discs were consumed) and live brine shrimp (*Artemia*) at least twice a week. At the conclusion of the study, *Fundulus* were euthanized with MS-222 and the tissues quickly excised. The intestinal lumens were purged with sterile PBS to remove any fecal matter and then preserved at -80°C until analyzed for cadmium content. A portion of the liver no more than 2-3 mm was fixed in at least 10 volumes of ice-cold Millonig's buffer + 2% glutaraldehyde. The remaining liver tissue was portioned and preserved at -80°C until analyzed for cadmium concentration via ICP-MS, oxidative stress biomarkers (total glutathione and lipid peroxidation), or changes in RNA expression of genes related to metal detoxification and oxidative stress (metallothionein, glutathione-s-transferase, glutathione peroxidase, and superoxide dismutases). The gonads, spleen, brain, and gills were also excised. Specimens were taken from abnormal tissues and preserved in 10% neutral buffered formalin. The remaining tissues were preserved at -80°C.

Transmission Electron Microscopy

Liver samples (2-3 mm thick) from fish fed the Standard Diet, SD + Lecithin, High QD, and CdCl₂ diets (N=2-4 individuals/diet) were fixed as above and stored at 4°C until processing. After rinsing (3X) in Millonig's phosphate buffer, the tissues were post-fixed in 2% osmium tetroxide /Millonig's buffer for 90 minutes at room temperature. Resultant secondarily fixed liver tissues were then rinsed 3X in distilled water and *en bloc* fixed in 2% aqueous uranyl acetate for 1 hour. The samples were dehydrated in a graded series of ethanol solutions ending in 3 changes of 100% ethanol. Samples were then rinsed (3X) in propylene oxide, placed in a 1:1 propylene oxide: Spurr's resin mixture for 1 hour, and transferred to a 1:2 propylene oxide: Spurr's resin mixture overnight. The next day, samples were transferred to a 1:3 propylene oxide: Spurr's resin mixture for 4.75 hours and then 100% Spurr's resin for 1 hour. After the initial infiltration, samples were placed in fresh 100% Spurr's resin for 1 hour, embedded in molds with fresh Spurr's resin (1 hour), and cured for at least 8 hours at 70°C. After polymerization, semithin sections (0.5 μm thick) were cut with a glass knife on a Reichert Ultracut E ultramicrotome, placed on glass histological slides, stained with Richardson's methylene blue/Azure II/ borate solution [216], coverslipped, and viewed. These high resolution sections proved useful for two purposes; first, to determine presence of liver in the block and second, to survey for alterations in liver structure.

With respect to the latter, the secondary osmium fixation preserved lipids and made it possible to directly detect lipid stores as vacuoles in hepatocytes. Imaging was performed using a Nikon Eclipse E600 light microscope, a Nikon DXM 1200 digital camera, and EclipseNet imaging software (Nikon, Melville, NY). Once liver tissue was verified in semithin sections, ultrathin sections (60-85 nm thick) were cut from the epon blocks using a diamond knife and affixed to copper grids. Resultant sections were stained with 2% aqueous uranyl acetate for 5 minutes followed by 0.4% aqueous lead citrate for 1.5 minutes. Grids were viewed on a Zeiss EM10CA transmission electron microscope. All processing and imaging of tissues for electron microscopy were performed at the University of Maryland, College Park.

Tissue Cd Measurement

Although QD concentrations can be determined via fluorescence in simple systems [217], its use in whole animals is limited. Thus, cadmium concentrations were measured to infer QD uptake and accumulation. Liver and intestinal tissues were weighed and placed in acid-washed polypropylene tubes. Tissues were homogenized in 200-300 μ l of 7 N nitric acid for 20 seconds. The samples were brought up to 1 ml of acid and digested overnight at room temperature. The next morning, samples were sonicated for 5 minutes (Branson 2510, Danbury, CT) and then 90 μ l of H₂O₂ was added.

The samples were vortexed intermittently over the next 6 hours and then transferred to trace-metal free 15 ml vials. Each sample was combined with 10 ml of internal standard solution and centrifuged at ~1,300 g for 10 minutes. One milliliter of supernatant was transferred to a fresh tube with 10 ml of internal standard solution. The samples were analyzed on a VG Plasmaquad 3 ICP-MS and compared to a cadmium standard curve. Recovery of cadmium spiked NIST bovine liver standard reference material (SRM 1577b) was 83.7%.

Total Glutathione (GSH) Assay

Total glutathione (N= 4-6 individuals/treatment/sex) was determined using the DTNB-GSSG Recycling Assay [204, 205] modified for 96-well plates. Livers were homogenized in 10 volumes of 5% sulfosalicylic acid (SSA) and then centrifuged at 6,000 g for 15 minutes at 4°C. The supernatant was diluted 1:10 with SSA. A 10 µl aliquot of sample was combined with 195 µl of reaction cocktail consisting of 0.238 mg/ml NADPH buffer, 10mM 5, 5'-dithiobis (2-nitrobenzoic acid), and sterile DI water. Glutathione reductase (50 U) was added to each well and read at 405 nm every 10 seconds for 2 - 2½ minutes on a SpectraMax 190 UV/VIS spectrophotometer (Sunnyvale, CA, USA). Samples were compared to a GSH standard curve and rates determined using linear

regression. Samples and standards were run in triplicate. Concentrations were expressed as nmol GSH per mg of tissue.

Lipid Peroxidation (LPo) Assay

Liver samples (N= 4-6 individuals/treatment/sex) were prepared and analyzed according to the protocols of Ringwood *et al.* [204] adapted from Ohkawa *et al.* [206]. Tissues were homogenized in 4 volumes of 150 mM TRIS, pH 7.5, 1mM EDTA buffer [207] and then centrifuged at 6000 g for 12 minutes at 4°C. A 50 µl aliquot of supernatant was combined with 700 µl 0.375% thiobarbituric acid and 7 µl 2% butylated hydroxytoluene. The samples were heated in a water-bath at 100°C for 15 minutes and centrifuged at 13,000 g for 5 minutes at room temperature. Then, 200 µl aliquots of the supernatant were measured spectrophotometrically at 532 nm and compared against a malondialdehyde tetraethylacetal (MDA) standard curve. Samples and standards were run in triplicate. Concentrations were expressed as nmol MDA per mg tissue.

Protein Assay

Liver protein content was determined using a Pierce Coomassie Protein Kit (Rockford, IL, USA). Briefly, a 5 µl aliquot of supernatant from the LPo assay was reacted with 250 µl of Coomassie blue reagent at room temperature. The solution was

measured spectrophotometrically at 595nm. Samples were compared to a bovine serum albumin standard curve.

Quantitative Real-Time PCR

All glassware was baked at 100°C for 1 week or soaked in 3% H₂O₂ for 15 minutes and rinsed in DEPC-treated water. The hand-held grinder, pipettes, and bench-top were cleaned with 70% EtOH and RNaseZap. RNase, DNase-free disposable pestles were rinsed with DEPC-treated water between samples. RNA was isolated from the livers of adult *Fundulus* using RNA-Bee reagent (Tel-Test, Inc.) according to the manufacturer's protocol with an additional chloroform phase separation and EtOH rinse of the pellet. The RNA/DNA ratio was measured spectrophotometrically at 260/280 nm on a Spectramax 190 microplate reader (Sunnyvale, CA) and the final concentration of RNA determined (ng RNA/μl). All samples had a 260/280 ratio of 1.9 or higher.

Reverse transcription was carried out using the Omniscript cDNA synthesis kit (Qiagen Inc., Valencia, CA) according to the kit's directions. Briefly, 500 ng of RNA, 10 μM oligo dT primers (Promega Corp., Madison, WI), and RNaseOut inhibitor (Invitrogen Corp., Carlsbad, CA) were combined and incubated at 37°C for 1 hour in an

Eppendorf Mastercycler (Hamburg, Germany). The cDNA was then diluted to a 2 ng/ μ l working concentration.

Table 4-2. Real-time PCR primer sequences for *F. heteroclitus*

Gene	GenBank ID	Primer Name	Primer Sequence (5'-3')
β -Actin ^a	AY735154	Fh-B-Actin-F Fh-B-Actin-R	ACCACACATTTCTCATACTCGGG CGCCTCCTTCATCGTTCCAGTTT
Metallothionein (mt)	AB426465	Fh-MT-F1 Fh-MT-R1	AAAGGGAAGACCTGCGACAA ACAAAGAAAGGCTCGGCGTA
Glutathione-S-transferase, mu class (gstmu)	AY725220	Fh-GSTmu-F1 Fh-GSTmu-R1	TATGTGCGGAGAGACTGAGG TCACAAAGCCGTTTCTGAAG
Glutathione peroxidase (gpx)	CN971701	Fh-GPX-F1 Fh-GPX-R1	TCACCGACGAGCACTACAGG TGAACAGCGGGAAGGAGACG
Cu/Zn Superoxide dismutase (sod1)	CV824930	Fh-SOD1-F1 Fh-SOD1-R1	AGCCGTGTGTGTCTGAAAG TGCCAAAGGGATTGTAGTGTGG
Mn Superoxide dismutase (sod2)	CN980747	Fh-SOD2-F1 Fh-SOD2-R2	ACACTTCCTGACCTGACATACGAC ATGATGCTTGCTGTGGTGGAG

^a primers originally described by Battle, L. [218]

Quantitative real-time PCR was carried out using previously published β -actin primers [218]. Target gene primers (Table 4-2) were designed using PrimerQuest software (Integrated DNA Technologies, Coralville, IA; <http://www.idtdna.com/Scitools/Applications/Primerquest>). Primer efficiencies were tested to confirm that β -actin and target genes amplified with comparable efficiency. QPCR was performed using SYBR Green PCR Master Mix (Applied Biosystems, Foster City, CA) following the manufacturer's protocol. Briefly, a 25 μ l reaction consisting of

200 nM of each primer, 12.5 µl 2x SYBR Green PCR Master Mix, 9.5 µl dH₂O, and 4 ng cDNA template was amplified using an Applied Biosystems 7300 Real-Time PCR System with the following thermal profile: 95°C for 10 min; 40 cycles of 95°C for 15 s, 60°C for 60 s. A dissociation curve was generated at the completion of the run. All samples were amplified in duplicate. Data were analyzed using ABI PRISM 7000 Software, Version 1.1 (Applied Biosystems Inc., Foster City, CA). Gene expression was calculated using relative quantification by the $2^{-\Delta\Delta C_T}$ method of Livak and Schmittgen [219]. Target gene expression, following normalization to β -actin, was compared to references (SD + Lecithin) to estimate average fold induction for each experimental group, and each target gene. Each biological replicate represents a single adult *Fundulus*, and each experimental group is represented by at least four individuals/treatment/sex. Data are presented as mean fold induction \pm standard error.

Histopathology

Testes from fish receiving the Standard Diet and Cd diet were fixed in 10% buffered formalin. After being rinsed with DI water overnight, the samples were dehydrated in a graded series of ethanol solutions, cleared in Citrisolv™ (Fisher Scientific, Pittsburgh, PA), and embedded in Paraplast® Plus (Oxford Labware, St. Louis, MO) using a Leica EG 1160 Embedding Center. The embedded livers were cut in 6 µm

sections using a HM 340E rotary microtome. Sections were stained with Harris hematoxylin (Fisher Scientific, Kalamazoo, MI) and Y eosin (EM Scientific, Gibbstown, NJ). Slides were imaged using a Nikon Eclipse E600 microscope and captured with a T45 camera (Diagnostic Images, Inc., Sterling Heights, MI) using Image-Pro Plus software (MediaCybernetics, Inc, Bethesda, MD).

Statistical Analysis

Cadmium concentrations for liver and intestinal tissues were log transformed and analyzed for significance using a 3-factor ANOVA (treatment, tissue, and sex) with a Tukey HSD post-hoc, $\alpha = 0.05$ (Fig. 4-3). Liver and intestinal cadmium concentrations without regard to sex (Table 4-3) were analyzed with a Kruskal-Wallis test with a Dunn's post-hoc comparison (N=10-12 individuals/treatment). For total glutathione and lipid peroxidation concentrations, a Kruskal-Wallis test with a Dunn's post-hoc comparison was used to compare across all treatment groups and between sexes (N=4-6 individuals/treatment/sex). For the qPCR analysis, the SD + Lecithin treatment served as the Control for statistical comparisons because the effects of the QDs and Cd, not the encapsulation material, were the focus of the study. A Kruskal-Wallis analysis with a Dunn's post-hoc test was used to determine significance (N=5-6 individuals/treatment/sex). When no statistical differences were seen between the sexes,

the data was merged. Statistical analysis of cadmium concentrations was performed using JMP, version 8.0.2 (SAS Institute Inc[®], Cary, NC). All other statistical analyses were performed using GraphPad Prism, version 5.0 (GraphPad Software, San Diego, CA).

Results

QD Characterization

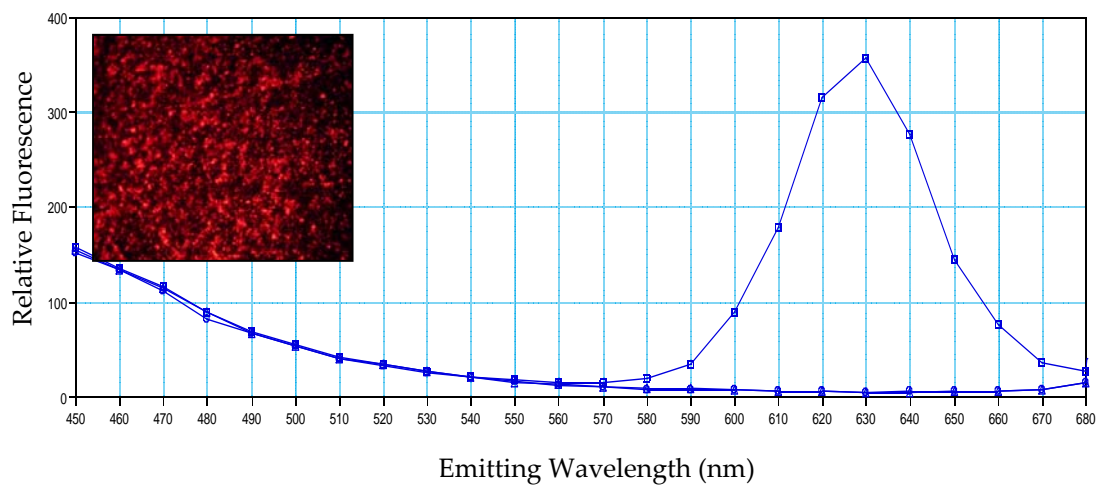


Figure 4-1. Emission profiles of the Lecithin-encapsulated QD suspension (□), Lecithin suspension (Δ), and sterile de-ionized water (○) when excited at 355 nm. The insert in the upper left corner is a fluorescent micrograph of the final QD suspension.

QDs fluoresce at discrete wavelengths according to their core-shell diameter, so degradation or aggregation can be inferred by evaluating the photoluminescence

emission spectrum of the prepared QD suspension. The spectrum (Fig. 4-1) shows a 10 nm right shift in the peak intensity (630 nm) from the manufacturer's listed peak wavelength of 620 nm [4] suggesting that there was a slight increase in particle size due to preparation methods. Flow field-flow fractionation analysis, which determines particle size and abundance in the 0-1000 nm range (Fig. 4-2), shows that the majority of the QD suspension particles were between 200 and 230 nm in radii with a calculated z-average RMS radius of 157.0 nm. The Lecithin suspension particles had a linear differential rms radius between 290 and 330 nm, and the z-average RMS radius was 324.1 nm.

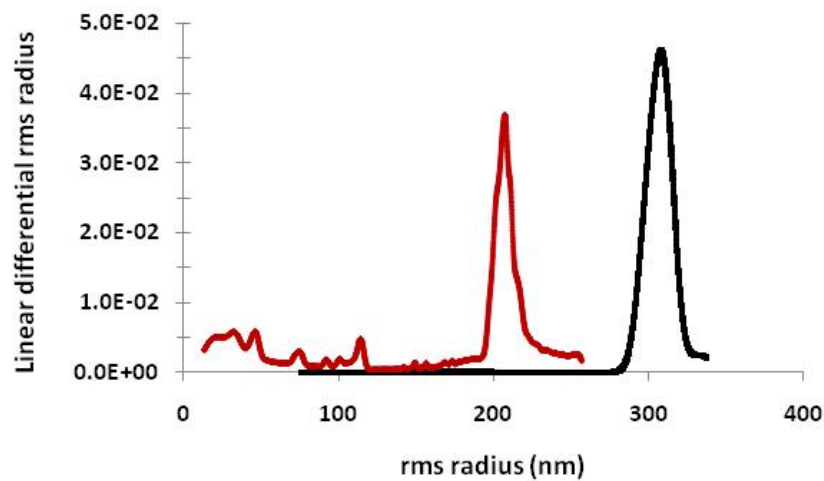


Figure 4-2. Particle size/abundance of the QD (red) and Lecithin (black) suspensions.

Dietary QD exposure

Despite monitoring the fish prior to the beginning of the study for aggressive behavior such as fin nipping and chasing, 2 female fish in the SD + Lecithin treatment died during the exposure portion of the study as a result of pair mis-match (male aggression). A female *Fundulus* from the High QD treatment group also died during the exposure period, but signs of aggressive behavior were absent, suggesting that QD exposure may have contributed to the death.

Bioavailability

Liver slices examined for the presence of QDs by transmission electron microscopy were inconclusive (Figures 4-3 through 4-5). Sections from fish fed the High QD diet showed the presence of dense bodies in lipid vacuoles; however, the dense bodies were also observed in SD + Lecithin and Cd tissues suggesting that they may be artifacts from staining or biological inclusions.

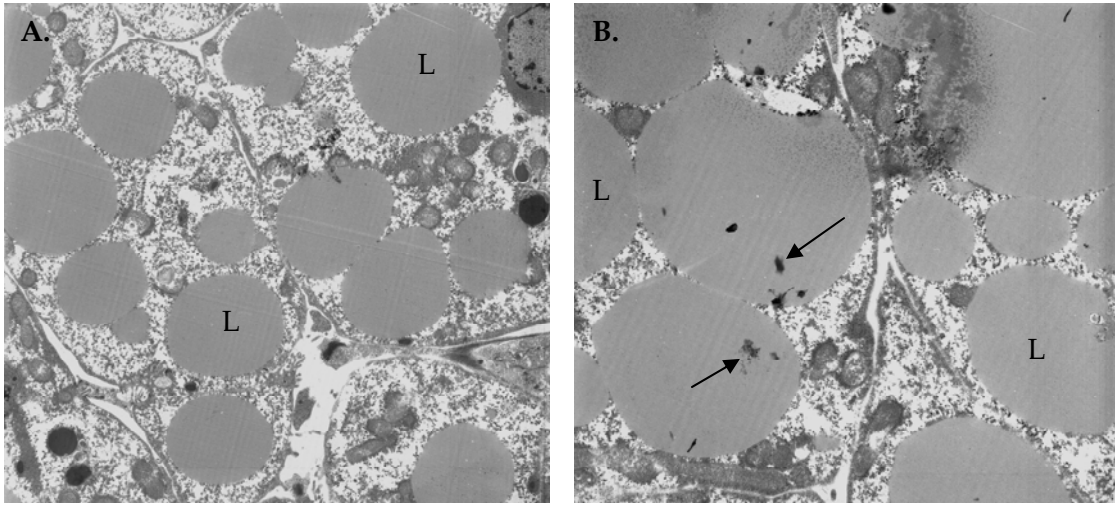


Figure 4-3. Electron micrographs of liver sections from a male *Fundulus* after dietary exposure to the SD + Lecithin diet for 85 days. Hepatic lipid vacuolation (L) is the major alteration. Note the unknown substances (arrows) in the vacuoles, which are believed to be cellular debris. Magnification: (A) 2,500 X (B) 4,000 X.

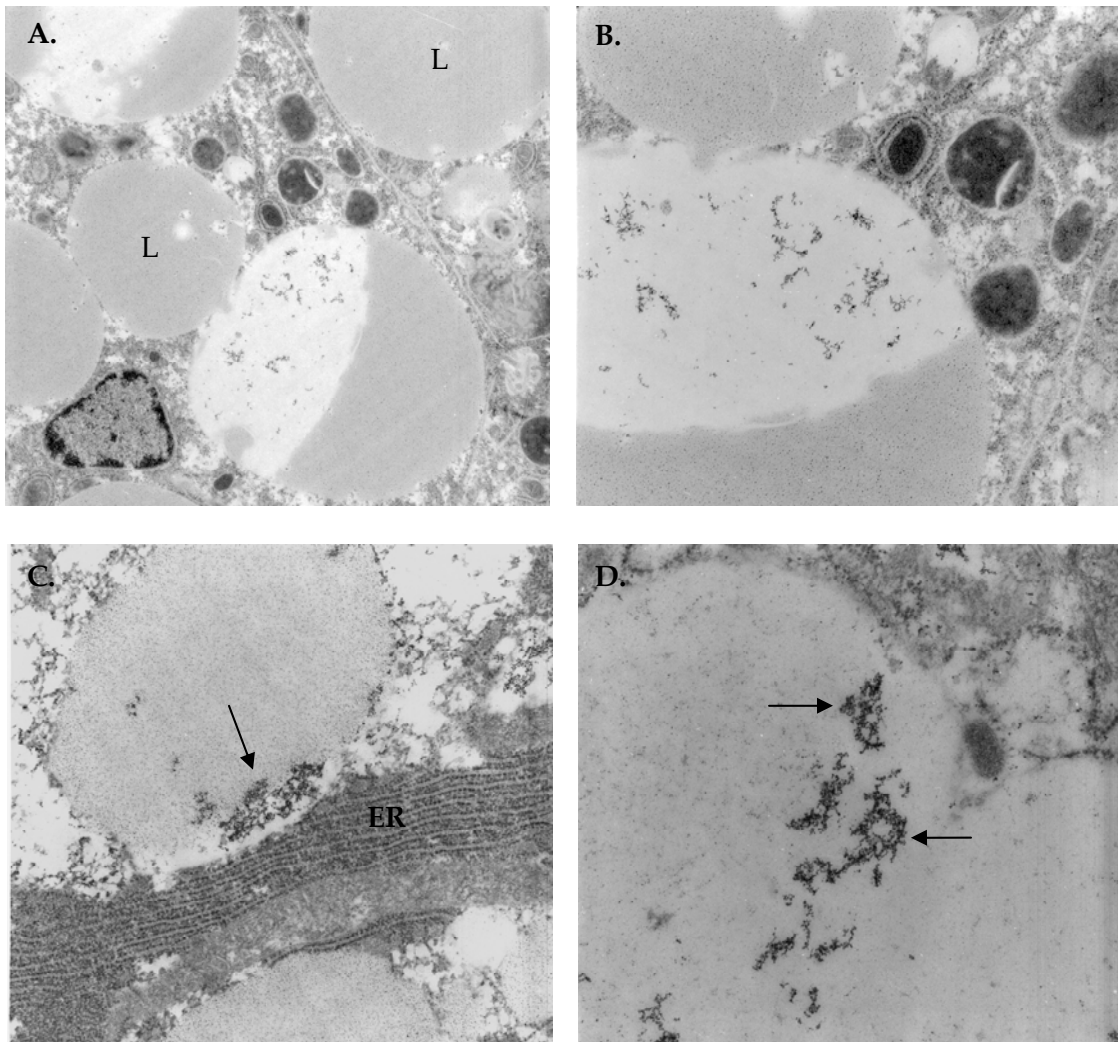


Figure 4-4. Electron micrographs of liver sections from a male (A, B) and female (C, D) *Fundulus* that have been fed the High QD diet for 85 days. The unknown substances (arrows) in the lipid vacuoles are presumed to be QD aggregates and show a different, more diffuse aggregate structure than the unknown substances present in Figure 4-3 above. L=lipid, ER=endoplasmic reticulum. Magnification: (A) 8,000 X, (B) 16,000 X, (C) 20,000 X, (D) 31,500 X.

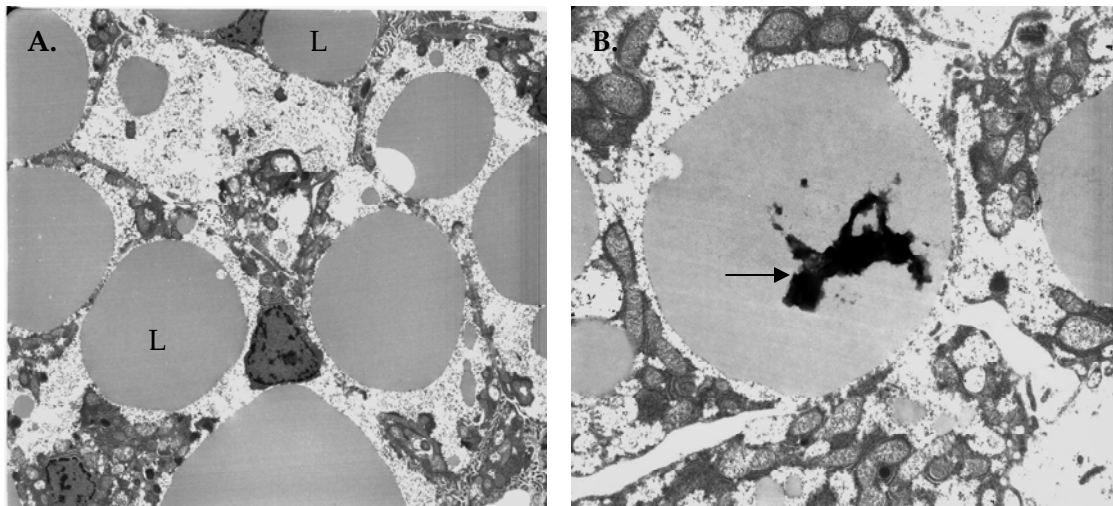
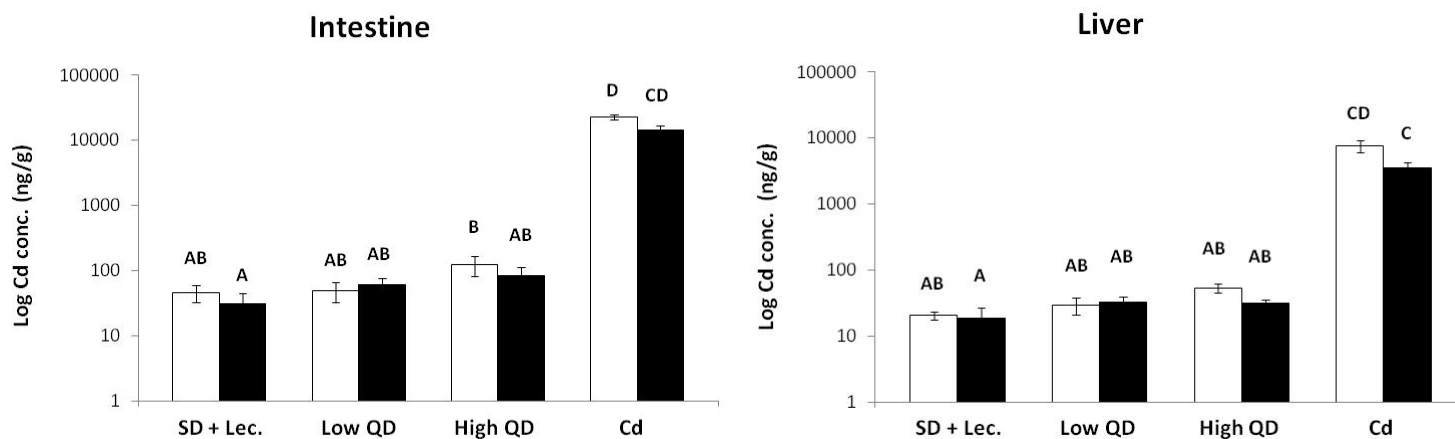


Figure 4-5. Electron micrographs of liver sections from a male *Fundulus* that has been fed the CdCl₂ diet for 85 days. Field A shows enhanced lipid vacuolation (L), while field B shows a lipid vacuole containing a large aggregate of unknown origin (arrow). Magnification: (A) 2,500 X (B) 6,300 X

QD uptake was also evaluated by measuring the cadmium concentrations in intestinal and liver tissues. Statistical analysis revealed that the intestinal Cd concentrations in male and female fish fed the CdCl₂ diet were significantly elevated from their SD + Lecithin counterparts (Fig. 4-6). Cd-treated females had an average intestinal Cd concentration of $23,017.3 \pm 2,110.8$ ng Cd/g tissue versus 46.1 ± 13.9 ng Cd/g tissue in females receiving the SD + Lecithin diet, while males receiving the Cd diet had an average intestinal concentration of $14,451.0 \pm 2,451.4$ ng Cd/g tissue compared with 31.3 ± 13.2 ng Cd/g tissue in the SD + Lecithin males. Similarly, liver cadmium

concentrations of both sexes were significantly increased in the Cd diet versus SD + Lecithin diet. In females, the average cadmium concentration in the liver was $7,680.4 \pm 1,620.2$ ng Cd/g tissue in Cd diet versus 20.8 ± 2.9 ng Cd/g tissue in the SD + Lecithin treatment. Males receiving the Cd diet had an average liver Cd concentration of $3,573.7 \pm 710.8$ ng Cd/g tissue compared to 18.7 ± 8.0 ng Cd/g tissue in males fed the SD + Lecithin treatment. Cadmium concentrations in the Low and High QD diets were not statistically different from the SD + Lecithin diet in either organ when combined in one data set for statistical comparison. However, the cadmium concentrations in the intestine and liver of *Fundulus* fed the High QD diet are statistically increased from the SD + Lecithin group when the data sets for each tissue are analyzed separately (see Table 4-3).

When uptake was examined with regard to sex-specific differences, it was determined that females acquired cadmium more readily than males ($P=0.0013$), but that this phenomenon was not affected by the treatment ($P=0.8096$). There were no statistical differences in cadmium concentrations between males and females within each treatment diet in either intestine or liver tissues (Fig. 4-6); therefore, male and female data were combined to calculate the average cadmium concentrations listed in Table 4-3.



Factor	p-value	Factor	p-value
Treatment	<0.0001	Treatment X Tissue	0.1007
Tissue	<0.0001	Treatment X Sex	0.8096
Sex	0.0013	Treatment X Tissue X Sex	0.5817

Figure 4-6. Cd concentrations of intestine and liver tissues in female (open) and male (filled) *Fundulus heteroclitus* after being treated for 85 days. Bars are mean \pm standard error. Bars not connected by the same letter are significantly different. A 3-factor ANOVA ($\alpha = 0.05$) was used for statistical analysis, thus comparisons can be made between treatments, sexes, and tissues. The table denotes the p-values for each statistical factor individually as well as the various crosses in the 3-factor ANOVA.

Cadmium concentrations were also affected by tissue type ($P < 0.0001$), though it may or may not have been influenced by treatment ($P = 0.1007$). Thus, statistical comparisons in Table 4-3 are non-parametric 1-factor ANOVAs and should not be compared between the tissues.

Table 4-3. Average Cd concentrations in the intestine and liver after the exposure

Treatment	Intestine (ng Cd/g tissue)	Liver (ng Cd/g tissue)
Std Diet (SD)	37.0 ± 6.0	43.9 ± 10.0
SD + Lecithin	38.7 ± 9.4	19.8 ± 4.1*
Low QD	55.9 ± 11.2 (< 0.01%)	31.4 ± 5.2 (< 0.01%)
High QD	102.8 ± 25.4 (< 0.01%) ^a	41.6 ± 5.7 (< 0.01%) ^a
Cd	18,734.2 ± 2011.5 (0.9%) ^a	5,627.0 ± 1046.3 (0.5%) ^a

* denotes a statistically significant difference between the Standard Diet and SD + Lecithin treatments; ^a statistically different from the SD + Lecithin treatment, $\alpha = 0.05$, $N = 10-12$.

Lecithin supplementation affected hepatic, but not intestinal cadmium concentrations. There was a significant difference in the hepatic Cd concentration between the Standard Diet and SD + Lecithin groups (Table 4-3). Cadmium was not incorporated into either diet (Table 4-1), so the cadmium detected was accumulated from the natural environment prior to this study. The decreased hepatic cadmium concentration in the SD + Lecithin treatment corresponds with the increased relative

liver size (Fig. 5-2), thus Lecithin supplementation diluted the accumulated cadmium over a larger organ.

Measurement of Cd uptake in intestine and liver tissues suggest QDs or their degradation products were bioavailable, but that they were not retained in appreciable amounts (Table 4-3). The total Cd dose administered over the course of the 85 day exposure period was 12.5 µg Cd/fish in the Low QD diet, 125.2 µg Cd in the High QD diet, and 240.8 µg Cd in the CdCl₂ diet based on the diet analysis (Table 4-1). Cd-exposed fish had significantly elevated cadmium levels in intestinal ($18,734.2 \pm 2,011.5$ ng Cd/g tissue) and liver ($5,627.0 \pm 1,046.3$ ng/g) tissues when compared to the SD + Lecithin tissues (38.7 ± 9.4 ng/g in the intestine and 19.8 ± 4.1 ng/g in the liver). No appreciable amount of cadmium was retained within the intestines or liver of *Fundulus* fed the Low QD diet; however, the average cadmium concentrations in the intestine and liver of animals fed the High QD diet were significantly increased (102.8 ± 25.4 and 41.6 ± 5.7 ng/g, respectively) from the SD + Lecithin diet. Given the Cd concentrations in the intestinal and liver tissues, it was determined in both QD treatments that less than 0.01% of the total dose was retained within the tissues. Alternately, 0.9% of the total cadmium administered was retained in the intestine and 0.5% retained within the liver of fish receiving the Cd diet.

Oxidative Stress Biomarkers

Oxidative stress biomarkers were measured in adult liver tissue to determine if the organisms elicited a response as a result of QD or Cd ingestion. Total glutathione (Fig. 4-7A) and lipid peroxidation levels (Fig. 4-7B) were not statistically different from the SD + Lecithin treatment. Furthermore, supplementation of the Standard Diet with Lecithin had no significant effect on total glutathione or lipid peroxidation levels (Figures A-1 and A-2).

While there were no sex-specific differences in glutathione levels, lipid peroxidation showed a different response pattern between sexes. Though statistically insignificant, males showed a very slight increase in MDA levels with treatment, whereas females showed variable MDA levels. Low and High QD females had elevated levels of MDA (35.0 ± 15.5 and 23.0 ± 8.7 nmol MDA/g tissue, respectively) when compared to the SD + Lecithin females (21.2 ± 6.3 nmol/g), while Cd-treated females had a lower MDA level (15.8 ± 2.1 nmol/g).

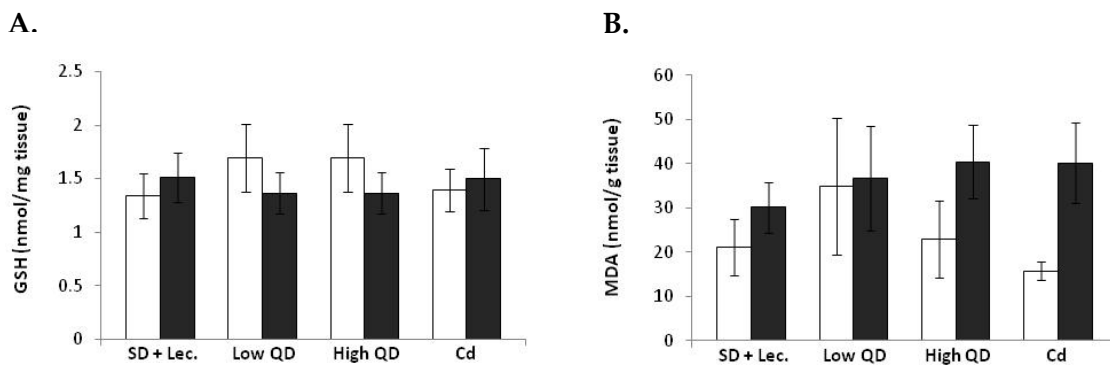


Figure 4-7. The average hepatic (A) total glutathione and (B) lipid peroxidation levels in female (open boxes) and male (filled boxes) *Fundulus heteroclitus* after 85 days of continuous dietary exposure to CdSe/ZnS nanocrystals. Bars are mean \pm standard error.

Gene Expression Changes

RNA expression of oxidative stress responsive genes (Fig. 4-8A) shows that *mt* was upregulated, though insignificantly, in response to Cd consumption (3.02 ± 0.7 fold induction versus 1.53 ± 0.4 in the SD + Lecithin diet). This increased expression was not observed in QD treated fish (1.14 ± 0.2 fold induction). Expression of *gstmu*, *gpx*, *sod1*, and *sod2* were not significantly affected by QD or Cd exposure. Sex-specific differences in expression were examined for each target gene (Figures A-3 through A-7); however, only *sod1* was differentially induced in males and females. Trends indicate that females given the High QD or Cd diets upregulated *sod1*, while expression in males did not change (Fig. 4-8B). Because of high individual variation, neither males nor females in the Cd treatment group had *sod1* levels that were significantly different from the SD +

Lecithin treatment. However, *sod1* expression in these two groups was significantly different from each other (0.86 ± 0.2 fold induction in males versus 3.59 ± 0.8 fold induction in females). Although statistically insignificant, the High QD females and males showed the same tendencies as those fish in the Cd diet with regard to *sod1* transcription.

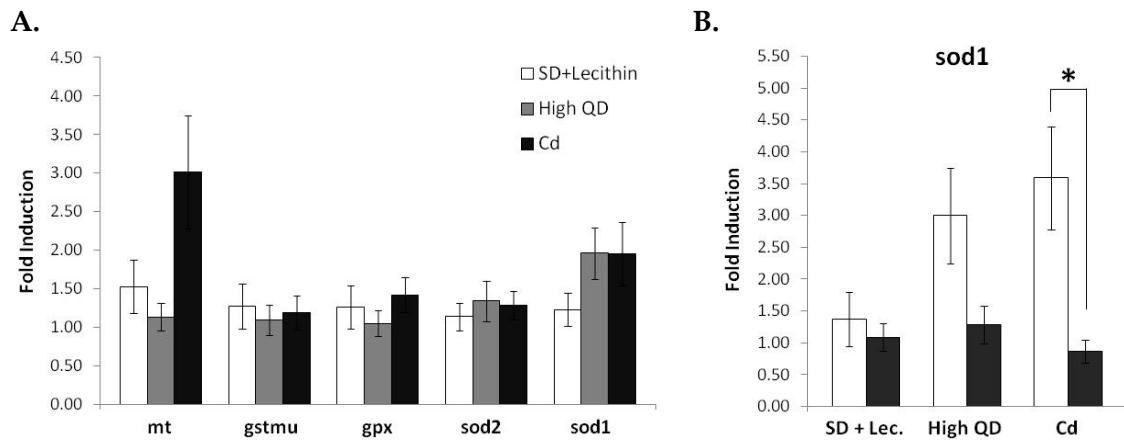


Figure 4-8. Expression changes (A) in metallothionein (*mt*), glutathione-*s*-transferase (*gstmu*), glutathione peroxidase (*gpx*), Mn-superoxide dismutase (*sod2*), and Cu/Zn-superoxide dismutase (*sod1*) hepatic RNA levels; and (B) sex-specific differences in *sod1* expression in female (open boxes) and male (filled boxes) *Fundulus heteroclitus* after 85 days of dietary exposure. Bars are mean fold induction \pm standard error. Asterisks indicate statistical differences between the sexes, $\alpha = 0.05$.

Histopathology

Upon dissection, it was noted that a male from the Cd diet had developed a testicular tumor measuring approximately 2.5 cm in length and weighing 1.50 grams, an order of magnitude greater than the average gonad weight across all males (0.1138 g) and of the Cd treated males (0.1 g). Histopathological examination revealed swelling and degenerative damage in the testes of the Cd-treated male (Fig. 4-9). The abundance of sperm was noticeably reduced when compared to a male *Fundulus* receiving the Standard Diet (Fig. 4-10).

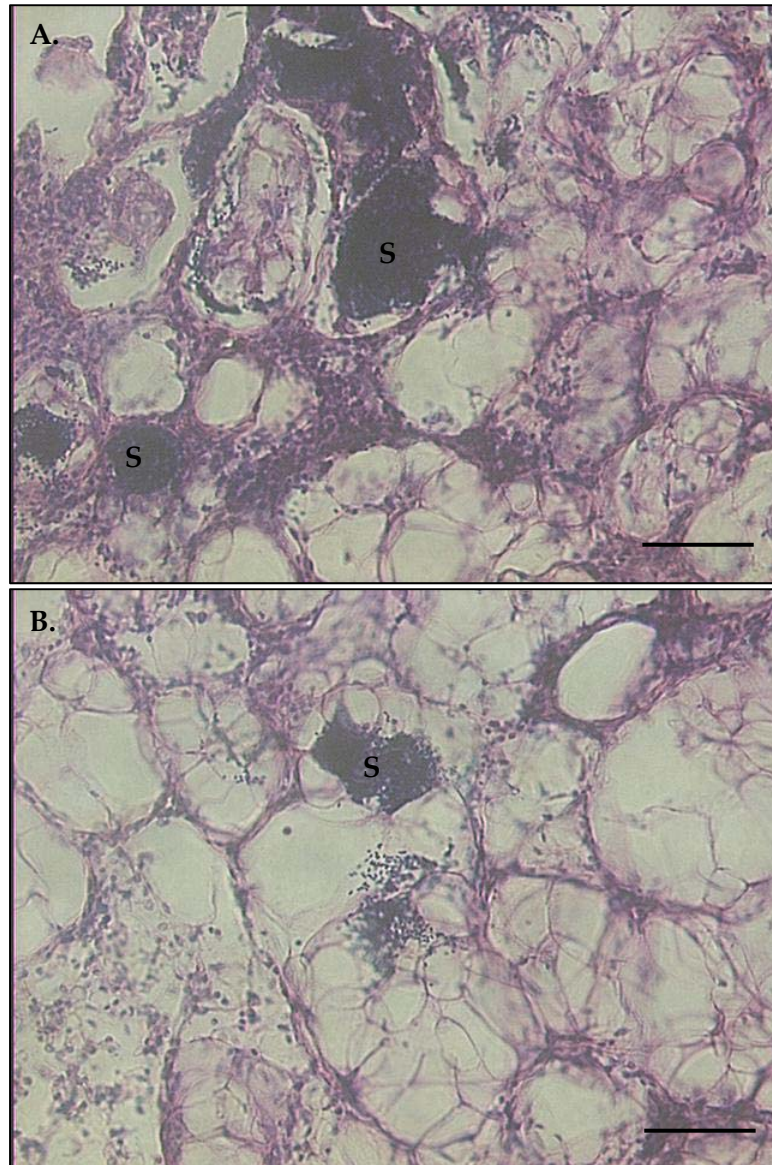


Figure 4-9. Light micrographs of 6 μm sections of testes from a *Fundulus* fed the Cd diet. Swelling and degeneration are apparent in both fields. Note the abundance of open spaces devoid of sperm (S). Magnification: 400X. Scale bar = 50 μm .

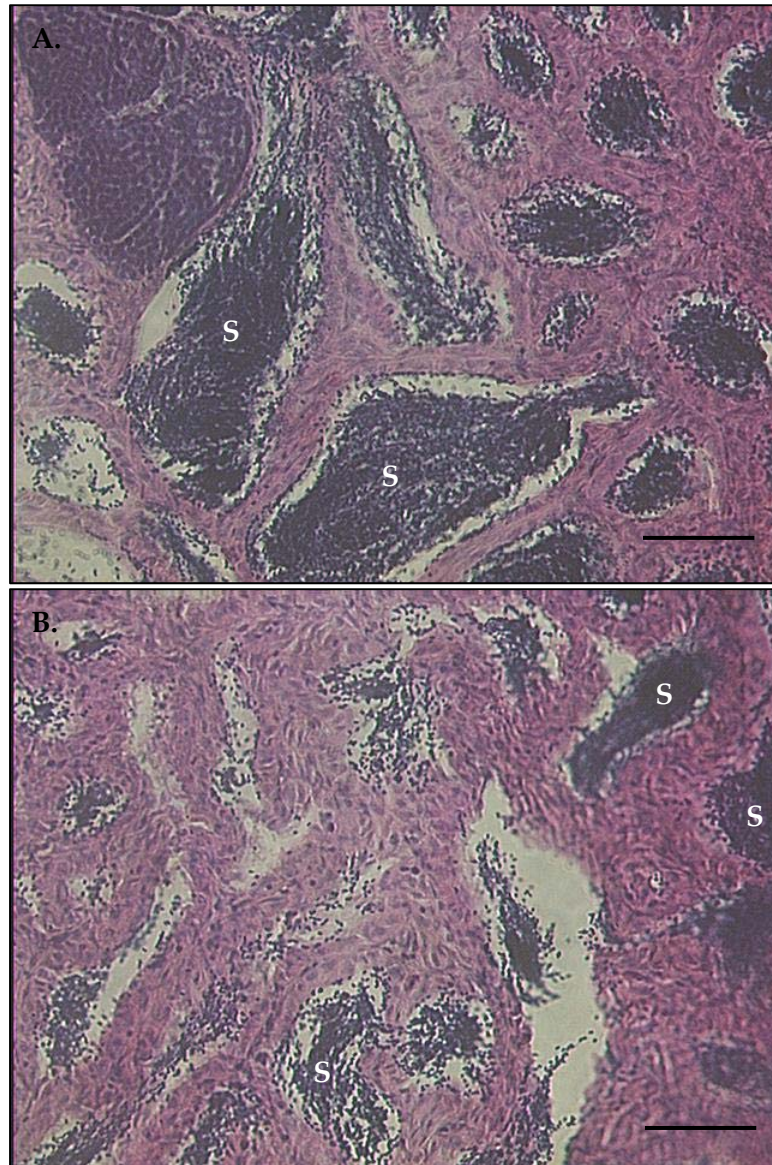


Figure 4-10. Light micrographs of testes from *Fundulus* fed the Standard Diet. The dark clusters are sperm (S). Compare the structure of the normal testes to that of Figure 4-9. Magnification: 400X. Scale bar = 50 μ m

Liver pathology was extended from the survey histopathology (Chapter 3) by examination of sections of epon embedded livers stained with Richardson's methylene blue/Azure II/ borate solution [216]. Male and female *Fundulus* livers showed enlarged hepatocytes with extensive vacuolation of lipid (as aquamarine staining material). This lipid vacuolation appeared regardless of the treatment diet (Figures 4-11 through 4-14). Spongiosis hepatitis is a degenerative lesion seen during serial investigations of the progression of liver carcinogenesis in fishes [220]. Thin extensions of stellate cells of Ito, the perisinusoidal cells that form the hepatic skeleton, delineate spaces once occupied by hepatocytes [221]. Spongiosis hepatitis was observed in livers of females fed the Standard, High QD, and Cd diets (Figures 4-11A, 4-12A, and 4-14B, respectively) suggesting that the appearance of this type of lesion was not a function of treatment, but reflected the stress due to aging and/or reproductive activity. Necrosis, however, was seen in female *Fundulus* fed the High QD diet (Fig. 4-13). Debris and necrotic hepatocytes were observed in the rounded spaces. Neither spongiosis hepatitis nor necrosis were observed in any of the liver sections from male fish (data not shown).

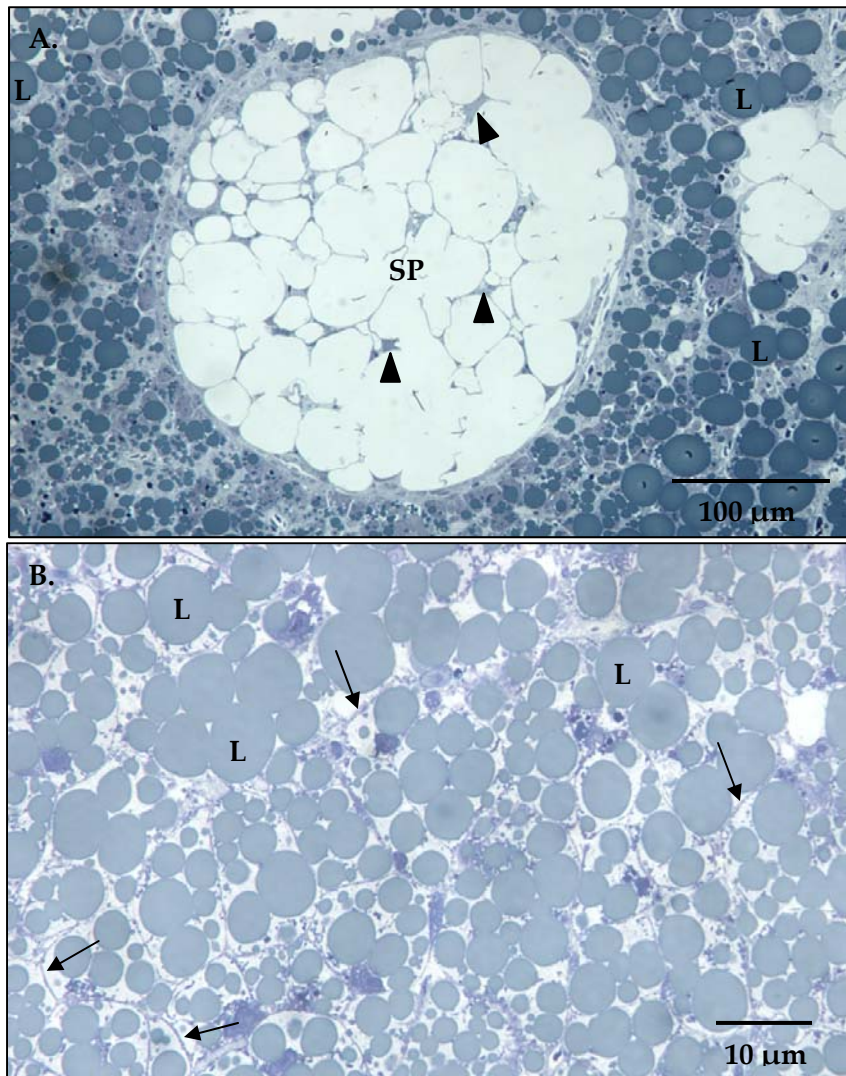


Figure 4-11. Light micrographs of liver sections from female *Fundulus* fed the Standard Diet. Micrograph A shows a spongiosis hepatis (SP) in center of field with septae of stellate cell cytoplasm partially dividing the lesion and appearing sponge like. Flattened nuclei are occasionally seen (arrowheads). Note the extensive hepatocyte lipid vacuolation (L) seen as aquamarine staining circular forms. Field B is from a different female fish fed the same diet. Arrows point to hepatocyte plasma membrane and show the extent of enlargement of these cells. 0.5 μm section of epon embedded liver stained with Richardson's methylene blue/Azure II/ borate solution [216]. Magnification: (A) 200X, and (B) 600X.

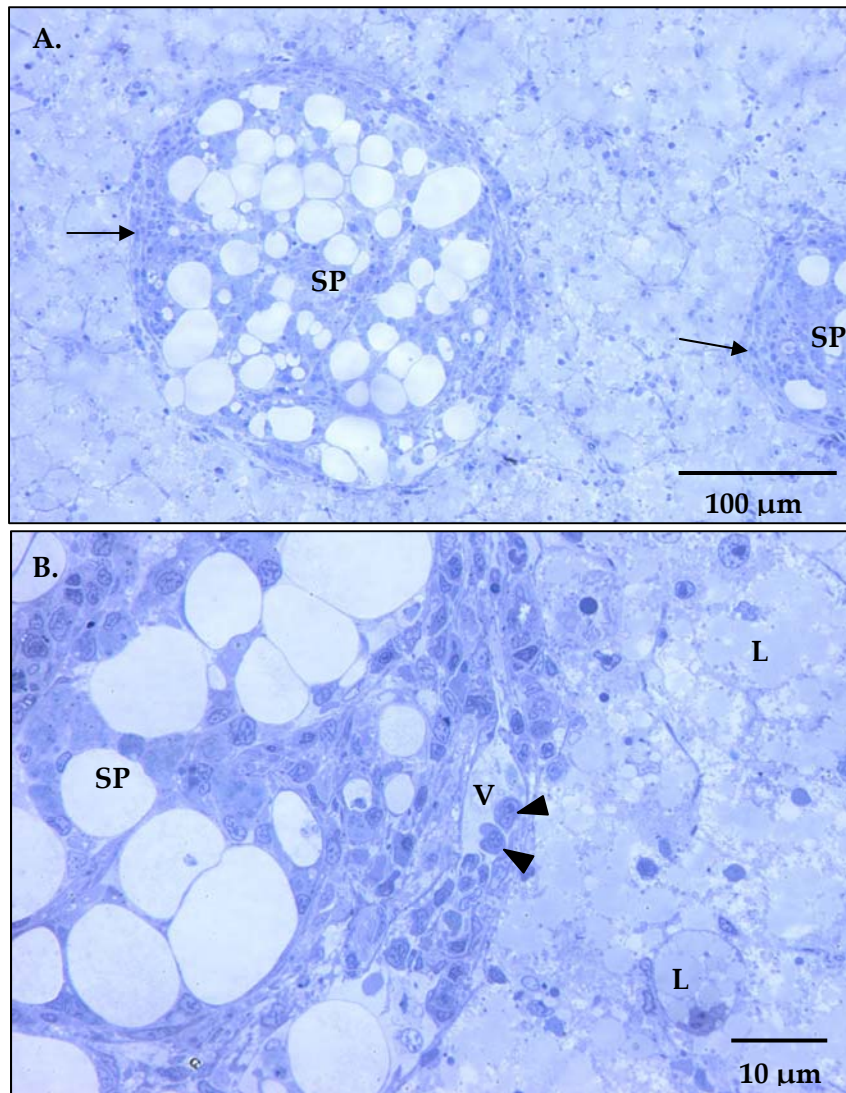


Figure 4-12. Light micrographs of liver sections from female *Fundulus* fed the SD + Lecithin diet. Field A shows two foci of inflammation with spongiosis hepatis (SP). At the margin of the lesions, note inflammatory cells (arrows). (B) is an enlarged view of the margin of spongiosis hepatis seen in A. Vessel (V) at margin of spongiosis shows margination of inflammatory cells (arrowheads). Hepatocytes fill right side of field and show marked lipid (L) in the cytoplasm. Lipid accumulation is associated with enhanced volume of hepatocytes. 0.5 µm section of epon embedded liver stained with Richardson's methylene blue/Azure II/ borate solution [216]. Magnification: (A) 200X, and (B) 600X.

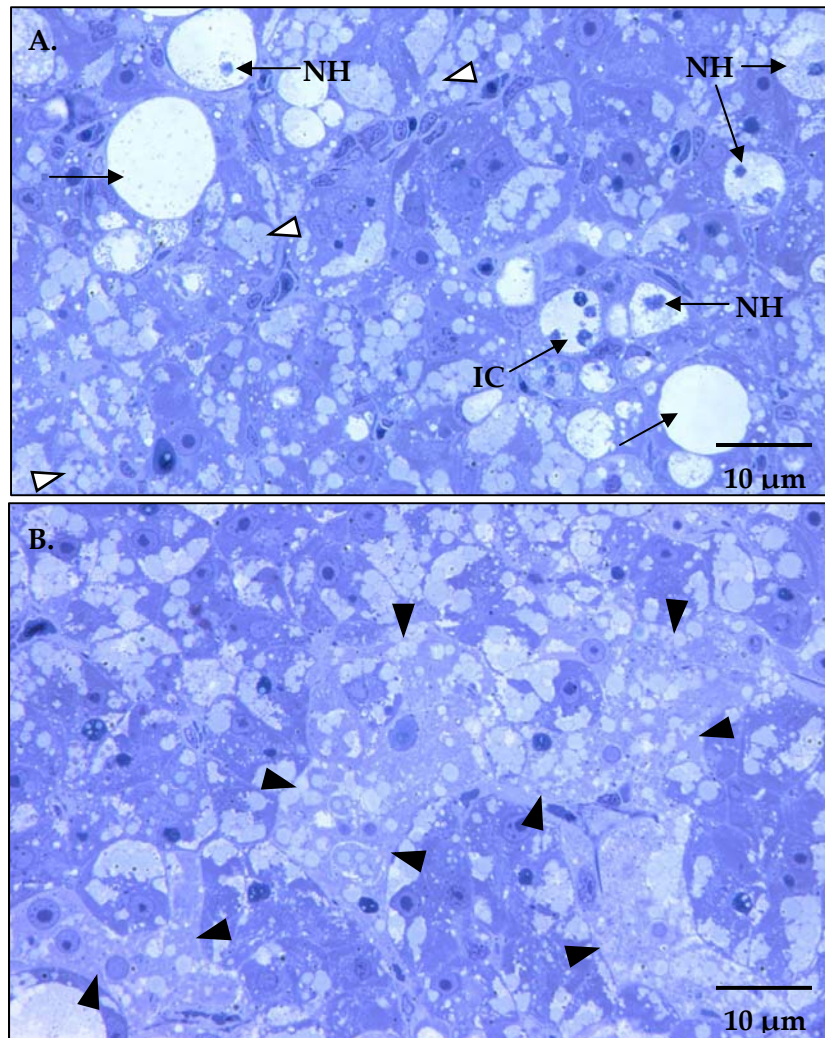


Figure 4-13. Liver of female *Fundulus* fed the High QD diet. (A) While lipid vacuoles are present in most hepatocytes of the field, they are smaller in diameter than seen under the SD or SD + Lecithin diets (open arrowheads). Large circular areas contain: clear space – and may represent fluid accumulation (arrows) or sites of debris from necrotic hepatocytes (NH); other spaces contain inflammatory cells (IC). (B) is another field from the liver of the female fish fed the High QD diet. Contiguous hepatocytes are undergoing necrosis (filled arrowheads). The majority of hepatocytes contain lipid and variable areas of cytoplasm showing darker staining. 0.5 μm section of epon embedded liver stained with Richardson’s methylene blue/Azure II/ borate solution [216]. Magnification: 600X.

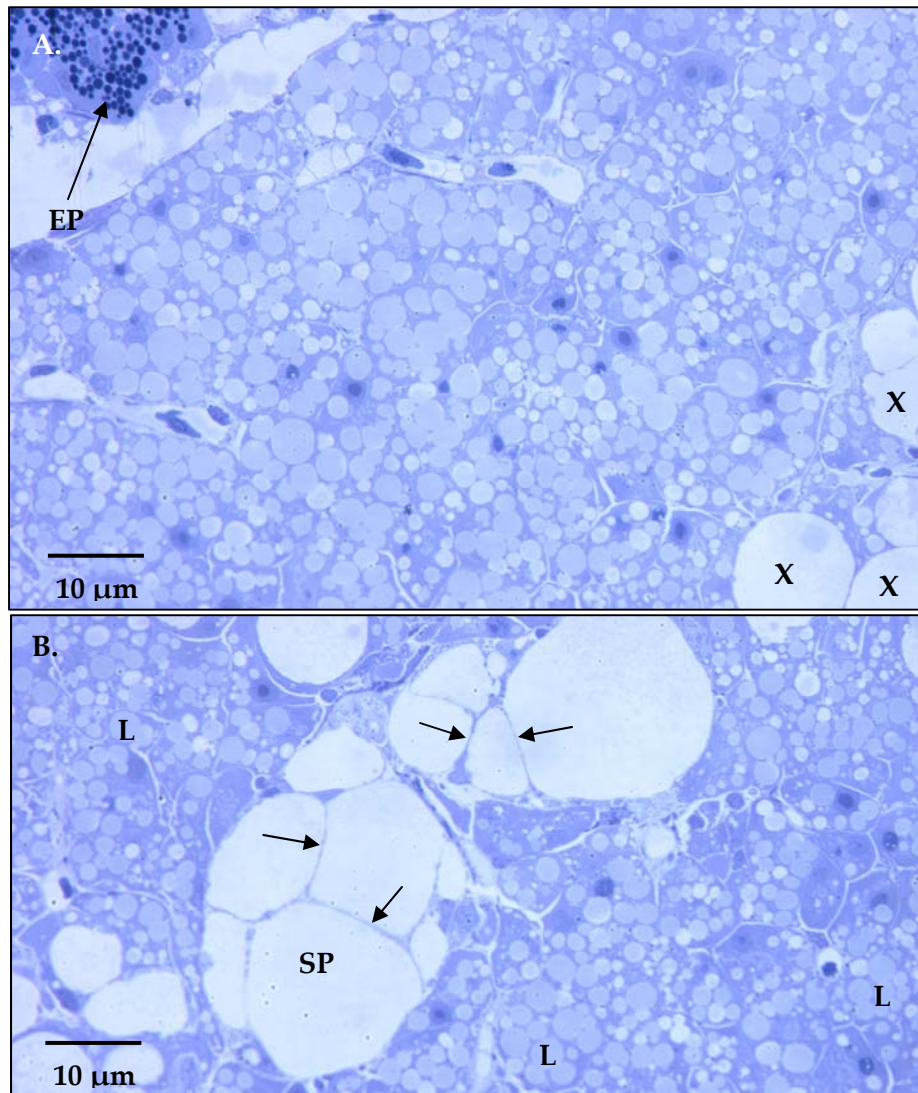


Figure 4-14. Light micrographs of a female *Fundulus* fed the Cd diet. The exocrine pancreas (EP) is in the upper left of field A. Importantly, the extent of lipid vacuolation is marked with all hepatocytes being affected. Larger clear vacuoles (X) are likely sites where hepatocytes once resided. Micrograph (B) shows a focus of spongiosis hepatis (SP). This lesion is comprised of large regions containing fluid or very lightly staining material. The thin septae (arrows) are comprised of hepatic stellate cells, the “skeleton” of the liver. Hepatocytes are filled with numerous lipid (L) vacuoles. 0.5 µm section of epon embedded liver stained with Richardson’s methylene blue/Azure II/ borate solution [216]. Magnification: 600X.

Discussion

Bioavailability

Given the increased production and commercial applications of quantum dots, it is prudent to evaluate how organisms respond to them. Cd analysis confirmed that QDs or their degradation products were taken up via diet and distributed to the liver, but not to the same extent as free cadmium. While the High QD diet contained roughly half as much cadmium as the Cd diet, the High QD intestinal and liver tissues had cadmium concentrations approximately 180 and 130 times lower than fish receiving the Cd diet. Evaluation of livers from exposed animals using TEM and confocal microscopy were inconclusive, so it remains to be determined if whole QDs were deposited to the liver, or if the particles degraded and free cadmium was re-distributed to the liver. At present, there are only a few publications in the literature that have examined uptake of ZnS shelled QDs in aquatic organisms. Carboxylated CdSe/ZnS QDs were observed in the digestive tracts of water fleas (*Ceriodaphnia dubia*) [222] and rotifers (*Brachionus calyciflorus*) [200], but QD distribution wasn't examined, thus it is not known if the QDs were assimilated. The fluorescent signal from PEG-functionalized CdSe/ZnS QDs was not observed in aqueously exposed zebrafish embryos/larvae (*Danio rerio*), but cadmium body burdens were elevated after 120 hours of exposure confirming uptake [195]. King-Heiden *et al.* [195] hypothesized that QDs were absorbed across the skin and gills, but

assimilation and distribution of cadmium to the tissues were not examined. However, Karabanovas *et al.* [60] used the fluorescent signal of CdSe/ZnS QDs to determine that whole QDs traversed the esophagus and duodenum when administered to Wistar rats. It has also been reported that core-shell QDs can be degraded by gastric fluids and enzymes *in vitro* [60, 223]. Taken together, this suggests that whole as well as degraded QDs will pass through the walls of the upper digestive tract.

Given the disparity in cadmium tissue concentrations between QD and Cd-treated fish, it is likely that QD uptake and accumulation were very low. There are notable differences in total cadmium retained in the tissues of fish receiving the QD and Cd diets. QD-treated fish retained less than 0.01% of the total dose administered in the intestine and liver (as it pertains to Cd content of the food versus the tissues), while *Fundulus* given the Cd diet retained 0.9% of the total dose in the intestinal tissue and 0.5% in the liver. These results suggest that while free cadmium uptake is relatively low, the configuration of the core-shell structure further inhibits QD bioavailability. The amount of free cadmium retained from the Cd diet is comparable to other sub-chronic dietary cadmium studies in fish ($\leq 1\%$ Cd accumulated) [55, 56]. Low retention occurs because a large amount of dietary Cd is bound in the digestive tract tissues (stomach, caecae, and intestines) [69] or eliminated via feces [56].

Although bioavailability of QDs and Cd from the diet was low, females had higher tissue cadmium concentrations than males. However, this phenomenon occurred independent of the treatment diet. This indicates that females, in general, are at risk of accumulating higher Cd burdens and are more susceptible to Cd toxicity than males. Though cadmium's endocrine disrupting capabilities are disputed in the literature [224-228], it is a known reproductive toxicant and teratogen [82, 229]. This implies that subsequent reproductive and developmental effects would cause declines in fish populations.

Oxidative Stress Biomarkers

Another potential consequence of QD or Cd uptake is the generation of reactive oxygen species. Excessive ROS causes oxidative stress, which can lead to DNA, lipid, protein, and enzyme damage [230-232]. *In vitro* studies have reported the generation of ROS and oxidative stress as a consequence of exposure to shelled and unshelled QDs [35, 38, 41, 42, 233, 234]. Yet, little is known about the ability of QDs to generate ROS and cause oxidative stress in whole animal models; thus, we measured the occurrence of molecular biomarkers for oxidative stress in exposed *Fundulus*. In our study, total glutathione and lipid peroxidation levels were not significantly altered by QDs, which is conceivable given that uptake of QDs or their degradation products was extremely low.

This is consistent with our 5 week dietary exposure of mummichogs to CdSe/ZnS QDs [235] and a 21 day aqueous exposure of sticklebacks (*Gasterosteus aculeatus*) to CdS QDs [199]. However, our results are in contrast to a study by Gagné and colleagues [61] where lipid peroxidation levels were significantly elevated in the gills of freshwater mussels (*Elliptio complanata*) acutely exposed to CdTe QDs. The conflicting results are likely due to differences in the type of QD, concentrations, exposure length, tissue type, and model organisms.

The stability of QDs is a function of structure and environmental conditions. Cho *et al.* [42] reported that unshelled CdTe QDs leached free Cd²⁺, while the ZnS-shelled QDs showed no detectable levels of free cadmium at 24 hours. However, shelling QDs does not provide absolute protection. A ZnS shell delays, but does not prevent oxidative degradation of QDs [19]. The liberation of cadmium from degraded QDs would affect antioxidant and lipid peroxidation levels as free cadmium indirectly generates ROS (superoxide anion, hydrogen peroxide, and the hydroxyl radical) [75]. As such, unshelled QDs are expected to more effectively induce an oxidative stress response than shelled QDs as long as a threshold level of free cadmium is attained.

The duration of the exposure also influences oxidative stress biomarkers. In acute QD exposures, detoxification biomolecules metallothionein and glutathione are depleted, while lipid peroxidation levels are elevated [49, 61, 62, 234]. Yet, in the only sub-chronic QD study published thus far, oxidized glutathione levels in sticklebacks were not altered by aqueous exposure to CdS QDs suggesting limited bioavailability and/or adaptation by the organism to the insult [199].

Changes in glutathione levels are dose- and time-dependent with respect to free cadmium exposure. In acute *in vitro* exposures, Pathak and Khandelwal [236] reported dose-dependent glutathione depletion. However, other studies have shown transient changes in glutathione levels; glutathione concentrations were initially elevated, but then fell to slightly above Control levels and were accompanied by increased lipid peroxidation [237, 238]. Transient effects on these molecular biomarkers were also noted during longer cadmium exposures. For example, hepatic total glutathione was elevated on day 14, but not day 28 in rainbow trout (*Oncorhynchus mykiss*) aqueously exposed to Cd [239]. Berntssen *et al.* [240] showed that even though hepatic cadmium concentrations were significantly elevated in Atlantic salmon (*Salmo salar*) after 1 month of dietary exposure to Cd (204 mg/kg), hepatic lipid peroxidation and total glutathione levels were unaltered. If intermediate time points were not taken, as was the case in our

study and that of Berntssen *et al.* [240], early changes in glutathione levels may have been missed. This adaptive response occurs because metal contaminants signal the synthesis of additional antioxidants to quench ROS and for metallothionein to bind/sequester un-necessary or excess free metals. Hence, the increased antioxidant levels may persist for a period of time, after which antioxidant levels fall despite continued contaminant exposure [239-241].

Certain forms of selenium have also been linked to the generation of superoxide anion and hydrogen peroxide [97, 242, 243]. Although selenide is one of the major components of CdSe/ZnS QDs, we did not measure selenium in this study because it is an essential micronutrient and the accuracy of detection was uncertain. While selenide is not a form of Se that is linked to ROS generation, possible transformation into one of the toxic forms of selenium is acknowledged and should be considered.

Gene Expression Changes

As mentioned previously, oxidative stress signals the upregulation of a suite of ROS-related genes including thioredoxin, metallothionein (mt), glutathione-s-transferase (gstmu), glutathione peroxidase (gpx), and superoxide dismutases (sod1 & sod2) [75, 244]. We determined that mt signaling was not altered by exposure to the High QD diet,

but that fish receiving the Cd diet had twice the amount of mt RNA as the SD + Lecithin diet. This slight increase in mt transcription is supported in the literature [239, 244-247]. Cadmium's affinity for metallothionein and its ability to displace zinc in the configuration of metallothionein is well known, as is the increase in metallothionein production that occurs when labile Zn is subsequently increased. Lange *et al.* [239] correlated transient hepatic mt mRNA levels with hepatic cadmium concentrations. Silver barb (*Puntius gonionotus*) aqueously exposed to Cd had elevated hepatic mt mRNA levels from day 5 to 56, though levels peaked at day 28 and subsequently declined [247]. Conversely, Roesijadi *et al.* [248] reported that dietary cadmium exposure of *Fundulus* for 7 days resulted in significantly increased intestinal mt mRNA, but insignificantly increased hepatic mt mRNA levels. The differences in reported effect emphasize the importance of exposure route. It's probable that like Lange *et al.* [239], the *Fundulus* livers hadn't accumulated or maintained sufficient cadmium to induce a change in metallothionein transcription.

Although none of the oxidative stress-related genes were significantly altered by QD or Cd exposure, there were sex-specific differences in sod1 mRNA levels. Females fed the High QD and Cd diet had sod1 levels that were elevated, though not significantly, whereas males had sod1 mRNA levels that were consistent with that of the

SD + Lecithin males. This is one possible explanation for the unusual trend observed in female lipid peroxidation levels. Though we did not measure actual SOD1 levels, if they were elevated as suggested by the upregulation of the signal, this would combat lipid peroxidation by quenching radicals and mitigating the damage of lipid radicals.

Histopathology

A testicular tumor was present in one of the *Fundulus* fed the Cd diet. While the linkage between cadmium and testicular tumors is well established in rodents [249], the correlation in fish is unsubstantiated by the literature. Acute cadmium exposure has been linked to testicular damage (hemorrhagic necrosis) in adult brook trout [250] as well as lesions (fibromas and granulomas) in the kidneys of rainbow trout [251], but no evidence of testicular tumors was recorded, perhaps due to the short duration of these studies.

Pathological examination of the liver revealed that females were more affected than male fish. Spongiosis hepatitis was only observed in female *Fundulus*. While this type of lesion has previously been linked to contaminant exposure, it was observed in females fed the Standard Diet suggesting that reproduction may have a significant impact on female liver morphology and that some changes likely resulted from this

physiological stressor. Spongiosis hepatitis is a degenerative lesion commonly seen in some strains of aging rats [252]. The lesion was also seen during serial investigations of the progression of liver carcinogenesis in fishes [220]. More dramatic changes in liver morphology occurred in female *Fundulus* fed the High QDs diet. QDs caused hepatic necrosis and inflammation. Little information is available in the literature regarding pathological alterations induced by QDs. Sanders *et al.* [199] reported that aqueous exposure to unshelled CdS QDs caused hepatocellular nuclear pleomorphisms in sticklebacks, while Ramot *et al.* [253] observed multifocal organizing thrombi in pulmonary arteries of NOD/SCID mice (T and B cell lymphocyte impaired) i.v. injected with QD-labeled stem cells. This suggests that QDs or their degradation products could have significant effects on morphology, and thus deserves continued study.

Conclusions

As the popularity of engineered nanoparticles grows, they will become ubiquitous in the environment due to use and disposal. In this simplified dietary study, pristine CdSe/ZnS quantum dots that were consumed by fish were minimally bioavailable and did not elicit an oxidative stress response. However, QDs did cause necrosis in female *Fundulus*. As more information comes to light regarding mechanisms of toxicity, trophic transfer, and the environmental fate of ENPs, we will be able to

determine if QDs pose a significant risk to aquatic organisms given their low bioavailability.

Chapter 5. Reproductive Toxicity and Maternal Transfer of CdSe/ZnS QDs in Mummichogs

Engineered nanoparticles have been detected in aqueous environments following their release from commercial products. Weather events caused leaching of nano-TiO₂ from building paints to surface waters [181], and antimicrobial socks released nano-Ag in wash water [182]. This presents an environmental dilemma as the ENPs that are revolutionizing medicine, environmental remediation technology, construction materials, and energy efficiency may cause toxicity in aquatic environments. Currently little information exists on the bioavailability and sub-lethal effects of ENPs to aquatic organisms. As such, there is a need for *in vivo* toxicological studies given the instability of ENPs in products.

ENPs such as fullerene (C₆₀) and titanium dioxide (TiO₂) have already been associated with reproductive and developmental impairment [212, 254-256]. Water-stirred fullerene (nC₆₀) decreased fecundity in water fleas (*Daphnia magna*) by delaying molting and subsequent breeding [212]. nC₆₀ also accumulated in neonates and caused reproductive impairment in greater than 90% of the daughter daphnids by delaying reproductive maturity [254]. Mice that were prenatally exposed to fullerene died as a result of severe head, tail, and yolk sac deformities, and maternally transferred TiO₂ was deposited in the brain and testes of male offspring, thus affecting genital and cranial nervous system development [255, 256].

We recently determined that quantum dots, a type of ENP that emits a fluorescent signal based on the diameter of its metallic core, are bio-available to estuarine fish. *Fundulus heteroclitus*, the mummichog, assimilated CdSe/ZnS QDs from its diet and distributed the QDs or their degradation products to the liver—the organ responsible for producing the egg-yolk precursor protein in teleosts. This suggests a potential risk to *Fundulus* progeny through maternal transfer. Moreover, QDs are known to degrade *in vivo* [60, 223]. QD constituents, cadmium and selenium, are known reproductive and developmental toxicants [82-84, 86, 107-110]. So, to evaluate the ability of QDs to cause reproductive and developmental effects in fish, Lecithin-encapsulated CdSe/ZnS QDs were incorporated into the diet of sexually mature *Fundulus* for approximately 3 months. The objectives of this study were to monitor reproduction, observe embryonic development, quantify cadmium uptake in eggs, and measure vitellogenin transcription in adult fish.

Materials and Methods

Chemicals

CdSe/ZnS Evidots (cat.# ED-C11-TOL-0620) were purchased from Evident Technologies (Troy, NY). Lecithin (102147) was purchased from MP Biomedicals, Inc. (Solon, OH, USA). CdCl₂ (202908) and gelatin (G-9382) was purchased from Sigma-

Aldrich (St. Louis, MO). Optima™ trace-metal free HNO₃ and H₂O₂ were purchased from Fisher Scientific (Pittsburgh, PA). The cadmium standard (CLCD-2-2Y) was purchased from Spex CertiPrep (Metuchen, NJ).

Quantum Dot Preparation

The preparation of the Lecithin-encapsulated CdSe/ZnS quantum dot (diameter = 5.2 nm, emit λ = 620 nm [4]) suspension is described in great detail in Chapter 4. Briefly, the QDs were precipitated from toluene, dried under vacuum, dissolved in chloroform, sonicated for 10 minutes in a bath sonicator, and stirred for 1 hour. Lecithin was added in a 1:1 Lecithin:QD ratio (by weight) to the chloroform-QD mixture and stirred in darkness overnight to encourage mono and bi-layer formation. The solvent was removed and sterile de-ionized water was added. The suspension was sonicated for 1 minute, mixed for 2 hours, and then sonicated again for 30 minutes to form small, uniform unilamellar vesicles [112]. The suspension was centrifuged at 125,000 g for 8 hours to break apart empty micelles [192]. After the supernatant was discarded, sterile DI water was added and the suspension was vortexed, transferred to a fresh glass vial, and sonicated for 5 minutes. The final QD suspension had a nominal concentration of 730 $\mu\text{g/ml}$ QD and 730 $\mu\text{g/ml}$ Lecithin. A Lecithin suspension was prepared in the same fashion and contained 730 $\mu\text{g/ml}$ Lecithin.

Diet Preparation

Five diets were prepared from the stock QD and Lecithin suspensions: the Standard Diet (SD), SD + Lecithin (0 μg QD and 10 μg Lec./day), Low QD (1 μg QD and 10 μg Lec./day), High QD (10 μg QD and 10 μg Lec./day), and CdCl₂ (3.4 μg Cd and 10 μg Lec./day). The diets were prepared by mixing 112.5 mg/ml ground tropical fish flakes (Aquatic Ecosystems, Apopka, FL), ~2% gelatin, and 250 μl /ml shrimp puree (1 shrimp homogenized in 10 ml of DI water) in sterile DI water. The appropriate amount of the QDs, Lecithin, and/or CdCl₂ were added to each food mixture and stirred for 5-10 minutes to obtain a homogeneous slurry. The diets were pipetted in 250 μl aliquots onto wax paper. After the discs cooled and solidified at room temperature, they were stored at -20°C until administered to the fish. The daily dose was achieved by feeding each fish two 250 μl discs per day (Table 4-1). Feeding was observed to ensure the discs were consumed.

While fluorescence is often used to determine QD concentrations in transparent suspensions [217], the complexity of the diets required the use of ICP-MS to measure the concentration of cadmium in each of the diets. The food cubes were digested and analyzed as previously mentioned (see Chapter 4). The SD and SD + Lecithin diets contained no cadmium, while the Low QD, High QD, and Cd diets contained 0.07, 0.74,

and 1.42 μg Cd per disc, respectively. The detection limit was 0.0005 μg of total Cd per sample or 0.002 ng/ml [201]. Recovery of cadmium spiked SD + Lecithin food discs was 86.8%.

Research Design

Thirty male-female pairs of sexually mature *Fundulus heteroclitus* were obtained from tidal creeks in Morehead City, NC. After acclimation to the laboratory, mating pairs were housed in partitioned tanks containing ~15 liters of well aerated, filtered natural seawater at ~23°C and 20 ± 2 ppt salinity. Fish were maintained on a 16:8 light:dark cycle. Partial water changes (~7 liters) occurred daily. Each pair received the Standard Diet for 27 days while being observed for spawning. Following the observation period, the treatment diets were administered daily for 85 days. Embryos were collected daily from egg traps. Subsets of eggs were raised in clean 20 ppt seawater during which development was monitored for morphological variations in the notochord, eyes, brain, heart, bladder, trunk, and fins [193]. Embryos with deformities were imaged using a Meiji Techno R2 dissecting microscope (Japan) and captured with aT45 camera (Diagnostic Images, Inc., Sterling Heights, MI) using Image-Pro Plus software (MediaCybernetics, Inc, Bethesda, MD). Additional eggs were preserved at -80°C for cadmium analysis. At the conclusion of the study, *Fundulus* were euthanized

and their organs quickly excised and weighed. A portion of the liver was preserved at -80°C for vitellogenin mRNA analysis.

Vitellogenin Analysis

RNA was isolated from the livers of adult *Fundulus* using RNA-Bee reagent (Tel-Test, Inc.) according to the manufacturer's protocol with an additional chloroform phase separation and EtOH rinse of the pellet. The RNA/DNA ratio was measured spectrophotometrically at 260/280 nm on a Spectramax 190 microplate reader (Sunnyvale, CA). The absorbance ratio was used to calculate the final RNA concentration in ng / μ l. All samples had a 260/280 ratio of 1.9 or higher.

Reverse transcription was carried out using the Omniscript cDNA synthesis kit (Qiagen Inc., Valencia, CA) according to the manufacturer's directions. Briefly, 500 ng of RNA, 10 μ M oligo dT primers (Promega Corp., Madison, WI), and RNaseOut inhibitor (Invitrogen Corp., Carlsbad, CA) were combined and incubated at 37°C for 1 hour in an Eppendorf Mastercycler (Hamburg, Germany). The cDNA was then diluted to a 2 ng/ μ l working concentration.

Table 5-1. Real-time PCR primer sequences for *F. heteroclitus*

Gene	GenBank ID	Primer Name	Primer Sequence (5'-3')
β -Actin ^a	AY735154	Fh-B-Actin-F	ACCACACATTTCTCATACACTCGGG
		Fh-B-Actin-R	CGCCTCCTTCATCGTTCAGTTT
Vitellogenin (vtg)	U07055	Fh-vg-F1	GCTCTTCCTGTTGATGTGCCTGAA
		Fh-vg-R1	GCTTGGATGTGTGTCTCCTGATTGG

^a β -actin primers designed by Battle, L. [218]

Quantitative real-time PCR was carried out using primers for β -actin [218] and vitellogenin. The *Fundulus* vitellogenin primers (Table 5-1) were designed using PrimerQuest software (Integrated DNA Technologies, Coralville, IA). Primer efficiencies were tested to confirm that β -actin and vtg amplified with comparable efficiency. QPCR was performed using SYBR Green PCR Master Mix (Applied Biosystems, Foster City, CA) following the manufacturer's protocol. Briefly, a 25 μ l reaction consisting of 200 nM of each primer, 12.5 μ l 2x SYBR Green PCR Master Mix, 9.5 μ l dH₂O, and 4 ng cDNA was amplified using an Applied Biosystems 7300 Real-Time PCR System with the following thermal profile: 95°C for 10 min; 40 cycles of 95°C for 15 s, 60°C for 60 s. A dissociation curve was generated at the completion of the PCR. All samples were run in duplicate. Data were analyzed using ABI PRISM 7000 Software, Version 1.1 (Applied Biosystems). Gene expression was calculated using relative quantification by the $2^{-\Delta\Delta C_T}$ method of Livak and Schmittgen [219]:

$$C_T(\text{vtg}) - C_T(\beta\text{-actin}) = \Delta C_T$$
$$\Delta C_T(\text{treatment}) - \Delta C_T(\text{SD} + \text{Lecithin}) = \Delta \Delta C_T$$
$$2^{(-\Delta \Delta C_T)} = \text{fold change}$$

Vitellogenin gene expression, following normalization to β -actin, was compared to references (SD + Lecithin) to estimate average fold induction for each experimental diet. Each biological replicate represents a single adult *Fundulus*, and each experimental group is represented by at least 4 individuals/treatment/sex. Data are presented as mean fold induction \pm standard error.

Embryo Cd Measurement

Eggs (N=10 per sample, 3-5 samples per diet) were homogenized in 200 μ l of 7 N nitric acid. The material was transferred to Teflon vials and 800 μ l of 15.8 N nitric acid was added to each sample. Samples were digested overnight at 90°C. The following day, the samples were sonicated for 5 minutes (Branson 2510, Danbury, CT) and 90 μ l of H₂O₂ was added. The samples were vortexed intermittently over the next 6 hours and then transferred to trace-metal free 15 ml vials. Each sample was combined with 10 ml of internal standard solution (10 ppb In, Tm, and Bi in ~2 % HNO₃) and then centrifuged at ~1,300 g for 10 minutes. One milliliter of supernatant was transferred to a fresh tube containing 10 ml of internal standard solution. The samples were analyzed on a VG

Plasmaquad 3 ICP-MS (ThermoScientific, Waltham, MA) and compared to a cadmium standard curve. The detection limit was 0.0005 µg of total Cd per sample or 0.002 ng/ml [201]. Recovery from cadmium spiked eggs was 79.0%.

Data Analysis and Statistics

Growth (final body wt-starting body wt) and hepatosomatic indices (HSI = liver wt/body wt X 100) in adults were analyzed for significance across all the treatment diets using a Kruskal-Wallis test with a Dunn's comparison post hoc. Gonadosomatic indices (GSI = gonad wt/body wt X 100) and vtg expression were analyzed with a Kruskal-Wallis test with a Dunn's comparison post hoc. Fecundity rates (eggs/day) for each spawn were determined for each individual breeding pair. Similarly, acute and chronic fecundity were calculated as the eggs per day in the observation period, spawns 2 and 3 (acute), and spawns 4 and 5 (chronic) for each breeding pair. The rates were then converted to percentages based on the pair's spawning rate on the Standard Diet prior to exposure (observational spawning rate (O)) and averaged for each treatment diet (N=3-6 pairs). Pairs that did not spawn during the observation period were not used to determine fecundity. If a pair did not complete a spawning interval, their rate was not included in the average for that time-point through the end of the study. Spawn-to-spawn fecundity was not evaluated for statistical significance given the low sample size

and missing values created when female fish died prior to the end of the study. Acute and chronic fecundity (compared to the SD + Lecithin treatment) was evaluated using a 2-way ANOVA with a Bonferroni post-test, $\alpha = 0.05$. Statistical analysis was performed using GraphPad Prism, version 5.0 (GraphPad Software, San Diego, CA). Embryonic development was assessed using a χ^2 test ($\alpha=0.05$) in Excel (Microsoft Corporation, Redmond, WA).

Results

During this study, no unusual behaviors were observed. It is common for male fish in confinement to develop aggressive behaviors toward females, which results in fin tears, scale loss, and occasionally death. As mentioned previously (Chapter 4), a female receiving the SD + Lecithin diet died during the treatment period and 2 females from the Low QD treatment died during the observational period due to pair-mismatch and subsequent aggression. However, the death of a High QD female during the exposure period was attributed to the contaminant as no signs of male aggression or disease were observed.

Upon dissection, it was noted that a male from the Cd diet had developed a testicular tumor measuring approximately 2.5 cm in length and weighing 1.50 grams, an

order of magnitude greater than the average gonad weight across all males (0.1138 g) and of the Cd treatment (0.1 g). This outlier was not included in growth, HSI, and GSI calculations. Histopathology of the tumor can be viewed in the Chapter 4 (Fig. 4-9).

The general condition of individuals was assessed through growth and relative liver size. Though there were no significant differences in growth as a result of treatment, trends indicate that males grew more than females (Fig. 5-1). In contrast, females had higher HSI than males (Fig. 5-2), though they weren't statistically different. Growth and hepatosomatic indices indicate that Lecithin supplementation was most likely responsible for the slight increase in the body and liver size of females.

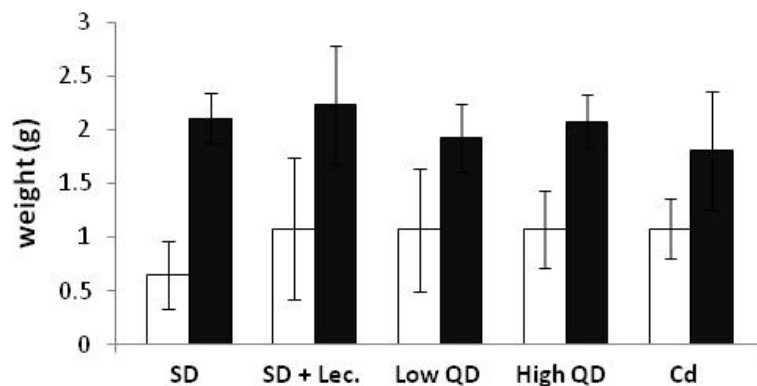


Figure 5-1. Growth of females (open boxes) and males (filled boxes) after dietary exposure to CdSe/ZnS QDs. Bars are mean \pm standard error.

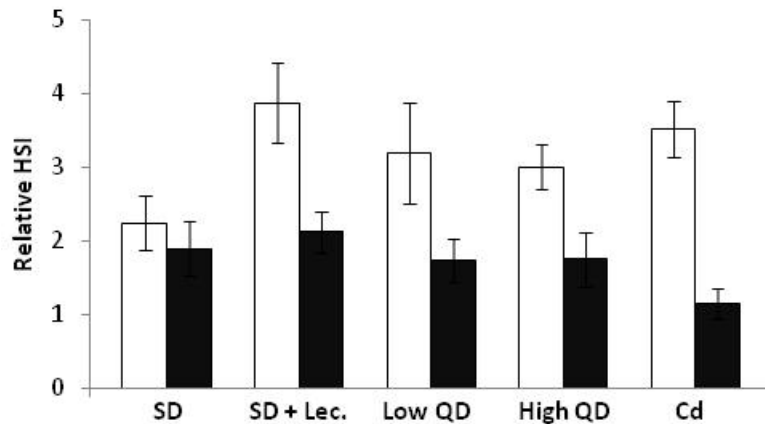


Figure 5-2. Hepatosomatic indices of females (open boxes) and males (filled boxes) after 85 days of continuous dietary exposure to CdSe/ZnS QDs. HSI = liver wt/body wt X 100. Bars are mean \pm standard error.

Evaluating reproduction on a spawn-to-spawn basis revealed that fecundity was altered by Lecithin, QDs, and Cd²⁺ (Fig. 5-3). Lecithin caused premature increases in fecundity as compared to that of the SD group. SD fecundity steadily increased over the breeding season until the last spawn. In comparison, the SD + Lecithin group had an immediate increase in fecundity during the transition spawn (1018% versus 219% in the SD) and was highly variable, ranging from 670% to 1967%, not including the last spawn. This increased fecundity was not observed in all the diets containing Lecithin. The High QD diet group had a minor increase in fecundity during the transition (116%) and subsequently declined below 100% for the remainder of the study. Fish fed the Low QD and Cd diets had an increase in fecundity during the transition (931% and 816%,

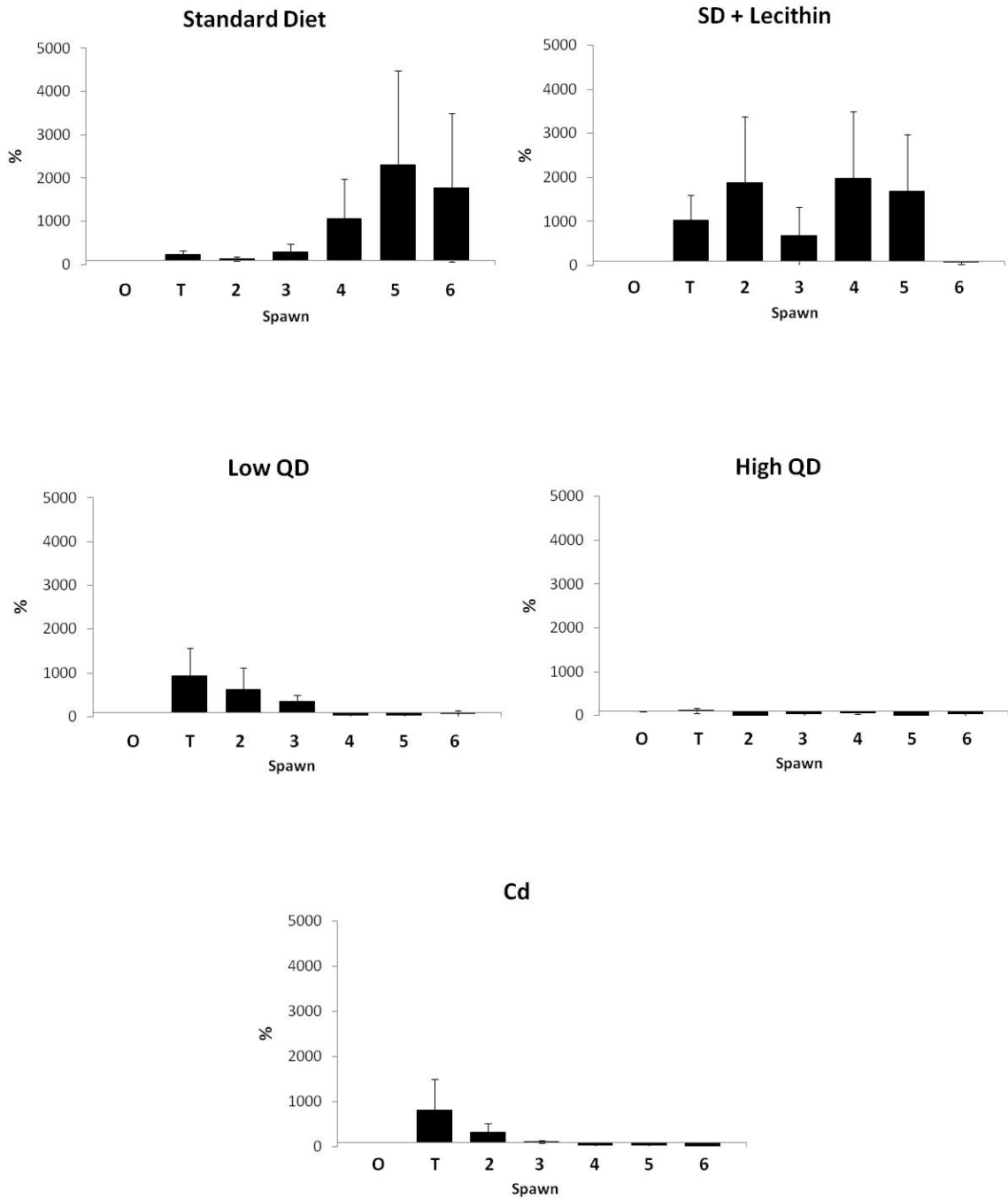


Figure 5-3. Fecundity shown as the eggs/day as a percent of the observational spawning rate (O). Fish were exposed from the transition spawn (T) through the sixth spawn. Bars are mean \pm standard error.

respectively), similar to the SD + Lecithin group (1018%), but egg numbers steadily declined post-transition and fell below 100% by the fourth spawn. These changes, though dramatic, could not be analyzed for statistical significance due to the small sample size (N=3-6 pairs/diet), thus only trends can be inferred.

Acute and chronic fecundity (Fig. 5-4) were also assessed to determine how fish tolerated shorter versus longer QD exposures. Even though it appears that Lecithin acutely increased fecundity (when compared to the Standard Diet), neither the acute or chronic fecundity were significantly different between the SD and SD + Lecithin treatments due to high variability. Similarly, neither acute nor chronic fecundity were statistically different between the SD + Lecithin and the QD- and Cd-treated diets.

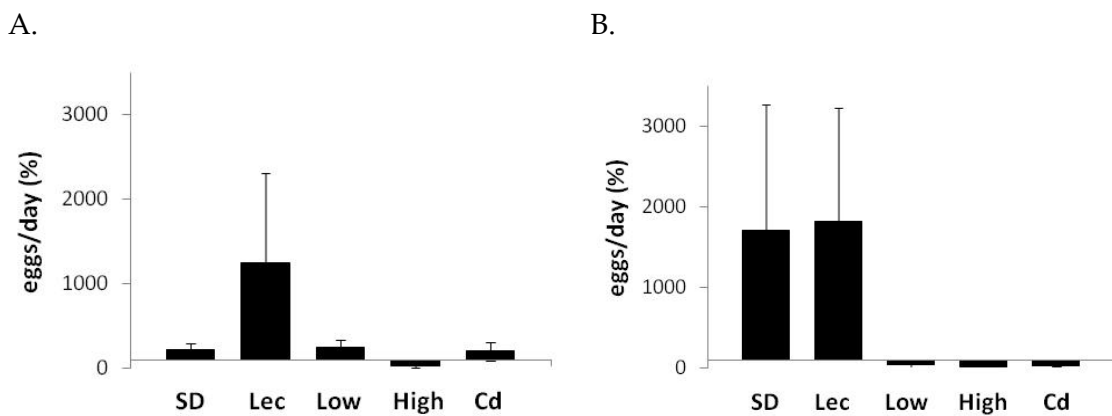


Figure 5-4. Acute (A) and chronic (B) fecundity. In both graphs, the horizontal axis crosses as 100%, the observational spawning rate. Bars are mean \pm std error.

Given the apparent reproductive toxicity of QDs, we examined the expression of vitellogenin (vtg) mRNA in the adults at the conclusion of the study (Figures 5-5 and A11). Hepatic vtg transcription was elevated, though insignificantly, in males consuming the High QD (13.6 ± 10.5) and Cd (9.3 ± 4.2) diets; the vtg levels were three to five times higher than the levels measured in the SD and SD + Lecithin animals (2.0 ± 1.5 and 2.7 ± 1.0 fold induction, respectively). Transcription of vtg was not induced in males consuming the Low QD diet (1.0 ± 0.5 fold induction). With the exception of the *Fundulus* with the testicular tumor, males fed the QD or Cd diets also tended to have smaller testes than those receiving the SD + Lecithin diet (Fig. 5-6). Female vtg transcription and gonadosomatic indices were not statistically different due to the extreme variability (Figures A-8 and A-9).

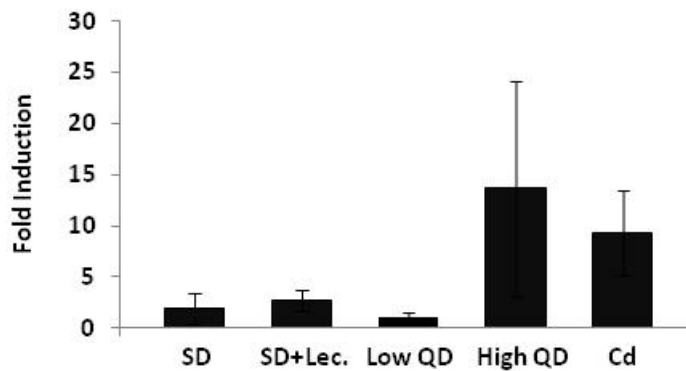


Figure 5-5. Male vtg mRNA levels after QD exposure. Bars are mean \pm std error.

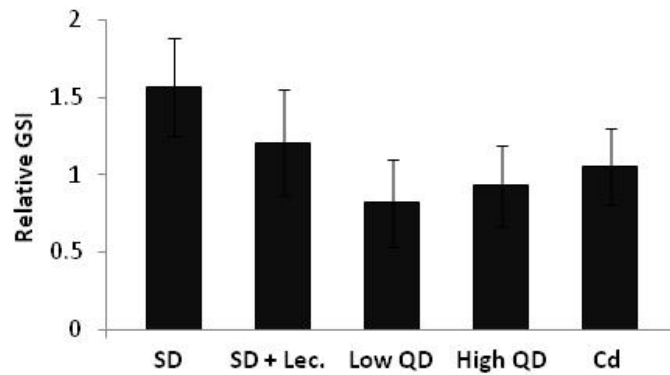


Figure 5-6. Male gonadosomatic indices in *Fundulus* after 85 days of dietary exposure. GSI = testis wt / body wt X 100. Bars are mean ± standard error.

Alterations in embryonic development can also be a sentinel for contaminant exposure. The addition of Lecithin to the diet (SD + Lecithin) caused a significant increase in the percentage of abnormally sized (3.9%) (Fig. 5-7) and malformed embryos (6.9%) during the first three treated spawns when compared to the Standard Diet (2.8% small and 1.6% malformed embryos). Yet, when embryos were parentally exposed to QDs or CdCl₂, they had significantly lower percentages of developmental deformities than the SD + Lecithin group (Table 5-2). Moreover, hatching percentages of embryos in the QD and Cd exposures were significantly higher than hatching percentages for embryos in the SD + Lecithin group (Table 5-2).

Table 5-2. Development and hatching of parentally exposed embryos ^a

Treatment	% Small ^b	% Abnormal ^c	% Hatched ^d
Standard Diet	2.8	1.6	64
SD + Lecithin	3.9 ^e	6.7 ^e	68 ^e
Low QD	1.7*	0.3*	84*
High QD	3.5*	3.1*	81*
Cd	0.0*	2.2*	98*

^a embryos were collected from spawns T, 2, and 3; ^b no deformities, but are half the size of normal embryos; ^c includes lethal and sub-lethal deformities; ^d includes both normally- and abnormally-developed fry; ^e significantly different from the SD; * statistically different from the SD + Lecithin treatment, $\alpha = 0.05$.

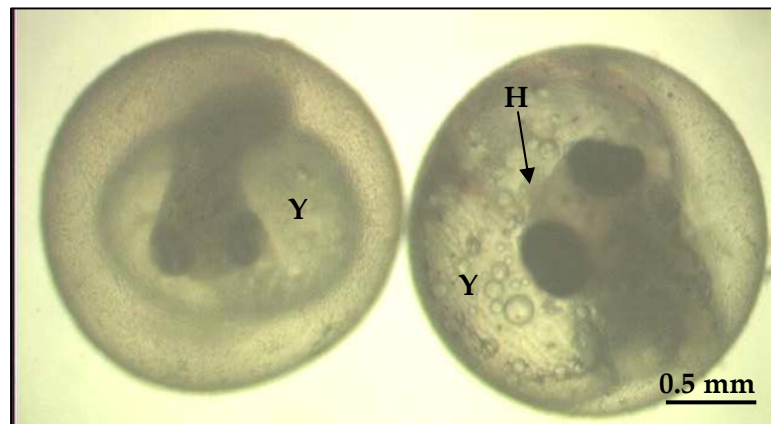


Figure 5-7. Embryos from parents that were fed the SD + Lecithin diet. The embryos are differently sized despite being the same age; the yolk (Y) fills the egg on the right, while it only fills half of the egg on the left. H = heart.

Ovo-deposition is one mechanism by which female *Fundulus* rid themselves of contaminants [190]. Analysis of embryos from the second and third treated spawns

revealed that none of the embryos contained detectable levels of cadmium. However, cadmium was detected in High QD embryos collected from the fourth spawn. Concentrations ranged from 0.0 to 0.7 ng Cd per sample with the average cadmium content being 0.244 ± 0.1 ng Cd/sample. Cadmium content could not be analyzed in the Low QD or CdCl₂ embryos from the fourth treated spawn due to insufficient egg production.

Discussion

Reproduction is an energetically demanding physiological process for female fish. Males expend little energy to produce thousands of gametes, while females expend copious amounts of energy to provide their oocytes the lipid-rich yolk necessary to survive during embryonic development and larval growth until active feeding begins. Growth and HSI measurements indicate that although the treatments did not significantly affect either parameter, males grew more than females, and females had a relatively larger liver size. Males have the advantage of spending energy on growth because they are not producing eggs. Sexually mature females, however, utilize their energy stores for reproduction. Newman *et al.* [257] reported that condition factor, relative liver size, and visceral fat stores were increased in cod (*Maccullochella peelii peelii*) prior to the spawning season. However, during the spawning season, the HSI and fat

stores declined as the GSI increased in cod and anglerfish (*Lophius litulon*) [257, 258].

Kamler [210] proposed that there is a trade-off in female fish between energy needed for metabolism and growth versus the energy needed for reproduction. In this study, it appears that females sacrificed growth to maintain their liver condition and improve the likelihood of producing successful progeny.

In the natural environment, *Fundulus* spawn multiple batches of eggs from April through September according to a semi-lunar cycle. Fecundity is extremely variable from individual to individual, and is dependent on several factors including maternal body size, hepatosomatic indices, age, food supply, temperature, photoperiod, and stressors [210, 259]. In this study, we monitored reproduction to determine the impact of long-term QD exposure on fish populations. While QDs did affect reproduction, it is obvious that the encapsulation agent also altered fecundity. Trends indicate that Lecithin hastened reproductive onset. With the exception of the High QD diet, all the diets supplemented with Lecithin exhibited increased fecundity during the transition spawning interval. Similar fecundity levels were not observed in the Standard Diet until the fourth spawn. Furthermore, acute fecundity was elevated almost 6-fold in the SD + Lecithin group compared to the SD group.

Lecithin is a membrane phospholipid and may have impacted reproduction by improving maternal condition. Female growth and hepatosomatic indices doubled from the Standard Diet group to the SD + Lecithin exposure group indicating that Lecithin served as a nutrient by improving both body and relative liver size. The changes in fecundity due to Lecithin ingestion are supported by the pilot study in which Lecithin (20 µg/day) significantly increased fecundity during the transition spawn in a 5 week dietary exposure (Chapter 3). However, the benefit of Lecithin was not sustained throughout the exposure as the subsequent spawn showed no changes in fecundity due to Lecithin or QD consumption. It is important to note that the pilot study used twice as much Lecithin as the current study, and it is possible that the excess phospholipid caused hepatic steatosis, which could have hindered reproduction. Therefore, Lecithin was decreased to 10 µg/day for the 3 month reproductive assessment to avoid potential liver damage and unduly influencing reproduction.

Despite the nutritional benefit provided by the encapsulation agent, reproduction after the transition period was decreased in the Low QD, High QD, and Cd exposures. The reproductive profiles suggest that the QD concentration impacted fecundity during acute exposures. Low QD fecundity was greater than the observational rate during the acute spawning interval, while High QD fecundity fell

below 100%. However, chronic QD ingestion severely depressed reproduction at both doses. Fish receiving the Cd diet also showed severely depressed fecundity with chronic exposure. This suggests that free cadmium might have played a role in reducing fecundity.

One potential mechanism for reduced fecundity is disruption of the endocrine system. However, almost no information is available regarding QDs and endocrine function. Based on the elevated vtg transcription in male *Fundulus*, it appears that QD and Cd ingestion feminized male fish. This differs from reports that aqueous exposure to CdS QDs for 21 days did not alter vitellogenin induction in male sticklebacks (*Gasterosteus aculeatus*) [199]. Saunders *et al.* [199] hypothesized that Cd²⁺ concentrations were too low to induce a change in vitellogenin levels, although they also conceded that the sticklebacks were not in the correct physiological state for reproductive assessment as all treatments showed a lack of nest building.

There are reports that free cadmium causes endocrine disruption in fish, but the studies are inconsistent. For instance, Haux *et al.* [260] reported that Cd exposure decreased plasma vitellogenin in female rainbow trout (*Oncorhynchus mykiss*) while plasma vitellogenin levels were unaltered by treatment in male and female Japanese

medaka (*Oryzias latipes*) [225]. In another study, male Japanese medaka exposed to cadmium *in ovo* had elevated hepatic vitellogenin levels [228]. Studies measuring plasma estradiol levels following cadmium exposure are similarly indeterminate. Circulating estradiol levels were reported as both elevated [224, 225] and diminished [225] in female fish aquously exposed to Cd. While cadmium has been shown to bind and activate the estrogen receptor-alpha (ER- α) in MCF-7 cells (human breast cancer) [227], selenite can also block estradiol and bind to ER- α [261]. Although Se concentrations were not measured in the adults, if QDs are degrading *in vivo*, selenide could be contributing to fecundity declines by feminizing males.

As early life stages are often more susceptible to toxicity, embryonic development is a good marker for contaminant exposure. In this study, Lecithin alone negatively affected development more than QD or Cd exposure. This is consistent with the pilot study, in which the proportion of *Fundulus* embryos that developed abnormally after parental exposure to the Standard Diet, SD + Lecithin, or QD diets were 3.6%, 5.9%, and 4.2%, respectively (Chapter 3). Furthermore, assessments investigating the developmental toxicity of aqueous exposure of eggs to Lecithin-encapsulated QDs strongly suggested that Lecithin was the cause of the hemorrhages, limb deformities, and mortality (Chapter 2).

Recent studies have shown that certain types of ENPs are bioavailable, and that they are transferred from parent to the offspring [254, 262, 263]. Ovo-deposition is a mechanism commonly employed by fish to rid themselves of contaminants, including metals [70, 110, 190, 264-266]. While previous studies have shown that Lecithin-encapsulated QDs are unable to traverse the *Fundulus* chorion in aqueous exposures due to QD aggregation (Chapter 2), maternal exposure to QDs would by-pass this physical defense mechanism by incorporating the QD or Cd into eggs prior to fertilization and extrusion. Metal analysis of embryos from the second, third, and fourth treated spawns showed that maternal transfer of QDs or their degradation products occurred after six to eight weeks of dietary exposure. This is the first study to report maternal transfer of QDs to offspring.

Conclusions

In summary, declining trends in fecundity suggest that while fish populations may be able to tolerate acute dietary exposure to QDs, chronic QD exposure could have dire consequences. QD uptake impacts reproduction by feminizing male fish. Moreover, maternal transfer of QDs or their degradation products to developing progeny circumvents the egg's chorion, thus directly impacting the offspring.

Chapter 6. Conclusions: The Potential Consequences of QDs in Estuarine Systems

The immense commercial potential of quantum dots ensures their continued production and development. QDs will enter the aquatic environment following manufacturing, use, and disposal where they will encounter organisms residing in the water column as well as the sediments. This dissertation sought to determine if, and how, Lecithin-encapsulated CdSe/ZnS QDs caused toxicity in larval and adult *Fundulus heteroclitus*. Specific aims were to: (1) determine bio-availability, (2) monitor reproduction, (3) observe embryonic development, (4) quantify biomarkers of oxidative stress, and (5) measure changes in the expression of genes associated with metal metabolism and oxidative stress.

Bioavailability

Aqueous exposure of developing *Fundulus* embryos to quantum dots showed that QDs were limited to the chorion, and thus, not bioavailable (Chapter 2). Conversely, QDs or their degradation products were detected in livers of adult *Fundulus* fed QDs (Chapter 4). Less than 0.01% of the cadmium from QDs was retained in the liver and intestinal tissues. In comparison, 0.9% of the Cd was retained in the intestine and 0.5% in the liver of fish fed the CdCl₂ diet. This indicates that the structure of the core-shell QD reduced uptake. Additionally, females assimilated cadmium more efficiently than males. Intestinal and hepatic cadmium concentrations were higher in

females than males regardless of the treatment diet. This implies that although bioavailability of QDs was very low, female fish might be more susceptible to toxicological effects than male fish.

Reproductive Effects

Fecundity was not significantly altered in sexually-mature *Fundulus* that were fed QDs for 35 days (Chapter 3). However, when the exposure duration was lengthened to 85 days, fecundity declined (Chapter 5). Assessment of vitellogenin transcription showed that males given 10 µg QD/day had vtg levels five times that of unexposed males. Relative gonad size was also reduced in QD exposed males. Similar trends occurred in males fed the CdCl₂ diet. Thus, it appears that declining fecundity occurred because the QDs, like free cadmium, feminized the male fish.

Developmental Toxicity

Fundulus embryos that were aqueously exposed to CdSe/ZnS quantum dots were protected by their chorion (Chapter 2). QDs formed large aggregates in seawater that were unable to traverse the chorion and therefore, did not disrupt embryonic development. However, QD aggregates that were attached to the chorion affected the ability of larval fish to hatch. Eggs from parents exposed to QDs confirmed that QDs or

their degradation products were maternally-transferred to the ova (Chapter 5). Thus, developing embryos were vulnerable to quantum dots whether aqueously- or maternally-exposed to QDs.

Oxidative Stress

Dietary exposure to QDs for 35 and 85 days did not elicit an oxidative stress response in adult *Fundulus*. Hepatic total glutathione and lipid peroxidation levels were not significantly altered at the conclusion of either study (Chapters 3 and 4).

Additionally, expression of genes related to metal metabolism and oxidative stress (*mt*, *gstmu*, *gpx*, *sod1*, and *sod2*) were not significantly altered after 85 days of continuous QD exposure (Chapter 4). This suggests that although QDs were bioavailable, the teleost adapted to the insult or uptake was not sufficient to induce oxidative stress.

Study Implications

In these studies, larval and adult *Fundulus* were exposed to pristine CdSe/ZnS QDs. However, in the natural environment QDs will be oxidized, enzymatically-altered, or bacterially-degraded. In the life-time of a core-shell QD, it may be ingested, metabolized, and excreted by multiple organisms, each time affecting the stability of the QD structure. So, although bioavailability was limited, the toxicological effects observed

during these studies would likely be magnified when the ZnS shell failed and free cadmium and selenium were released *in vivo*.

Future Studies

QD toxicity in teleosts was a function of the concentration and duration of the exposures. Observations made during these studies also showed that environmental conditions play a significant role in the fate of QDs. Salinity caused aggregation and precipitation to the sediments, suggesting that benthic organisms are more likely to be exposed to QDs than pelagic fish. Thus, future studies with engineered nanoparticles should focus on assessing toxicity using concentrations, exposure routes, ecosystem conditions, and animal models that are environmentally-relevant. This will clarify if the effects seen in the laboratory will occur in the natural environment.

Appendix

Fundulus were evaluated for sex-specific differences in hepatic total glutathione (Fig. A-1) and lipid peroxidation levels (Fig. A-2) after 85 days of dietary exposure to the Standard Diet, SD + Lecithin, Low QD, High QD, or Cd diets. The graph on the left shows the effect of Lecithin supplementation of the Standard Diet, while the graph on the right is a comparison of all the treatment diets. Statistical analysis using a Kruskal-Wallis test with a Dunn's comparison post hoc ($\alpha = 0.05$) revealed no significant differences between the treatments.

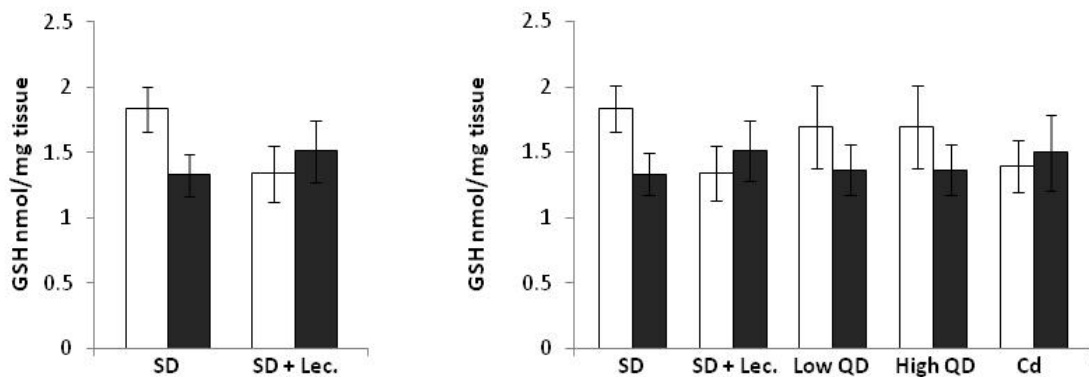


Figure A-1. The average hepatic total glutathione levels in female (open boxes) and male (filled boxes) *Fundulus heteroclitus* after 85 days of continuous dietary exposure to CdSe/ZnS QDs. Bars are mean \pm standard error.

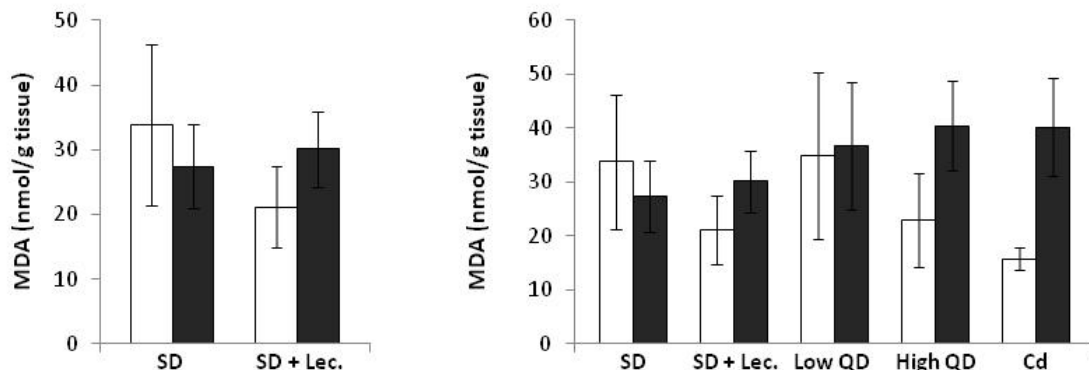


Figure A-2. The average hepatic lipid peroxidation levels in female (open boxes) and male (filled boxes) *Fundulus heteroclitus* after 85 days of continuous dietary exposure to CdSe/ZnS nanocrystals. Bars are mean \pm standard error.

Transcription of genes related to oxidative stress and metal detoxification were also evaluated for sex-specific differences after 85 days of dietary exposure to the various treatments (Figures A-3 through A-7). The graph on the left shows the effect of Lecithin supplementation of the Standard Diet, while the graph on the right is a comparison of all the treatment diets. Statistical analysis using a Kruskal-Wallis test with a Dunn's comparison post hoc ($\alpha = 0.05$) revealed that Lecithin supplementation did not affect the expression of the genes evaluated. Moreover, there were no sex-specific differences in the expression of *mt*, *gstmu*, *gpx*, and *sod2*. However, female *Fundulus* fed the Cd diet had significantly elevated *sod1* mRNA levels versus their male counterparts.

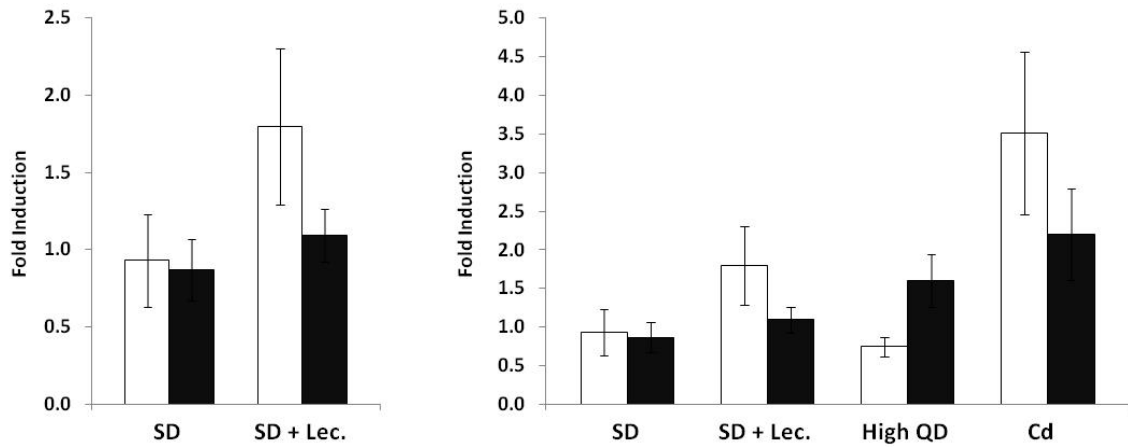


Figure A-3. Changes in hepatic metallothionein (mt) expression in female (open boxes) and male (filled boxes) *Fundulus heteroclitus*. Bars are mean fold induction \pm standard error.

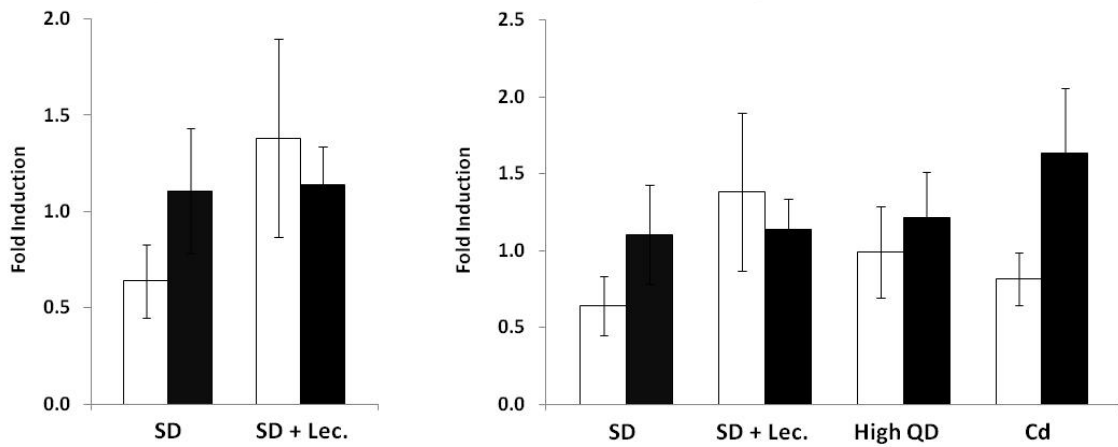


Figure A-4. Changes in glutathione-s-transferase (gstmu) hepatic RNA levels in female (open boxes) and male (filled boxes) *Fundulus*. Bars are mean fold induction \pm standard error.

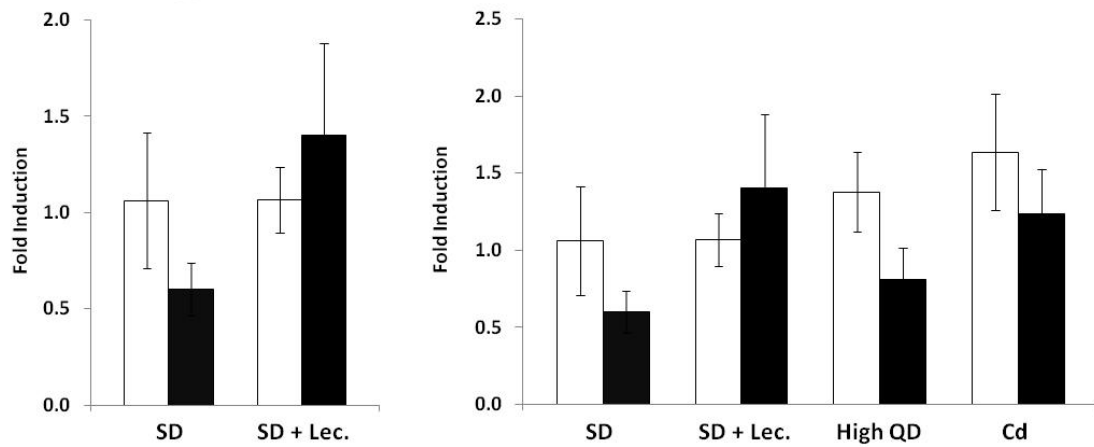


Figure A-5. Changes in hepatic glutathione peroxidase (gpx) RNA levels in female (open boxes) and male (filled boxes) *Fundulus heteroclitus*. Bars are mean fold induction \pm standard error.

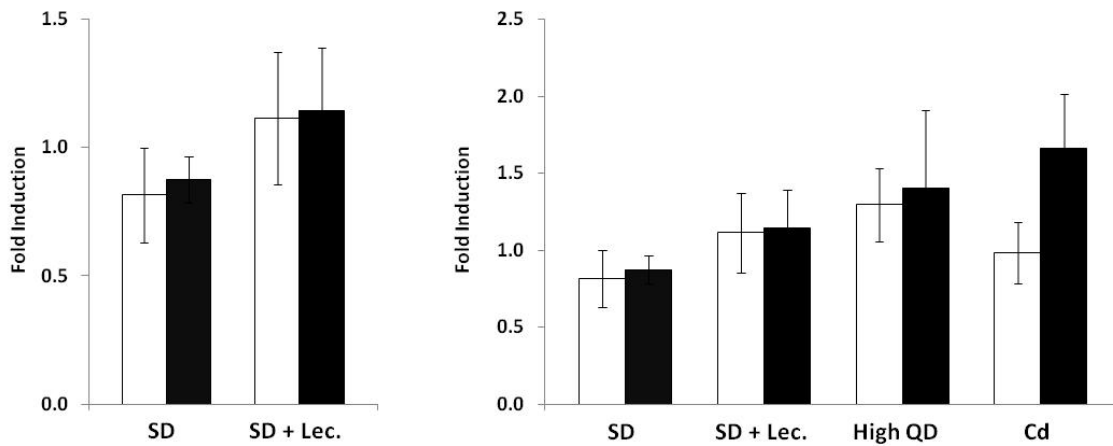


Figure A-6. Changes in Mn-superoxide dismutase (sod2) hepatic RNA levels in female (open boxes) and male (filled boxes) *Fundulus heteroclitus*. Bars are mean fold induction \pm standard error.

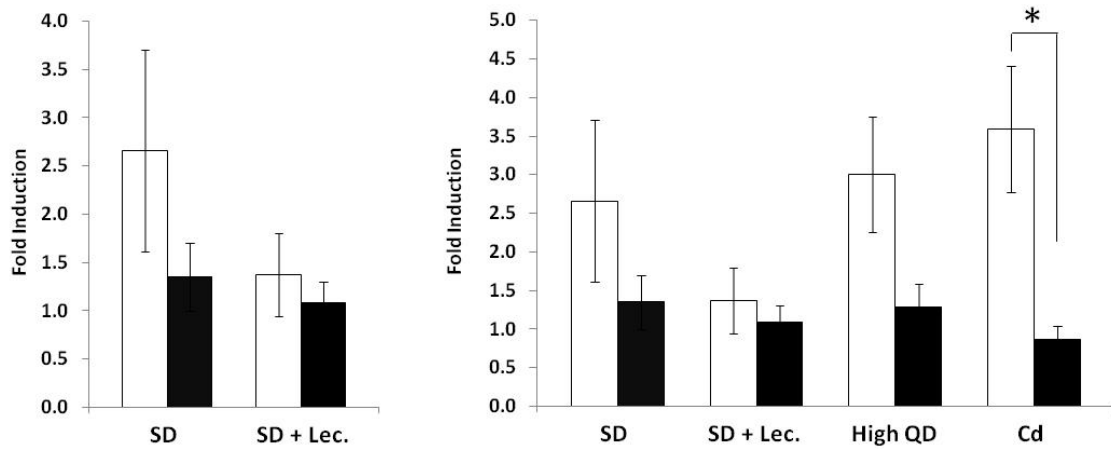


Figure A-7. Changes in hepatic Cu/Zn-superoxide dismutase (sod1) expression in female (open boxes) and male (filled boxes) *Fundulus heteroclitus*. Bars are mean fold induction \pm standard error, $\alpha = 0.05$.

The vitellogenin levels (Fig. A-8) of female *Fundulus* exposed to QDs or Cd for 85 days were measured to determine if they might have an impact on fecundity. However, there were no statistical differences between treatment groups due to the high variability. This is not uncommon as vtg levels in female fish vary depending upon their individual reproductive cycle. Similarly, female gonadosomatic indices (Fig. A-9) were not altered by the treatment diets. Gonad weight in females is based on how recently the individual spawned, and as such, is not a good marker for comparison.

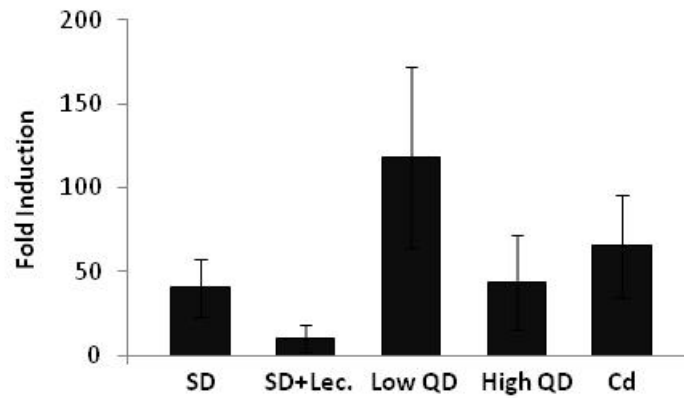


Figure A-8. Female hepatic vitellogenin mRNA levels after 85 days of dietary QD exposure. Bars are mean \pm standard error.

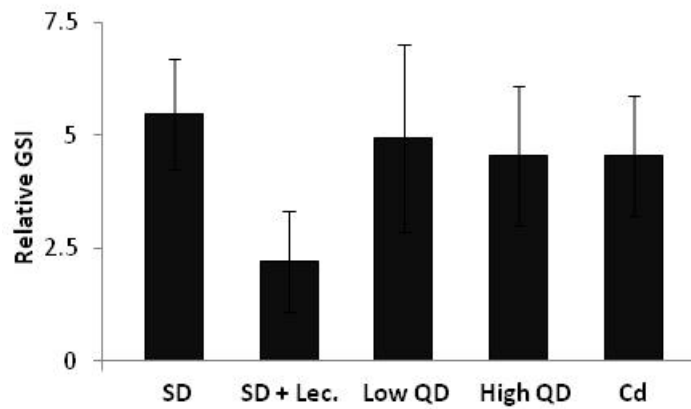


Figure A-9. Female gonadosomatic indices after 85 days of QD exposure. Bars are mean \pm standard error.

References

1. Kroto, H.W., J.R. Heath, S.C. O'Brien, R.F. Curl, and R.E. Smalley. 1985. C₆₀: Buckminsterfullerene. *Nature*, **318**: p. 162-163.
2. Roco, M.C. 2001. International strategy for nanotechnology research and development. *J. Nanopart.Res.*, **3**(5-6): p. 353-360.
3. Iijima, S. 1991. Helical microtubules of graphitic carbon. *Nature*, **354**: p. 56-58.
4. EvidentTechnologies. 2008 [cited 8.28.2008]; Available from: www.evidenttech.com.
5. Bawendi, M.G., P.J. Carrol, W.L. Wilson, and L.E. Brus. 1992. Luminescence properties of CdSe quantum crystallites: Resonance between interior and surface localized states. *J.Chem.Phys.*, **96**(2): p. 946-954.
6. Kortan, A.R., R. Hull, R.L. Opila, M.G. Bawendi, M.L. Steigerwald, P.J. Carrol, and L.E. Brus. 1990. Nucleation and growth of CdSe on ZnS quantum crystallite seeds, and vice versa, in inverse micelle media. *J.Am.Chem.Soc.*, **112**: p. 1327-1332.
7. Steigerwald, M.L., A.P. Alivisatos, J.M. Gibson, T.D. Harris, R. Kortan, A.J. Muller, A.M. Thayer, T.M. Duncan, D.C. Douglass, and L.E. Brus. 1988. Surface derivatization and isolation of semiconductor cluster molecules. *J.Am.Chem.Soc.*, **110**: p. 3046-3050.
8. Murray, C.B., D.J. Norris, and M.G. Bawendi. 1993. Synthesis and characterization of nearly monodisperse CdE (E=S, Se, Te) semiconductor nanocrystallites. *J.Am.Chem.Soc.*, **115**: p. 8706-8715.
9. Kirmse, H., R. Schneider, D. Scheerschmidt, D. Conrad, and W. Neumann. 1999. TEM characterization of self-organized CdSe/ZnSe quantum dots. *J. of Microsc.*, **194**(1): p. 183-191.

10. Maehashi, K. 2000. Formation and characterization of self-organized CdSe quantum dots. *J. Electron.Mater.*, **29**(5): p. 542-549.
11. Su, Y.-W., C.-S. Wu, C.-C. Chen, and C.-D. Chen. 2003. Fabrication of two-dimensional arrays of CdSe pillars using E-beam lithography and electrochemical deposition. *Adv.Mater.*, **15**(1): p. 49-51.
12. Yu, M., G.W. Fernando, R. Li, F. Papadimitrakopoulous, N. Shi, and R. Ramprasad. 2006. First principles study of CdSe quantum dots: Stability, surface unsaturations, and experimental validation. *App.Phys.Lett*, **88**: p. 231910.
13. Alivisatos, A.P. 1996. Perspectives on the physical chemistry of semiconductor nanocrystals. *J.Phys.Chem.*, **100**: p. 13226-13239.
14. Henglein, A. 1989. Small-particle research: Physicochemical properties of extremely small colloidal metal and semiconductor particles. *Chem.Rev.*: p. 1861-1873.
15. Hines, M.A. and P. Guyot-Sionnest. 1996. Synthesis and characterization of strongly luminescing ZnS-capped CdSe nanocrystals. *J.Phys.Chem.*, **100**: p. 468-471.
16. Dabbousi, B.O., J. Rodriguez-Viejo, F.V. Mikulee, J.R. Heine, H. Mattoussi, R. Ober, K.F. Jensen, and M.G. Bawendi. 1997. (CdSe)ZnS core-shell quantum dots: Synthesis and characterization of a size series of highly luminescent nanocrystallites. *J.Phys.Chem. B*, **101**: p. 9463-9475.
17. Chan, W.C.W. and S. Nie. 1998. Quantum dot bioconjugates for ultrasensitive nonisotopic detection. *Science*, **281**(5385): p. 2016-2018.
18. Kloepper, J.A., R.E. Mielke, and J.L. Nadeau. 2005. Uptake of CdSe and CdSe/ZnS quantum dots into bacteria via purine-dependent mechanisms. *Appl.Environ.Microbiol.*, **71**(5): p. 2548-2557.
19. Derfus, A.M., W.C.W. Chan, and S.N. Bhatia. 2004. Probing the cytotoxicity of semiconductor dots. *Nano Lett.*, **4**(1): p. 11-18.

20. Hoshino, A., K. Fujioka, T. Oku, M. Suga, Y.F. Sasaki, T. Ohta, M. Yasuhara, K. Suzuki, and K. Yamamoto. 2004. Physicochemical properties and cellular toxicity of nanocrystal quantum dots depend on their surface modification. *Nano Lett.*, **4**(11): p. 2163-2169.
21. Shiohara, A., A. Hoshino, K.-I. Hanaki, K. Suzuki, and K. Yamamoto. 2004. On the cyto-toxicity caused by quantum dots. *Microbiol. Immunol.*, **48**(9): p. 669-675.
22. Akerman, M.E., W.C.W. Chan, P. Laakkonene, S.N. Bhatia, and E. Ruoslahti. 2002. Nanocrystal targeting in vivo. *Proc.Natl.Acad.Sci.*, **99**(20): p. 12617-12621.
23. Chen, F. and D. Gerion. 2004. Fluorescent CdSe/ZnS nanocrystal-peptide conjugates for long-term, nontoxic imaging and nuclear targeting in living cells. *Nano Lett.*, **4**(10): p. 1827-1832.
24. Cai, W., D.-W. Shin, K. Chen, O. Gheysens, Q. Cao, S.X. Wang, S.S. Gambhir, and X. Chen. 2006. Peptide-labeled near-infrared quantum dots for imaging tumor vasculature in living subjects. *Nano Lett.*, **6**(4): p. 669-676.
25. Rozenzhak, S.M., M.P. Kadakia, T.M. Caserta, T.R. Westbrook, M.O. Stone, and R.R. Naik. 2005. Cellular internalization and targeting of semiconductor quantum dots. *Chem. Commun.*: p. 2217-2219.
26. Clarke, S.J., C.A. Hollmann, Z. Zhang, D. Suffern, S.E. Branforth, N.A. Dimitrijevic, W.G. Minarik, and J.L. Nadeau. 2006. Photophysics of dopamine-modified quantum dots and effects on biological systems. *Nat. Mater.*, **5**: p. 409-417.
27. Yang, D., Q. Chen, W. Wang, and S. Xu. 2008. Direct and indirect immunolabelling of HeLa cells with quantum dots. *Luminescence*, **23**(3): p. 169-174.
28. Heath, J.R. and J.J. Shiang. 1998. Covalency in semiconductor quantum dots. *Chem.Soc.Rev.*, **27**: p. 65-71.
29. Aldana, J., Y.A. Wang, and X. Peng. 2001. Photochemical instability of CdSe nanocrystals coated by hydrophilic thiols. *J.Am.Chem.Soc.*, **123**: p. 8844-8850.

30. Bowen Katari, J.E., V.L. Colvin, and A.P. Alivisatos. 1994. X-ray photoelectron spectroscopy of CdSe nanocrystals with applications to studies of the nanocrystal surface. *J.Phys.Chem.*, **98**: p. 4109-4117.
31. van Sark, W.G.J.H.M., P.L.T.M. Frederix, D.J. van den Heuvel, A.A. Bol, J.N.J. van Lingen, C. de Mello Donega, H.C. Gerritsen, and A. Meijerink. 2002. Time-resolved fluorescence spectroscopy study on the photophysical behavior of quantum dots. *J. Fluoresc.*, **12**(1): p. 69-76.
32. Navarro, D.A., D.F. Watson, D.S. Aga, and S. Banerjee. 2009. Natural organic matter-mediated phase transfer of quantum dots in the aquatic environment. *Environ.Sci.Technol.*
33. Kirchner, C., T. Liedl, S. Kudera, T. Pellegrino, A.M. Javier, H.E. Gaub, S. Stolzle, N. Fertig, and W.J. Parak. 2005. Cytotoxicity of colloidal CdSe and CdSe/ZnS nanoparticles. *Nano Lett.*, **5**(2): p. 331-338.
34. Ryman-Rasmussen, J.P., J.E. Rivier, and N.A. Monteriro-Riviere. 2006. Surface coatings determine cytotoxicity and irritation potential of quantum dot nanoparticles in epidermal keratinocytes. *J. Invest.Dermatol.*, **127**: p. 143-153.
35. Green, M. and E. Howman. 2005. Semiconductor quantum dots and free radical induced DNA nicking. *Chem.Commun.*: p. 121-123.
36. Liang, J., Z. He, S. Zhang, S. Huang, Z. Ai., H. Yang, and H. Han. 2007. Study of DNA damage induced by CdSe quantum dots using nucleic acid molecular "light switches" as probe. *Talanta*, **71**: p. 1675-1678.
37. Aryal, B.P., K.P. Neupane, M.G. Sandros, and D.E. Benson. 2006. Metallothioneins initiate semiconducting nanoparticle cellular toxicity. *Small*, **2**(10): p. 1159-1163.
38. Ipe, B.I., M. Lehnig, and C.M. Niemeyer. 2005. On the generation of free radical species from quantum dots. *Small*, **1**(7): p. 706-709.
39. Chan, W.-H., N.-H. Shiao, and P.-Z. Lu. 2006. CdSe quantum dots induce apoptosis in human neuroblastoma cells via mitochondrial-dependent pathways and inhibition of survival signs. *Toxicol.Lett.*, **167**: p. 191-200.

40. Lovric, J., H.S. Bassi, Y. Cuie, G.R.A. Fortin, F.M. Winnik, and D. Maysinger. 2005. Differences in subcellular distribution and toxicity of green and red emitting CdTe quantum dots. *J. Mol. Med.*, **83**: p. 377-385.
41. Lovric, J., S.J. Cho, F.M. Winnik, and D. Maysinger. 2005. Unmodified cadmium telluride quantum dots induce reactive oxygen species formation leading to multiple organelle damage and cell death. *Chem.Biol.*, **12**: p. 1227-1234.
42. Cho, S.J., S. Maysinger, M. Jain, B. Roder, S. Hackbarth, and F.M. Winnik. 2007. Long-term exposure to CdTe quantum dots causes functional impairments in live cells. *Langmuir*, **23**: p. 1974-1980.
43. Henry, T.B., F.-M. Menn, J.T. Flemming, J. Wilgus, R.N. Compton, and G.S. Saylor. 2007. Attributing effects of aqueous C60 nano-aggregates to tetrahydrofuran decomposition products in larval zebrafish by assessment of gene expression. *Environ.Health Perspec.*, **115**(7): p. 1059-1065.
44. Oberdorster, E. 2004. Manufactured Nanomaterials (Fullerenes, C₆₀) Induce Oxidative Stress in the Brain of Juvenile Largemouth Bass. *Environ.Health Perspec.*, **112**(10): p. 1058-1062.
45. Sayes, C.M., A.M. Gobin, K.D. Ausman, J. Mendez, J.L. West, and V.L. Colvin. 2005. Nano-C₆₀ cytotoxicity is due to lipid peroxidation. *Biomaterials*, **26**: p. 7587-7595.
46. de la Torre, F.R., A. Salibian, and L. Ferrari. 2000. Biomarkers assessment in juvenile *Cyprinus carpio* exposed to waterborne cadmium. *Environ.Poll.*, **109**: p. 277-282.
47. Ali, C., D.M. Reda, R. Rachid, and B. Houria. 2009. Cadmium induced changes in metabolic function of mitochondrial isolated from potatoe tissue (*Solanum tuberosum* L.). *Am.J. Biochem. Biotech.*, **5**(1): p. 35-39.
48. Almeida, J.A., E.L.B. Novelli, M.D.P. Silva, and R. Alves Junior. 2001. Environmental cadmium exposure and metabolic responses of the Nile tilapia, *Oreochromis niloticus*. *Environ.Poll.*, **114**: p. 169-175.

49. Gagne, F., D. Maysinger, C. Andre, and C. Blaise. 2008. Cytotoxicity of aged cadmium-telluride quantum dots to rainbow trout hepatocytes. *Nanotoxicology*, **2**(3): p. 113-120.
50. Ballou, B., B.C. Lagerholm, L.A. Ernst, M.P. Bruchez, and A.S. Waggoner. 2004. Noninvasive imaging of quantum dots in mice. *Bioconj.Chem.*, **15**: p. 79-86.
51. Fischer, H.C., L. Liu, K.S. Pang, and W.C.W. Chan. 2006. Pharmacokinetics of nanoscale quantum dots: In vivo distribution, sequestration, and clearance in the rat. *Adv.Funct.Mater.*, **16**: p. 1299-1305.
52. Gopee, N.V., D.W. Roberts, P. Webb, C.R. Cozart, P.H. Siitonen, A.R. Warbritton, W.W. Yu, V.L. Colvin, N.J. Walker, and P.C. Howard. 2007. Migration of intradermally injected quantum dots to sentinel organs in mice. *Toxicol. Sci.*, **98**(1): p. 249-257.
53. Yang, R.S.H., L.W. Chang, J.-P. Wu, M.-H. Tsai, H.-J. Wang, Y.-C. Kuo, T.-K. Yeh, C.S. Yang, and P. Lin. 2007. Persistent tissue kinetics and redistribution of nanoparticles, quantum dot 705, in mice: ICP-MS quantitative assessment. *Environ.Health Perspec.*, **115**(9): p. 1339-1343.
54. Chowdhury, M.J., D.G. McDonald, and C.M. Wood. 2004. Gastrointestinal uptake and fate of cadmium in rainbow trout acclimated to sublethal dietary cadmium. *Aquatic Tox.*, **69**: p. 149-163.
55. Franklin, N.M., C.N. Glover, J.A. Nicol, and C.M. Wood. 2005. Calcium/cadmium interaction at uptake surfaces in rainbow trout: waterborne versus dietary routes of exposure. *Environ.Toxicol.Chem.*, **24**(11): p. 2954-2964.
56. Harrison, S.E. and J.F. Klaverkamp. 1989. Uptake, elimination, and tissue distribution of dietary and aqueous cadmium by rainbow trout (*Salmo gairdneri*) and lake whitefish (*Coregonus clupeaformis*). *Environ.Toxicol.Chem.*, **8**: p. 87-97.
57. Norey, C.G., A. Cryer, and J. Kay. 1990. Induction of metallothionein gene expression by cadmium and the retention of the toxic metal in the tissues of rainbow trout (*Salmo gairdneri*). *Comp. Biochem. Physiol.*, **97**(2): p. 215-220.

58. Szebedinszky, C., J.C. McGeer, D.G. McDonald, and C.M. Wood. 2001. Effects of chronic Cd exposure via the diet or water on internal organ-specific distribution and subsequent gill Cd uptake kinetics in juvenile rainbow trout (*Oncorhynchus mykiss*). *Environ.Chem.Toxicol.*, **20**(3): p. 597-607.
59. Ryman-Rasmussen, J., J.E. Riveier, and N.A. Monteiro-Riveier. 2006. Penetration of intact skin by quantum dots with diverse physicochemical properties. *Toxicol.Sci.*, **91**(1): p. 159-165.
60. Karabanovas, V., E. Zakarevicius, A. Sukackaite, G. Streckyte, and R. Rotomskis. 2008. Examination of the stability of hydrophobic (CdSe)ZnS quantum dots in the digestive tract of rats. *Photochem.Photobiol.Sci.*, **7**: p. 725-729.
61. Gagne, F., J. Auclair, P. Turcotte, M. Fournier, C. Gagnon, S. Suave, and C. Blaise. 2008. Ecotoxicity of CdTe quantum dots to freshwater mussels: Impacts on immune system, oxidative stress and genotoxicity. *Aquat.Toxicol.*, **86**: p. 333-340.
62. Peyrot, C., C. Gagnon, F. Gagne, K.J. Wilkinson, P. Turcotte, and S. Sauve. 2009. Effects of cadmium telluride quantum dots on cadmium bioaccumulation and metallothionein production to the freshwater mussel, *Elliptio complanata*. *Comp. Biochem. Physiol., C*, **150**: p. 246-251.
63. Klaasen, C.D., *Casarett & Doull's Toxicology: The Basic Science of Poisons*. 6 ed. 2001, New York: McGraw-Hill.
64. de Smet, H. and R. Blust. 2001. Stress response and changes in protein metabolism in carp *Cyprinus carpio* during cadmium exposure. *Ecotox.Environ.Saf.*, **48**: p. 255-262.
65. Jessen-Eller, K. and J.F. Crivello. 1998. Changes in metallothionein mRNA and protein after sublethal exposure to arsenite and cadmium chloride in juvenile winter flounder. *Environ.Toxicol.Chem*, **17**(5): p. 891-896.
66. Pan, L. and H. Zhang. 2006. Metallothionein, antioxidant enzymes and DNA strand breaks as biomarkers of Cd exposure in a marine crab, *Charybdis japonica*. *Comp.Biochem.Phys., Part C*, **144**: p. 67-75.

67. Chen, W.-Y., J.A.C. John, C.-H. Lin, and C.-Y. Chang. 2007. Expression pattern of metallothionein, MTF-1 nuclear translocation, and its DNA-binding activity in zebrafish (*Danio rerio*) induced by zinc and cadmium. *Environ.Toxicol.Chem.*, **26**(1): p. 110-117.
68. Urani, C., P. Melchiorretto, C. Canevali, and G.F. Crosta. 2005. Cytotoxicity and induction of protective mechanisms in HepG2 cells exposed to cadmium. *Toxicol. in Vitro*, **19**: p. 887-892.
69. Chowdhury, M.J., D.G. McDonald, and C.M. Wood. 2004. Gastrointestinal uptake and fate of cadmium in rainbow trout acclimated to sublethal dietary cadmium. *Aquat.Toxicol.*, **69**: p. 149-163.
70. Sellin, M.K. and A.S. Kolok. 2006. Cadmium exposures during early development: Do they lead to reproductive impairment in fathead minnows? *Environ.Toxicol.Chem.*, **25**(11): p. 2957-2963.
71. Shackley, S.E., P.E. King, and S.M. Gordon. 1981. Vitellogenesis and trace metals in a marine teleost. *J.Fish Biol.*, **18**(3): p. 349-352.
72. Ghosh, P. and P. Thomas. 1995. Binding of metals to red drum vitellogenin and incorporation into oocytes. *Mar.Environ.Res.*, **39**: p. 165-168.
73. Kim, J. and R.P. Sharma. 2006. Cadmium-induced apoptosis in murine macrophages is antagonized by antioxidants and caspase inhibitors. *J.Toxicol.Environ.Health, Part A*, **69**: p. 1181-1201.
74. Oh, S.-H. and S.-C. Lim. 2006. A rapid and transient ROS generation by cadmium triggers apoptosis via caspase-dependent pathway in HepG2 cells and this is inhibited through *N*-acetylcysteine-mediated catalase upregulation. *Toxicol.Appl.Pharm.*, **212**: p. 212-223.
75. Waisberg, M., P. Joseph, B. Hale, and D. Beyersmann. 2003. Molecular and cellular mechanisms of cadmium carcinogenesis. *Toxicology*, **192**: p. 95-117.
76. Stohs, S.J. and D. Bagchi. 1995. Oxidative mechanisms in the toxicity of metal ions. *Free Radical Biol.Med.*, **18**(2): p. 321-336.

77. Basha, P.S., and A.U. Rani. 2003. Cadmium-induced antioxidant defense mechanism in freshwater teleost *Oreochromis mossambicus* (Tilapia). *Ecotox. Environ. Saf.*, **56**: p. 218-221.
78. Almeida, J.A., Diniz, Y.S., Marques, S.F.G., Faine, L.A., Ribas, B.O., Burneiko, R.C., and E.L.B. Novelli. 2002. The use of oxidative stress response as biomarkers in Nile tilapia (*Oreochromis niloticus*) exposed to in vivo cadmium contamination. *Environ. Int.*, **27**: p. 673-679.
79. Dally, H. and A.Hartwig. 1997. Induction and repair inhibition of oxidative DNA damage by nickel (II) and cadmium (II) in mammalian cells. *Carcinogenesis*, **18**(5): p. 1021-1026.
80. Hartmann, M. and A. Hartwig. 1998. Disturbance of DNA damage recognition after UV-irradiation by nickel (II) and cadmium (II) in mammalian cells. *Carcinogenesis*, **19**(4): p. 617-621.
81. Potts, R.J., R.D. Watkin, and B.A. Hart. 2003. Cadmium exposure down-regulates 8-oxoguanine DNA glycosylase expression in rat lung and alveolar epithelial cells. *Toxicology*, **184**: p. 189-202.
82. Cheng, S.H., A.W.K. Wai, C.H. So, and R.S.S. Wu. 2000. Cellular and molecular basis of cadmium-induced deformities in zebrafish embryos. *Environ. Toxicol. Chem.*, **19**(12): p. 3024-3031.
83. Chow, E.S.H. and S.H. Cheng. 2003. Cadmium affects muscle type development and axon growth in zebrafish embryonic somitogenesis. *Toxicol. Sci.*, **73**: p. 149-159.
84. Chan, P.K. and S.H. Cheng. 2003. Cadmium-induced ectopic apoptosis in zebrafish embryos. *Arch. Toxicol.*, **77**: p. 69-79.
85. Agency for Toxic Substances and Disease Registry, A., *ToxFAQs for Selenium*.
86. Lemly, A.D. 1997. A teratogenic deformity index for evaluating impacts of selenium on fish populations. *Ecotox. Environ. Saf.*, **37**: p. 259-266.

87. Lemly, A.D. 2002. Symptoms and implications of selenium toxicity in fish: the Belews Lake case example. *Aquat.Toxicol.*, **57**: p. 39-49.
88. Kleinow, K.M. and A.S. Brooks. 1986. Selenium compounds in the fathead minnow (*Pimephales promelas*) - 1. Uptake, distribution, and elimination of orally administered selenate, selenite, and l-selenomethionine. *Comp. Biochem. Physiol. C*, **83**(1): p. 61-69.
89. Hilton, J.W., P.V. Hodson, and S.J. Slinger. 1980. The requirement and toxicity of Selenium in Rainbow trout (*Salmo gairdneri*). *J. Nutr.*, **110**: p. 2527-2535.
90. Sato, R., Y. Ose, and T. Sakai. 1980. Toxicological effects of Selenium on fish. *Env. Poll. A*, **21**: p. 217-224.
91. Baumann, P.C. and R.B. Gillespie. 1986. Selenium bioaccumulation in gonads of largemouth bass and bluegill from three power plant cooling reservoirs. *Environ.Toxicol.Chem.*, **5**: p. 695-701.
92. Coyle, J.J., D.R. Buckler, C.G. Ingersoll, J.F. Fairchild, and T.W. May. 1993. Effect of dietary Selenium on the reproductive success of bluegills (*Lepomis Macrochirus*). *Environ.Toxicol.Chem.*, **12**: p. 551-565.
93. Ogle, R.S. and A.W. Knight. 1989. Effects of elevated foodborne selenium on growth and reproduction of the fathead minnow (*Pimephales promelas*). *Arch.Environ.Contam.Toxicol*, **18**: p. 795-803.
94. Letavayova, V.V., and J. Brozmanova. 2006. Selenium: from cancer prevention to DNA damage. *Toxicology*, **227**: p. 1-14.
95. Spallholz, J.E. 1994. On the nature of selenium toxicity and carcinostatic activity. *Free Radical Biol.Med.*, **17**(1): p. 45-64.
96. Shen, H.-M., C.-F. Yang, J. Liu, and C.-N. Ong. 2000. Dual role of glutathione in selenite-induced oxidative stress and apoptosis in human hepatoma cells. *Free Radical Biol.Med.*, **28**(7): p. 1115-1124.

97. Yan, L. and J.E. Spallholz. 1993. Generation of reactive oxygen species from the reaction of selenium compounds with thiols and mammary tumor cells. *Biochem.Pharm.*, **45**(2): p. 429-437.
98. Shen, H.-M., Yang, C.-F., and C.-N. Ong. 1999. Sodium selenite-induced oxidative stress and apoptosis in human hepatoma HepG₂ cells. *Int.J.Cancer*, **81**: p. 820-828.
99. Spyrou, G., Bjornstedt, M., Kumar, S., and A. Holmgren. 1995. AP-1 DNA-binding activity is inhibited by selenite and selenodigluathione. *FEBS Lett.*, **368**: p. 59-63.
100. Nordberg, J. and E.S.J. Arner. 2001. Reactive oxygen species, antioxidants, and the mammalian thioredoxin system. *Free Rad. Biol. Med.*, **31**(11): p. 1287-1312.
101. Miller, L.L., F. Wang, V.P. Palace, and A. Hontela. 2007. Effects of acute and subchronic exposures to waterborne selenite on the physiological stress response and oxidative stress indicators in juvenile rainbow trout. *Aquat.Toxicol.*, **83**: p. 263-271.
102. Zhang, J.-S., X.-Y. Gao, L.-D. Zhang, and Y.-P. Bao. 2001. Biological effects of a nano red elemental selenium. *Biofactors*, **15**: p. 27-38.
103. Lu, J., M. Kaeck, C. Jiang, A.C. Wilson, and H.J. Thompson. 1994. Selenite induction of DNA strand breaks and apoptosis in mouse leukemic L1210 cells. *Biochem.Pharm.*, **47**(9): p. 1531-1535.
104. Zhou, N., H. Xiao, T.-K. Li, A. Nur-E-Kamal, and L.F. Liu. 2003. DNA damage-mediated apoptosis induced by selenium compounds. *J.Biol.Chem.*, **278**: p. 29532-29537.
105. Abul-Hassan, K.S., B.E. Lehnert, L. Guant, and R. Walmsley. 2004. Abnormal DNA repair in selenium-treated human cells. *Mut.Res.*, **565**: p. 45-51.
106. Blessing, H., S. Kraus, P. Heindle, W. Bal, and A. Hartwig. 2004. Interaction of selenium compounds with zinc finger proteins involved in DNA repair. *Eur.J.Biochem.*, **271**: p. 3190-3199.

107. Pyron, M. and T.L. Beitinger. 1989. Effect of selenium on reproductive behavior and fry of fathead minnows. *Bull.Environ.Contam.Toxicol.*, **42**: p. 609-613.
108. Teh, S.J., X. Deng, F.-C. Teh, and S.O. Hung. 2002. Selenium-induced teratogenicity in Sacramento splittail (*Pogonichthyhy macroepidotus*). *Mar.Environ.Res.*, **54**: p. 605-608.
109. Woock, S.E., W.R. Garrett, W.E. Partin, and W.T. Bryson. 1987. Decreased survival and teratogenesis during laboratory selenium exposures to Bluegill, *Lepomis macrochirus*. *Bull.Environ.Contam.Toxicol.*, **39**: p. 998-1005.
110. Schultz, R. and R. Hermanutz. 1990. Transfer of toxic concentrations of selenium from parent to progeny in fathead minnow (*Pimephales promelas*). *Bull.Environ.Contam.Toxicol.*, **45**: p. 568-573.
111. Woock, S.E., Garrett, W.R., Partin, W.E., and W.T. Bryson. 1987. Decreased survival and teratogenesis during laboratory selenium exposures to Bluegill, *Lepomis macrochirus*. *Bull.Environ.Contam.Toxicol.*, **39**: p. 998-1005.
112. Shchipunov, Y.A. 1997. Self-organising structures of lecithin. *Russ.Chem.Rev.*, **66**(4): p. 301-322.
113. Brook, J.G., S. Linn, and M. Aviram. 1986. Dietary soy lecithin decreases plasma triglyceride levels and inhibits collagen- and ADP-induced platelet aggregation. *Biochem. Med. Metab. Biol.*, **35**(1): p. 31-39.
114. Mastellone, I., E. Polichetti, S. Gres, C. de la Maisonneuve, N. Domingo, V. Marin, A.-M. Lorec, C. Farnarier, H. Portugal, G. Kaplanski, and F. Chanussot. 2000. Dietary soybean phosphatidylcholines lower lipidemia: Mechanisms at the levels of intestine, endothelial cell, and hepato-biliary axis. *J. Nutr. Biochem.*, **11**: p. 461-466.
115. *Aventi Polar Lipids, Inc.* [cited Jan. 16, 2009]; Available from: www.aventilipids.com.
116. Gabriel, N.E. and M.F. Roberts. 1984. Spontaneous formation of stable unilamellar vesicles. *Biochemistry*, **23**(18): p. 4011-4015.

117. Huang, C.-H. 1969. Studies on phosphatidylcholine vesicles. Formation and physical characteristics. *Biochemistry*, **8**(1): p. 344-351.
118. Nii, T. and F. Ishii. 2005. Encapsulation efficiency of water-soluble and insoluble drugs in liposomes prepared by the microencapsulation vesicle method. *Int.J.Pharm.*, **298**: p. 198-205.
119. Papahadjopoulos, D., S. Nir, and S. Ohki. 1971. Permeability properties of phospholipid membranes: Effect of cholesterol and temperature. *Biochim. Biophys. Acta*, **266**: p. 561-583.
120. Yesair, D.W., *Phosphatidyl choline and lysophosphatidyl choline in mixed lipid micelles as novel drug delivery systems*. Phospholipids, ed. I.a.G.P. Hanin. 1990, New York: Plenum Press.
121. Mackiewicz, M.R., B.R. Ayres, and S.M. Reed. 2008. Reversible, reagentless solubility changes in phosphatidylcholine-stabilized gold nanoparticles. *Nanotechnology*, **19**.
122. Fiume, Z. 2001. Final report on the safety assessment of Lecithin and hydrogenated Lecithin. *Int. J. Toxicol.*, **20**(suppl.1): p. 21-45.
123. Moreno, M.A., M.P. Ballesteros, and P. Frutos. 2003. Lecithin-based oil-in-water microemulsions for parental use: Pseudoternary diagrams, characterization, and toxicity studies. *J. Pharm.Sci.*, **92**(7): p. 1428-1437.
124. Hamza, N., M. Mhelti, I.B. Khemis, C. Cahu, and P. Kestemont. 2008. Effect of dietary phospholipid levels on performance, enzyme activities, and fatty acid composition of pikeperch (*Sander lucioperca*) larvae. *Aquaculture*, **275**: p. 274-282.
125. Coutteau, P., E.K.M. Kontara, and P. Sorgeloos. 2000. Comparison of phosphatidylcholine purified from soybean and marine fish roe in the diet of postlarval *Penaeus vannamei*. *Aquaculture*, **181**: p. 331-345.
126. Administration, U.F.a.D. *Guidance for Industry: Guidance on the labeling of certain uses of lecithin derived from soy under section 403(w) of the federal food, drug, and cosmetic act*. [cited October 14, 2009]; Available from: www.fda.gov.

127. Shertzer, H.G., Nebert, D.W., Puga, A., Ary, M., Sonntag, D., Dixon, K., Robinson, L.J., Cianciolo, E., and T.P. Dalton. 1998. Dioxin causes a sustained oxidative stress response in the mouse. *Biochem. Biophys. Res. Commun.*, **253**: p. 44-48.
128. Valko, M., Leibfritz, D., Moncol, J., Cronin, M.T.D., Mazur, M., and J. Telser. 2007. Free radicals and antioxidants in normal physiological functions and human disease. *International Journal of Biochemistry & Cell Biology*, **39**: p. 44-84.
129. Davies, K.J. 2000. Oxidative stress, antioxidant defenses, and damage removal, repair, and replacement systems. *IUBMB Life*, **50**: p. 279-289.
130. Marnett, L.J. 1999. Lipid peroxidation-DNA damage by malondialdehyde. *Mutation Research*, **424**: p. 83-95.
131. Marnett, L.J. 2000. Oxyradical and DNA damage. *Carcinogenesis*, **21**(3): p. 361-370.
132. West, J.D., and L.J. Marnett. 2006. Endogenous reactive intermediates as modulators of cell signaling and cell death. *Chemical Research in Toxicology*, **19**(2): p. 173-194.
133. Livingstone, D.R. 2001. Contaminant-stimulated reactive oxygen species production and oxidative damage in aquatic organisms. *Mar.Poll.Bull.*, **42**(8): p. 656-666.
134. Droge, W. 2002. Free radicals in the physiological control of cell function. *Physiol.Rev.*, **82**: p. 47-95.
135. Stohs, S.J., and D. Bagchi. 1995. Oxidative mechanisms in the toxicity of metal ions. *Free Radical Biology & Medicine*, **18**(2): p. 321-336.
136. Valko, M., Rhodes, C.J., Moncol, J., Izakovic, M., and M. Mazur. 2006. Free radicals, metals and antioxidants in oxidative stress-induced cancer. *Chem-Biol.Interactions*, **160**: p. 1-40.
137. Martindale, J.L. and N.J. Holbrook. 2002. Cellular response to oxidative stress: Signaling for suicide and survival. *J.Cell.Physiol.*, **192**: p. 1-15.

138. Davies, K.J. 1999. The broad spectrum of responses to oxidants in proliferating cells: a new paradigm for oxidative stress. *IUBMB Life*, **48**: p. 41-47.
139. Weise, A.G., R.E. Pacifici, and K.J.A. Davies. 1995. Transient adaptation to oxidative stress in mammalian cells. *Arch.Biochem.Biophys.*, **318**(1): p. 231-240.
140. Cadet, J., Delatour, T., Douki, T., Gasparutto, D., Pouget, J.-P., Ravanat, J.-L., and S. Sauvaigo. 1999. Hydroxyl radicals and DNA base damage. *Mut.Res.*, **424**: p. 9-21.
141. Dizdaroglu, M., Jaruga, P., Birincioglu, M., and H. Rodriguez. 2002. Free radical-induced damage to DNA: mechanisms and measurement. *Free Radical Biology & Medicine*, **32**(11): p. 1102-1115.
142. Evans, M.D., Dizdaroglu, M., and M.S. Cooke. 2004. Oxidative DNA damage and disease: induction, repair, and significance. *Mut.Res.*, **567**: p. 1-61.
143. Kasprzak, K.S. 2002. Oxidative DNA and protein damage in metal-induced toxicity and carcinogenesis. *Free Radical Biology & Medicine*, **32**(10): p. 958-967.
144. Lloyd, D.R., and D.H. Philips. 1999. Oxidative DNA damage mediated by copper(II), iron (II), and nickel (II) Fenton reactions: evidence for site-specific mechanisms in the formation of double-strand breaks, 8-hydroxydeoxyguanosine and putative intrastrand cross-links. *Mut.Res.*, **424**: p. 23-36.
145. Kelly, S.A., C.M. Havrilla, T.C. Brady, K.H. Abramo, and E.D. Levin. 1998. Oxidative stress in toxicology: Established mammalian and emerging piscine model systems. *Environ.Health Perspec.*, **106**(7): p. 375-384.
146. Kinoshita, A., Wanibuchi, H., Wei, M., Yunoki, T., and S. Fukushima. 2007. Elevation of 8-hydroxydeoxyguanosine and cell proliferation via generation of oxidative stress by organic arsenicals contributes to their carcinogenicity in the rat liver and bladder. *Tox.Appl.Pharm.*, **221**: p. 295-305.

147. Wang, S.C., Chung, J.-G., Chen, C.-H., and S.-C. Chen. 2006. 2- and 4-Aminobiphenyls induce oxidative DNA damage in human hepatoma (HepG2) cells via different mechanisms. *Mut.Res.*, **593**: p. 9-21.
148. Arnaiz, S.L., Llesuy, S., Cutrin, J.C., and A. Boveris. 1995. Oxidative stress by acute acetaminophen administration in mouse liver. *Free Rad. Biol. Med.*, **19**(3): p. 303-310.
149. Kamata, H., and H. Hirata. 1999. Redox regulation of cellular signalling. *Cell.Signal.*, **11**(1): p. 1-14.
150. Thannickal, V.J., and B.L. Fanburg. 2000. Reactive oxygen species in cell signaling. *Am.J.Physiol.Lung.Cell.Mol.Physiol.*, **279**: p. L1005-L1028.
151. Bagchi, D., Bagchi, M., Tang, L., and S.J. Stohs. 1997. Comparative in vitro and in vivo protein kinase C activation by selected pesticides and transition metal salts. *Tox.Lett.*, **91**: p. 31-37.
152. Clemens, M.J., Trayner, I., and J. Menaya. 1992. The role of protein kinase C isoenzymes in the regulation of cell proliferation and differentiation. *Journal of Cell Science*, **103**: p. 881-887.
153. Gopalakrishna, R., and S. Jaken. 2000. Protein kinase C signaling and oxidative stress. *Free Radical Biology & Medicine*, **28**(9): p. 1349-1361.
154. Konishi, H., M. Tanaka, Y. Takemura, H. Matsuzaki, Y. Ono, U. Kikkawa, and Y. Nishizuka. 1997. Activation of protein kinase C by tyrosine phosphorylation in response to H₂O₂. *Proc.Natl.Acad.Sci.*, **94**: p. 11233-11237.
155. Wijeratne, S.S.K., Cuppett, S.L., and V. Schlegel. 2005. Hydrogen peroxide induced oxidative stress damage and antioxidant enzyme response in Caco-2 human colon cells. *J.Agric. Food Chem.*, **53**: p. 8768-8774.
156. Allen, R.G., and M. Tresini. 2000. Oxidative stress and gene regulation. *Free Radical Biology & Medicine*, **28**(3): p. 463-499.
157. Martindale, J.L., and N.J. Holbrook. 2002. Cellular response to oxidative stress: Signaling for suicide and survival. *J.Cell.Physiol.*, **192**: p. 1-15.

158. Storez, P. 2006. Mitochondrial ROS-radical detoxification, mediated by protein kinase D. *Trends in Cell Biology*, **17**(1): p. 13-18.
159. Kanthasamy, A.G., Kitazawa, M., Kanthasamy, A., and V. Anantharam. 2003. Role of proteolytic activation of protein kinase C in oxidative stress-induced apoptosis. *Antioxidants and Redox Signaling*, **5**(5): p. 609-620.
160. Allen, R.G. and M. Tresini. 2000. Oxidative stress and gene regulation. *Free Radical Biol.Med.*, **28**(3): p. 463-499.
161. Iryo, Y., M. Matsuoka, B. Wispriyono, T. Sugiura, and H. Igisu. 2000. Involvement of the extracellular signal-regulated protein kinase (ERK) pathway in the induction of apoptosis by cadmium chloride in CCRF-CEM cells. *Biochem.Pharm.*, **60**: p. 1875-1882.
162. Turner, N.A., Xia, F., Azhar, G., Zhang, X., Liu, L., and J.Y. Wei. 1998. Oxidative stress induces DNA fragmentation and caspase activation via the c-jun NH₂-terminal kinase pathway in H9c2 cardiac muscle cells. *J.Mol.Cell.Cardiol.*, **30**: p. 1789-1801.
163. West, J.D. and L.J. Marnett. 2006. Endogenous reactive intermediates as modulators of cell signaling and cell death. *Chem.Res.Toxicol.*, **19**(2): p. 173-194.
164. Storez, P., H. Doppler, and A. Toker. 2005. Protein kinase D mediates mitochondrion-to-nucleus signaling and detoxification from mitochondrial reactive oxygen species. *Molec.Cell.Biol.*, **25**(19): p. 8520-8530.
165. Storez, P. 2006. Mitochondrial ROS-radical detoxification, mediated by protein kinase D. *Trends Cell.Biol.*, **17**(1): p. 13-18.
166. Wang, X.-T., K.D. McCullough, X.-J. Wang, G. Carpenter, and N.J. Holbrook. 2001. Oxidative stress-induced phospholipase C- γ 1 activation enhances cell survival. *J.Bio.Chem.*, **276**(30): p. 28364-28371.
167. Guyton, K.Z., Y. Liu, M. Gorospe, Q. Xu, and N.J. Holbrook. 1996. Activation of mitogen-activated protein kinase by H₂O₂. *J.Bio.Chem.*, **271**(8): p. 4138-4142.

168. Weber, H., S. Huhns, L. Jonas, G. Sparmann, M. Bastian, and P. Schuff-Werner. 2007. Hydrogen peroxide-induced activation of defense mechanisms against oxidative stress in rat pancreatic acinar AR42J cells. *Free Radical Biol.Med.*, **42**: p. 830-841.
169. Whisler, R.L., M.A. Goyette, I.S. Grants, and Y.G. Newhouse. 1995. Sublethal levels of oxidant stress stimulate multiple serine/threonin kinases and suppress protein phosphatases in Jurkat T cells. *Arch.Biochem.Biophys.*, **319**(1): p. 23-35.
170. Han, H., H. Long, H. Wang, J. Wang, Y. Zhang, and Z. Wang. 2004. Progressive apoptotic cell death triggered by transient oxidative insult in H9c2 rat ventricular cells: a pattern of apoptosis and the mechanisms. *Am.J. Physiol.Heart Circ. Physiol.*, **286**: p. H2169-2182.
171. Song, J., J. Li, A. Lulla, B.M. Evers, and D.H. Chung. 2006. Protein kinase D protects against oxidative stress-induced intestinal epithelial cell injury via Rho/ROK/PKC pathway activation. *Am.J. Physiol.Cell Physiol.*, **290**: p. C1469-C1476.
172. Kurata, S. 2000. Selective activation of p38 MAPK cascade and mitotic arrest caused by low level oxidative stress. *J.Bio.Chem.*, **275**(31): p. 23413-23416.
173. Kim, S.D., C.K. Moon, S.-Y. Eun, P.D. Ryu, and S.A. Jo. 2005. Identification of ASK1, MKK4, JNK, c-Jun, and caspase-3 as a signaling cascade involved in cadmium-induced neuronal cell apoptosis. *Biochem.Biophys.Res.Comm.*, **328**: p. 326-334.
174. Sharma, P., and K.P. Mishra. 2006. Aluminium-induced maternal and developmental toxicity and oxidative stress in rat brain: Response to combined administration of Tiron and glutathione. *Reproductive Toxicology*, **21**: p. 313-321.
175. Hoffman, D.J., Marn, C.M., Marois, K.C., Sproul, E., Dunne, M., and J.P. Skorupa. 2002. Sublethal effects in avocet and stilt hatchlings from selenium-contaminated sites. *Enviro.Tox.Chem*, **21**(3): p. 561-566.

176. Pagano, G., de Biase, A., Deeva, I., Degan, P., Doronin, Y.K., Iaccarino, M., Oral, R., Trieff, N.M., Warnau, M., and L.G. Korkina. 2001. The role of oxidative stress in developmental and reproductive toxicity of tamoxifen. *Life Sciences*, **68**: p. 1735-1749.
177. Zhao, Z., and E.A. Reece. 2005. Nicotine-induced embryonic malformations mediated by apoptosis from increasing intracellular calcium and oxidative stress. *Birth Defects Research, Part B*, **74**: p. 383-391.
178. Williams, F.E., Sickelbaugh, T.J., and E. Hassoun. 2006. Modulation by ellagic acid and DCA-induced developmental toxicity in the zebrafish. *J.Bio.Chem.Molec.Tox.*, **20**(4): p. 183-190.
179. Korkina, L.G., Deeva, I., de Biase, A., Degan, P., Iaccarino, M., Oral, R., Warnau, M., and G. Pagano. 2000. Redox-dependent toxicity of diepoxybutane and mitomycin C in sea urchin embryogenesis. *Carcinogenesis*, **21**(2): p. 213-220.
180. Buryskova, B., Hilscherova, K., Blaha, L., Marsalek, B., and I. Holoubek. 2006. Toxicity and modulation of biomarkers in *Xenopus laevis* embryos exposed to polycyclic aromatic hydrocarbons and their N-heterocyclic derivatives. *Enviro.Tox.* , **21**: p. 590-598.
181. Kaegi, R., A. Ulrich, B. Sinnet, R. Vonbank, A. Wichser, S. Zuleeg, H. Simmler, S. Brunner, H. Vonmont, M. Burkhardt, and M. Boller. 2008. Synthetic TiO₂ nanoparticle emission from exterior facades into the aquatic environment. *Environ.Poll.*, **156**: p. 233-239.
182. Benn, T.M. and P. Westerhoff. 2008. Nanoparticle silver released into water from commercially available sock fabrics. *Environ.Sci.Technol.*, **42**: p. 4133-4139.
183. Lee, K.J., P.D. Nallathamby, L.M. Browning, C.J. Osgood, and X.-H. N. Xu. 2007. In Vivo imaging of transport and biocompatibility of single silver nanoparticles in early development of zebrafish embryos. *ACS Nano*, **1**(2): p. 133-143.
184. Asharani, P.V., Y.L. Wu, Z. Gong, and S. Valiyaveetil. 2008. Toxicity of silver nanoparticles in zebrafish models. *Nanotechnology*, **19**: p. 255102-255109.

185. Blickley, T.M. and P. McClellan-Green. 2008. Toxicity of aqueous fullerene in adult and larval *Fundulus heteroclitus*. *Environ.Toxicol.Chem.*, **27**(9): p. 1964-1971.
186. Cheng, J., E. Flahaut, and S.H. Cheng. 2007. Effect of carbon nanotubes on developing zebrafish (*Danio rerio*) embryos. *Environ.Toxicol.Chem.*, **26**(4): p. 708-716.
187. Jiang, J., G. Oberdorster, and P. Biswas. 2009. Characterization of size, surface charge, and agglomeration state of nanoparticle dispersions for toxicological studies. *J. Nanopart. Res.*, **11**: p. 77-89.
188. Kashiwada, S. 2006. Distribution of nanoparticles in the see-through medaka (*Oryzias latipes*). *Environ.Health Perspec.*, **114**(11): p. 1697-1702.
189. King-Heiden, T., R.J. Hutz, and M.J. Caravan, III. 2005. Accumulation, tissue distribution, and maternal transfer of dietary 2,3,7,8-Tetrachlorodibenzo-p-dioxin: Impacts on reproductive success in zebrafish. *Toxicol.Sci.*, **87**(2): p. 497-507.
190. Monteverdi, G.H. and R.T. DiGiulio. 2000. Oocytic accumulation and tissue deposition of 2,3,7,8-tetrachlorodibenzene-p-dioxin and benzo[a]pyrene in gravid *Fundulus heteroclitus*. *Environ.Toxicol.Chem.*, **19**(10): p. 2512-2518.
191. Cheng, S.H., Wai, A.W.K., So, C.H., and R.S.S. Wu. 2000. Cellular and molecular basis of cadmium-induced deformities in zebrafish embryos. *ET&C*, **19**(12): p. 3024-3031.
192. Dubertret, B., P. Skourides, D.J. Norris, V. Noireaux, A.H. Brivanlou, and A. Libchaber. 2002. *In vivo* imaging of quantum dots encapsulated in phospholipid micelles. *Science*, **298**: p. 1759-1762.
193. Armstrong, P.B. and J.S. Child. 1965. Stages in the normal development of *Fundulus Heteroclitus*. *Biol.Bull.*, **128**(2): p. 143-167.
194. Holbrook, D. 2008. personal communication

195. King-Heiden, T.C., P.N. Wicinski, A.N. Mangham, K.M. Metz, D. Nesbit, J.A. Pedersen, R.J. Hamers, W. Heideman, and R.E. Peterson. 2009. Quantum dot nanotoxicity assessment using zebrafish embryo. *Environ.Sci.Technol.*, **43**: p. 1605-1611.
196. Michibata, H. 1981. Uptake and distribution of calcium in the egg of the teleost, *Oryzia latipes*. *J. Fish Biol.*, **19**: p. 691-696.
197. Burnett, K.G., L.J. Bain, W.S. Baldwin, G.V. Callard, S. Cohen, R.T. Di Giulio, D.H. Evans, M. Gomez-Chiarri, M.E. Hahn, C.A. Hoover, S.I. Karchner, F. Katoh, D.L. MacLatchy, W.S. Marshall, J.N. Meyer, D.E. Nacci, M.F. Oleksiak, B.B. Rees, T.D. Sinder, J.J. Stegeman, D.W. Towle, P.A. Van Veld, W.K. Vogelbein, A. Whitehead, R.N. Winn, and D.L. Crawford. 2007. *Fundulus* as the premier teleost model in Environmental Biology: Opportunities for new insights using genomics. *Comp. Biochem. Physiol., D* **2**(4): p. 257-286.
198. Green, M., and E. Howman. 2005. Semiconductor quantum dots and free radical induced DNA nicking. *Chem.Commun.*: p. 121-123.
199. Sanders, M.B., M. Sebire, J. Sturve, P. Christian, I. Katsiadaki, B.P. Lyons, D. Sheahan, J.M. Weeks, and S.W. Feist. 2008. Exposure of sticklebacks (*Gasterosteus aculeatus*) to cadmium sulfide nanoparticles: Biological effects and the importance of experimental design. *Mar.Environ.Res.*, **66**(1): p. 161-163.
200. Holbrook, R.D., K.E. Murphy, J.B. Morrow, and K.D. Cole. 2008. Trophic transfer of nanoparticles in a simplified invertebrate food web. *Nat. Nanotechnol.*, **3**: p. 352-355.
201. Taylor, H.E., *Inductively coupled plasma mass spectrometry: practices and techniques*. 2001: Academic Press.
202. Bush, C.P. and J.S. Weis. 1983. Effects of salinity on fertilization success in two populations of *Fundulus heteroclitus*. *Biol.Bull.*, **164**: p. 406-417.
203. Ohtsuka, E. 1960. On the hardening of the chorion of the fish egg after fertilization. III. The mechanism of chorion hardening in *Oryzia latipes*. *Biol.Bull.*, **118**: p. 120-128.

204. Ringwood, A.H., J. Hoguet, C.J. Keppler, M.L. Gielazyn, B.P. Ward, and A.R. Rourk. January 2003. < <http://ciceet.unh.edu/powerpoint/ringwood-methods.pdf> >. Cellular Biomarkers (Lysosomal Destabilization, Glutathione & Lipid Peroxidation) in Three Common Estuarine Species: A Methods Handbook.
205. Andersen, M.E. 1985. Determination of glutathione and glutathione disulfide in biological samples. *Method Enzymol.*, **113**: p. 548-555.
206. Ohkawa, H., N. Ohishi, and K. Yagi. 1979. Assay for lipid peroxides in animal tissues by thiobarbituric acid reaction. *Anal.Biochem.*, **95**: p. 351-358.
207. Orbea, A., M. Ortiz-Zarragoitia, M. Sole, C. Porte, and M.P. Cajaraville. 2002. Antioxidant enzymes and peroxisome proliferation in relation to contaminant body burdens of PAHs and PCBs in bivalve mollusks, crabs, and fish from the Urdaibai and Plentzia estuaries (Bay of Biscay). *Aquat.Toxicol.*, **58**: p. 75-98.
208. Ott, R.L. and M. Longnecker, *An Introduction to statistical methods and data analysis*. 5 ed. 2001, Pacific Grove, CA: Duxbury.
209. Babkin, B.P. and D.J. Bowie. 1928. The digestive system and its function in *Fundulus heteroclitus*. *Biol.Bull.*, **54**(3): p. 254-277.
210. Kamler, E. 2005. Parent-egg-progeny relationships in teleost fishes: an energetics perspective. *Rev.Fish Biol.Fish.*, **15**: p. 399-421.
211. Kumar, V., A.K. Abbas, and N. Fausto., *Pathologic Basis of Disease*. 7 ed. 2005, Philadelphia: Elsevier Saunders.
212. Oberdorster, E., S. Zhu, T.M. Blickey, P. McClellan-Green, and M.L. Haasch. 2006. Ecotoxicology of Carbon-Based Engineered Nanoparticles: Effects of Fullerene on Aquatic Organisms. *Carbon*, **44**(1112-1120).
213. Cumberland, S.A. and J.R. Lead. 2009. Particle size distribution of silver nanoparticles at environmentally relevant conditions. *J.Chromatogr. A*, **1216**: p. 9099-9105.

214. French, R.A., A.R. Jacobson, B. Kim, S.L. Isley, R.L. Penn, and P.C. Baveye. 2009. Influence of ionic strength, pH, and cation valence on aggregation kinetics of titanium dioxide nanoparticles. *Environ.Sci.Technol.*, **43**: p. 1354-1359.
215. Szoka, F. and D. Papahajopoulos. 1980. Comparative properties and methods of preparation of lipid vesicles (liposomes). *Annu. Rev. Biophys. Bioeng.*, **9**: p. 467-508.
216. Richardson, K.C., L. Jarett, and E.H. Finke. 1960. Embedding in epoxy resins for ultrathin sections in electron microscopy. *Stain Tech.*, **35**(313-323).
217. Yu, W.W., L.H. Qu, W.Z. Guo, and X.G. Peng. 2003. Experimental determination of the extinction coefficient of CdTe, CdSe, and CdS nanocrystals. *Chem.Mat.*, **15**: p. 2854-2860.
218. Battle, L.P., *The role of biotransformation on the toxic effects of polycyclic aromatic hydrocarbons in the Atlantic killifish (Fundulus heteroclitus)*. 2008, Duke University: Durham. p. 198.
219. Livak, K.J. and T.D. Schmittgen. 2001. Analysis of relative gene expression data using real-time quantitative PCR and the $2^{-\Delta\Delta CT}$ method. *Methods*, **25**: p. 402-408.
220. Hinton, D.E., *Cells, cellular responses, and their markers in chronic toxicity of fishes*. Aquatic Toxicology, ed. G.K. Ostrander and D.M. Malins. 1993: Lewis Publishers/CRC Press.
221. Boorman, G.A., S. Boots, T.E. Bunton, J.W. Fournie, J.C. Harshbarger, W.E. Hawkins, D.E. Hinton, M.P. Joikinen, M.S. Okihiro, and M.J. Wolfe. 1997. Diagnostic criteria for degenerative, inflammatory, proliferative nonneoplastic and neoplastic liver lesions in medaka (*Oryzias latipes*): Consensus of a National Toxicology Program pathology working group. *Toxicol.Pathol.*, **25**: p. 202-210.
222. Ingle, T.M., R. Alexander, J. Bouldin, and R.A. Buchanan. 2008. Absorption of semiconductor nanocrystals by the aquatic invertebrate *Ceriodaphnia dubia*. *Bull.Environ.Contam.Toxicol.*, **81**: p. 249-252.
223. Wiecinski, P.N., K.M. Metz, A.N. Mangham, K.H. Jacobson, R.J. Hamers, and J.A. Pedersen. 2009. Gastrointestinal biodurability of engineered nanoparticles: Development on an in vitro assay. *Nanotoxicology*, **3**(3): p. 202-214.

224. Thomas, P. 1989. Effects of Aroclor 1254 and cadmium on reproductive endocrine function and ovarian growth in Atlantic croaker. *Mar. Environ. Res.*, **28**: p. 499-503.
225. Tilton, S., C.M. Foran, and W.B. Benson. 2003. Effect of cadmium on the reproductive axis of Japanese medaka (*Oryzias latipes*). *Comp. Biochem. Physiol. C*, **136**: p. 265-276.
226. Vetillard, A. and T. Bailhache. 2005. Cadmium: An endocrine disruptor that affects gene expression in the liver and brain of juvenile Rainbow trout. *Biol. Reprod.*, **72**: p. 119-126.
227. Stoica, A., B.S. Katzenellenbogen, and M.B. Martin. 2000. Activation of estrogen receptor- α by the heavy metal cadmium. *Molec. Endocrinol.*, **14**: p. 545-553.
228. Foran, C.M., B.N. Peterson, and W. H. Benson. 2002. Influence of parental and developmental cadmium exposure on endocrine and reproductive function in Japanese medaka (*Oryzias latipes*). *Comp. Biochem. Physiol. C*, **133**: p. 345-354.
229. Thompson, J. and J. Bannigan. 2008. Cadmium: Toxic effects on the reproductive system and the embryo. *Reprod. Toxicol.*, **25**: p. 304-315.
230. Ercal, N., H. Gurer-Orhan, and N. Aykin-Burns. 2001. Toxic metals and oxidative stress Part 1: Mechanisms involved in metal induced oxidative damage. *Curr. Top. Med. Chem.*, **1**: p. 529-539.
231. Valavanidis, A., R. Vlahogiani, M. Dassenakis, and M. Scoullas. 2006. Molecular biomarkers of oxidative stress in aquatic organisms in relation to toxic environmental pollutants. *Ecotox. Environ. Saf.*, **64**: p. 178-189.
232. Valko, M., C.J. Rhodes, J. Moncol, M. Izakovic, and M. Mazur. 2006. Free radicals, metals and antioxidants in oxidative stress-induced cancer. *Chem. Biol. Interact.*, **160**: p. 1-40.
233. Choi, A.O., S.J. Cho, J. Desbarats, J. Lovric, and D. Maysinger. 2007. Quantum dot-induced cell death involves Fas upregulation and lipid peroxidation in human neuroblastoma cells. *J. Nanobiotechnology*, **5**(1).

234. Li, K.G., J.T. Chen, S.S. Bai, X. Wen, S.Y. Song, Q. Yu, J. Li, and Y.Q. Wang. 2009. Intracellular oxidative stress and cadmium ions release induce cytotoxicity of unmodified cadmium sulfide quantum dots. *Toxicol. in Vitro*, **23**: p. 1007-1013.
235. Blickley, T.M., D. Rittschof, and P. McClellan-Green. 2010. The reproductive and developmental toxicity of quantum dots in the mummichog, *Fundulus heteroclitus*: A pilot study. *Mar. Environ. Res.*
236. Pathak, N. and S. Khandelwal. 2006. Influence of cadmium on murine thymocytes: Potentiation of apoptosis and oxidative stress. *Toxicol. Lett.*, **165**: p. 121-132.
237. Wolf, M.B. and J.W. Baynes. 2007. Cadmium and mercury cause an oxidative stress-induced endothelial dysfunction. *BioMetals*, **20**: p. 73-81.
238. Nzengue, Y., R. Steiman, C. Garrel, E. Lefebvre, and P. Guiraud. 2008. Oxidative stress and DNA damage induced by cadmium in the human keratinocyte HaCaT cell line: Role of glutathione in the resistance to cadmium. *Toxicology*, **243**: p. 193-206.
239. Lange, A., O. Ausseil, and H. Segner. 2002. Alterations of tissue glutathione levels and metallothionein mRNA in rainbow trout during single and combined exposure to cadmium and zinc. *Comp. Biochem. Physiol. C*, **131**: p. 231-243.
240. Berntssen, M.H., A.-K. Lundebye, and K. Hamre. 2000. Tissue lipid peroxidation responses in Atlantic salmon (*Salmo salar* L.) parr fed high levels of dietary copper and cadmium. *Fish Physiol. Biochem.*, **23**: p. 35-48.
241. Basha, P.S. and A.U. Rani. 2003. Cadmium-induced antioxidant defense mechanism in freshwater teleost *Oreochromis mossambicus* (Tilapia). *Ecotox. Environ. Saf.*, **56**: p. 218-221.
242. Spallholz, J.E., V.P. Palace, and T.W. Reid. 2004. Methioninase and selenomethionine but not Se-methylselenocysteine generate methylselenol and superoxide in an *in vitro* chemiluminescent assay: implications for the nutritional carcinostatic activity of selenoamino acids. *Biochem. Pharm.*, **67**: p. 547-554.

243. Spallholz, J.E. 1997. Free radical generation by selenium compounds and their prooxidant toxicity. *Biomed. Environ. Sci.*, **10**: p. 260-270.
244. Sheader, D.L., T.D. Williams, B.P. Lyons, and J.K. Chipman 2006. Oxidative stress response of European flounder (*Platichthys flesus*) to cadmium determined by a custom cDNA microarray. *Mar. Environ. Res.*, **62**: p. 33-44.
245. Olsson, P.-E., P. Kling, C. Petterson, and C. Silversand. 1995. Interaction of cadmium and oestradiol-17B on metallothionein and vitellogenin synthesis in rainbow trout (*Oncorhynchus mykiss*). *Biochem. J.*, **307**: p. 197-203.
246. Olsson, P.-E., A. Larsson, A. Maage, C. Haux, D. Bonham, M. Zafarullah, and L. Gedamu. 1989. Induction of metallothionein synthesis in rainbow trout, *Salmo gairdneri*, during long-term exposure to waterborne cadmium. *Fish Physiol. Biochem.*, **6**(4): p. 221-229.
247. Wangsongsak, A., S. Utarnpongsa, M. Druatrachue, M. Ponglikitmonkol, P. Pokethitiyook, and T. Sumranwanich. 2007. Alterations of organ histopathology and metallothionein mRNA expression in silver barb, *Puntius gonionotus* during subchronic cadmium exposure. *J. Environ. Sci.*, **19**: p. 1341-1348.
248. Roesijadi, G., S. Rezvankhah, A. Perez-Matus, A. Mitelberg, K. Torruellas, and P.A. Van Veld. 2009. Dietary cadmium and benzo(a)pyrene increased intestinal metallothionein expression in the fish *Fundulus heteroclitus*. *Mar. Environ. Res.*, **67**: p. 25-30.
249. Waalkes, M.P. 2003. Cadmium carcinogenesis. *Mut. Res.*, **533**: p. 107-120.
250. Sangalang, G.B. and M.J. O'Halloran. 1973. Adverse effects of cadmium on brook trout testis and on in vitro testicular androgen synthesis. *Biol. Reproduction*, **9**: p. 394-403.
251. Iliopoulou-Georgudaki, J. and N. Kotsanis. 2001. Toxic effects of cadmium and mercury in rainbow trout (*Oncorhynchus mykiss*): A short-term bioassay. *Bull. Environ. Contam. Toxicol.*, **66**: p. 77-85.
252. Karbe, E. and R.L. Kerlin. 2002. Review article: Cystic degeneration/spongiosis hepatitis in rats. *Toxicol. Pathol.*, **30**: p. 216-227.

253. Ramot, Y., M. Steiner, V. Morad, S. Leibovitch, N. Amouyal, M.F. Cesta, and A. Nyska. 2010. Pulmonary thrombosis in the mouse following intravenous administration of quantum dot-labeled mesenchymal cells. *Nanotoxicology*, **4**(1): p. 98-105.
254. Tao, X., J.D. Fortner, B. Zhnag, Y. He, Y. Chen, J.B. Hughes. 2009. Effects of aqueous stable fullerene nanocrystals (nC60) on *Daphnia magna*: Evaluation of sub-lethal reproductive responses and accumulation. *Chemosphere*, **77**: p. 1482-1487.
255. Takeda, K., K.-i. Suzuki, A. Ishihara, M. Kubo-Irie, R. Fujimoto, M. Tabata, S. Oshio, R. Nihei, R. Ihara, and M. Sugamata. 2009. Nanoparticles transferred from pregnant mice to their offspring can damage the genital and cranial nerve systems. *J. Health Science*, **55**(1): p. 95-102.
256. Tsuchiya, T., I. Oguri, Y. Nakajima, and N. Miyata. 1996. Novel harmful effects of [60] fullerene on mouse embryos in vitro and in vivo. *FEBS Letters*, **393**: p. 139-145.
257. Newman, D.M., P.L. Jones, and B.A. Ingram. 2007. Temporal dynamics of oocyte development, plasma sex steroids and somatic energy reserves during seasonal ovarian maturation in captive Murray cod *Maccullochella peelii peelii*. *Comp. Biochem. Physiol., A*, **148**: p. 876-887.
258. Yoneda, M., M.T.H. Fujita, N.T.K. Takeshita, and M.M.S. Matsuura. 2001. Reproductive cycle, fecundity, and seasonal distribution of the anglerfish *Lophius litulon* in the East China and Yellow seas. *Fish.Bull.*, **99**: p. 356-370.
259. Galloway, B.J. and K.R. Munkittrick. 2006. Influence of seasonal change in relative liver size, condition, relative gonad size and variability in ovarian development in multiple spawning fish species used in environmental monitoring programmes. *J.Fish Biol.*, **69**: p. 1788-1806.
260. Haux, C., B.Th. Bjornsson, and L. Forlin. 1988. Influence of cadmium exposure on plasma calcium, vitellogenin and calcitonin in vitellogenic rainbow trout. *Mar.Environ.Res.*, **24**: p. 199-202.

261. Stoica, A., E. Pentecost, and M.B. Martin. 2000. Effects of selenite on estrogen receptor- α expression and activity in MCF-7 breast cancer cells. *J.Cell.Biochem.*, **79**: p. 282-292.
262. Snell, T.W. and D.G. Hicks. 2010. Assessing toxicity of nanoparticles using *Brachionus manjavacas* (Rotifera). *Environ.Toxicol.* , **In Press**.
263. Lin, S., J. Reppert, Q. Hu, J.S. Hudson, M.L. Reid, T.A. Ratnikova, A.M. Rao, H. Luo, and P.C. Ke. 2009. Uptake, translocation, and transmission of carbon nanomaterials in rice plant. *Small*, **5**(10): p. 1128-1132.
264. Nyholm, J.R., A. Norman, L. Norrgren, P. Haglund, and P.L. Andersson. 2008. Maternal transfer of brominated flame retardants in zebrafish (*Danio rerio*). *Chemosphere*, **73**: p. 203-208.
265. Hammerschmidt, C.R. and M.B. Sandeirich. 2005. Maternal diet during oogenesis is the major source of methylmercury in fish embryos. *Environ.Sci.Technol.*, **39**: p. 3580-3584.
266. Hall, A.T. and J.T. Oris. 1991. Anthracene reduces reproductive potential and is maternally transferred during long-term exposure in fathead minnows. *Aquat.Toxicol.*, **19**: p. 249-264.

Biography

T. Michelle Blickley was born in Columbus, Ohio in August of 1981. She is the oldest daughter of Bill and Twyla Blickley. The family relocated to Lake Jackson, Texas in 1988. The aquatic environments in Texas inspired Blickley to pursue a career in marine science. In 2003, she graduated from the University of South Carolina, Columbia, SC with a Bachelors of Science in Marine Science. After graduation, Blickley took a position as the laboratory manager for the USC Marine Science Program. In the fall of 2004, Blickley began her graduate career at Duke University under the direction of Patricia McClellan-Green of North Carolina State University and Professor Daniel Rittschof of the Duke University Marine Laboratory. Blickley also obtained a certificate from the Integrated Toxicology & Environmental Health Program at Duke.

Twyla Michelle Blickley

Education

Duke University, Durham, NC

Doctor of Philosophy, received March 25th, 2010

Nicholas School of the Environment

Integrated Toxicology & Environmental Health Program

University of South Carolina, Columbia, SC

Bachelors of Science, received May 10th, 2003

Major: Marine Science

Grants, Awards, and Honors

NRC Resident Research Associateship, NIST, Gaithersburg, MD, 2010-2012

Society for Environmental Toxicology and Chemistry (SETAC)/Proctor and Gamble

Fellowship for Doctoral Research in Environmental Science, 2009

Sally Hughes-Schrader Sigma Xi Travel Award, 2008

Duke University Marine Lab Fellowship, 2008-2009

SETAC Conference Travel Award, 2006

Phi Beta Kappa, honor society, University of South Carolina

Peer-reviewed Publications

Blickley, T.M., D. Rittschof, and P. McClellan-Green. 2010. The Reproductive and Developmental Toxicity of Quantum Dots in the Mummichog, *Fundulus heteroclitus*: A Pilot Study. *Marine Environmental Research* (submitted)

Blickley, T.M. and P. McClellan-Green. 2008. Toxicity of Aqueous Fullerene in Adult and Larval *Fundulus heteroclitus*. *Environmental Toxicology & Chemistry* 27 (9): 1964-1971.

Oberdorster, E., S. Zhu, **T.M. Blickley**, P. McClellan-Green, and M.L. Haasch. 2006. Ecotoxicology of Carbon-Based Engineered Nanoparticles: Effects of Fullerene on Aquatic Organisms. *Carbon* 44: 1112-1120.

Luther, III, G.W., S. Ma, R. Trouwborst, B. Glazer, **M. Blickley**, R. Scarborough, and M. Mensinger. 2004. The Roles of Anoxia, H₂S, and Storm Events in Fish Kills of Dead-end Canals of Delaware Inland Bays. *Estuaries* 27 (3): 551-560.

Book Chapters

McClellan-Green, P., E. Oberdorster, S. Zhu, **T. M. Blickley**, and M.L. Haasch. "Impacts of Nanoparticles on Aquatic Organisms." Nanotoxicology: Characterization, Dosing and Health Effects. Ed. N. Monteiro-Riviere, and C.L. Tran. Informa Healthcare USA, Inc.: New York, 2007. 391-404.

Posters & Presentations

Toxicological Effects of Quantum Dot Exposure in Fish. **T.M. Blickley**, C. Matson, D. Rittschof, R. Di Giulio, and P. McClellan-Green. SETAC North America Meeting. New Orleans, LA. Nov. 22, 2009. (presentation)

Toxicological Effects of CdSe/ZnS Nanocrystals in the Mummichog, *Fundulus heteroclitus*. **T.M. Blickley**, D. Rittschof, and P. McClellan-Green. International Conference on Environmental Implications and Applications of Nanotechnology. University of Massachusetts, Amherst, MA. June 9-11, 2009. (poster)

Toxicological Effects of Nanocrystal Exposure in Teleosts. **T.M. Blickley**, D. Rittschof, and P. McClellan-Green. International Conference on Particle Separation and Nanoparticles in Water. Center for Environmental Implications of Nanotechnology (CEINT), Duke University, Durham, NC. June 3-5th, 2009. (presentation)

Investigating the Eco-toxicity of CdSe/ZnS Quantum Dots in the Mummichog, *Fundulus heteroclitus*. **T. M. Blickley**, P. McClellan-Green, and D. Rittschof. SETAC North America Meeting. Tampa, FL. November 17, 2008. (poster)

Investigating the Eco-toxicity of Engineered Nanomaterials in the Mummichog, *Fundulus heteroclitus*. **T.M. Blickley**. International Water Association World Water Congress. Vienna, Austria. Sept. 8, 2008. (invited presentation)

Investigating the Eco-toxicity of CdSe/ZnS Quantum Dots in *Fundulus heteroclitus*. **T.M. Blickley**, D. Rittschof, and P. McClellan-Green. Carolinas SETAC regional meeting. Morehead City, NC. April 4, 2008. (presentation)

Fate and Toxicological Effect of Fullerene Ingestion in *Fundulus heteroclitus*.
T.M. Blickley, B. Fair, and P. McClellan-Green. SETAC North America Meeting.
Milwaukee, WI. November 13th, 2007. (invited presentation)

Behavior of Water-soluble Fullerenes (nC₆₀) in Seawater and their Developmental Effects
in Teleost Embryos. **T. M. Blickley**, P. McClellan-Green, and E. Oberdorster. SETAC
North America Meeting. Montreal, Quebec. November 8th, 2006. (poster)

Ecotoxicology of Fullerene (C₆₀) in Five Aquatic Species. E. Oberdorster, S. Zhu,
T.M. Blickley, P. McClellan-Green, and M.L. Haasch. 1st International Conference on
Nanotoxicology: Biomedical Aspects. Miami Beach, FL. January 31st, 2006.
(presentation)

Foraminiferal-based Predictions of Metal Bioavailabilities in Estuarine Sediments. **C.J.**
Hintz, **T. M. Blickley**, G.T. Chandler, and T. Shaw. SETAC North America Meeting.
Austin, TX. Nov. 9-13th, 2003. (poster)

Development of Seasonal Anoxia in a Shallow Lagoon-Delaware Inland Bays." **S. Ma**,
M. Blickley, M.G. Mensinger, R. Scarborough, B. Glazer, R. Trouwborst, R. Tyler, and
G. Luther, III. Gordon Conference on Chemical Oceanography. Tilton, N.H. August 13-
14th, 2001. (poster)